

Palaeoenvironmental change from the Hettangian to Toarcian in Moyeni (Quthing District), southwestern Lesotho

By

T'Nielle Haupt

HPTTNI001



Supervisor: Dr Emese M. Bordy

Dissertation presented for the degree of Master of Science in Geology in the
Department of Geological Sciences at the University of Cape Town



September 2018

The copyright of this thesis vests in the author. No quotation from it or information derived from it is to be published without full acknowledgement of the source. The thesis is to be used for private study or non-commercial research purposes only.

Published by the University of Cape Town (UCT) in terms of the non-exclusive license granted to UCT by the author.

Plagiarism Declaration

1. I acknowledge that plagiarism is wrong. Plagiarism is to use another's work and pretend that it is one's own.
2. I have used the South African Journal of Geology convention for citation and referencing. Each contribution to, and quotation, in this project from the work(s) of other people has been attributed, cited and referenced.
3. This project is my own work.
4. I have not allowed, and will not allow, anyone to copy my work with the intention of passing it off as his or her own work.

Signature:

Signed by candidate

Date: 07/09/2018

Acknowledgements

I would like to thank my supervisor Dr Emese Bordy for all your support and dedication throughout the duration of this project. Thank you for all the effort you have put in and for all the encouragement and knowledge that you have instilled in me. Thank you for also being a helpful hand in the field as well as the continuous support before and during the writing process.

A very special thanks also goes to Dr Alastair Sloan for taking your time to help me with the structural geology, both in and outside the field.

I would also like to thank my colleagues and friends Miengah Abrahams, Lara Sciscio, Akhil Rampersadh and Mhairi Reid for their assistance during my fieldwork. Thank you to the rest of the UCT SedsPalaeo team and all the technical staff in the Department of Geological Sciences at UCT, who helped with sample preparation.

I also wish to thank family and friends for their constant motivation and support.

Last but not least, I would also like to acknowledge the following financial sources:

- National Research Foundation Grants (African Origins Platform and Competitive Programme for Rated Researchers: # NRF 98825, 113394, 93544) to my supervisor, Dr Bordy to cover operational costs (including conference participation costs, bursary top up) in 2017 and 2018.
- Palaeontological Scientific Trust's (PAST) conference grant to my supervisor, Dr Bordy to attend the 20th Biennial Conference of the Palaeontological Society of Southern Africa, Bloemfontein, South Africa, July 2018.
- International Association of Sedimentologists for the conference grant to attend the International Meeting of Sedimentology (IMS), Toulouse, France, October 10-13, 2017.
- NRF/DST Centre of Excellence in Palaeosciences (CoE-Pal) for MSc bursary in 2017 and 2018.

Opinions expressed, and conclusions arrived at, are those of the author and are not necessarily to be attributed to the NRF or CoE-Pal.

Contents

Plagiarism Declaration.....	ii
Acknowledgements.....	iii
Abstract.....	vi
1 Introduction	1
1.1 Rationale for undertaking research	1
1.2 Geological Background	4
1.3 Tectonic setting of the main Karoo Basin.....	5
1.4 Stratigraphy of the Karoo Supergroup	9
2 Methodology and study area.....	15
2.1 An Overview	15
2.2 Sedimentary Facies Analysis.....	16
2.2.1 Sedimentary Facies	16
2.2.2 Facies Models.....	18
2.3 Ichnological Analysis.....	21
2.4 Geological mapping.....	23
2.5 Petrographic analysis.....	24
3 Results.....	25
3.1 Description of the main stratigraphic units and their lithofacies assemblages.....	29
3.1.1 The upper Elliot Formation (uEF)	29
3.1.2 The Clarens Formation.....	36
3.1.3 The Drakensberg Group.....	38
3.1.4 Breccia Facies	47
3.2 Petrographic analysis.....	49
3.2.1 Upper Elliot Formation.....	49
3.2.2 Clarens Formation.....	49
3.2.3 Barkly East Formation	50
3.3 Ichnology of Moyeni	52
3.3.1 Lower Moyeni ichnosite.....	52
3.3.2 Upper Moyeni ichnosite.....	55
3.3.3 Phahameng ichnosite	59
3.4 Geological Map of Moyeni.....	26
3.5 Structural geology near Moyeni.....	60
3.5.1 Faults in eastern Moyeni	60

3.5.3 Faults in western Moyeni	63
4 Discussion.....	65
4.1 Interpretation of the facies analysis results	65
4.1.1 The upper Elliot formation (uEF).....	65
4.1.2 The Clarens Formation.....	68
4.1.3 The Barkly East Formation (lowermost Drakensberg Group)	71
4.2 Petrographic analysis.....	77
4.2.1 Mineral composition and grain size	77
4.2.2 Sorting.....	79
4.2.3 Maturity	79
4.2.4 Source rocks	79
4.2.5 Sandstone classification.....	80
4.3 Ichnology.....	82
4.3.1 Lower Moyeni.....	82
4.3.2 Upper Moyeni.....	84
4.3.2 Phahameng.....	85
4.4 Structural geology of Moyeni	86
4.4.1 Normal Faulting	86
4.4.2 Timing of the faulting.....	87
4.4.3 Breccia Facies	76
4.5 Palaeoenvironmental changes	91
4.5.1 Hettangian	91
4.5.2 Sinemurian – Pliensbachian	92
4.5.3 Pliensbachian – Toarcian.....	93
4.5.4 Early Jurassic Palaeogeography	93
5 Conclusion	95
6 References.....	97
7 Appendix	111

Abstract

The upper Karoo Supergroup of southern Africa encompasses the Late Triassic-Early Jurassic geological evolution of southern Gondwana. The environment is known to have shifted from wet swamps to a semi-arid fluvio-lacustrine and then to an aeolian system, preceding the outpouring of the Karoo continental flood basalts. The study area at Moyeni in SW Lesotho, exposes the richly fossiliferous Lower Jurassic upper Elliot and Clarens Formations (Stormberg Group) as well as the Barkly East Formation (lowermost Drakensberg Group). With the aid of integrated geological methods (e.g., field mapping, sedimentology, ichnofacies analysis), this research aims to document Early Jurassic palaeoenvironmental and tectonic changes in this region.

The upper Elliot Formation comprises very fine- to fine-grained sandstone units with either massive or with ripple cross-lamination, low-angle cross-bedding as well as sandy siltstone with *in-situ* carbonate nodules, desiccation cracks, bone fossils and a diverse ichnofauna (e.g., algal mats, vertebrate burrows, tracks of theropods, ornithischians, amphibians, crocodylomorphs). Sedimentological evidence indicates that in the Hettangian the area was prone to flash floods and drying in a low energy depositional system with small rivers and shallow lakes. The bulk of the Clarens Formation comprises very thick, tabular, fine- to medium-grained, massive to large-scale cross-bedded arenites. However, the lower part of the Clarens also preserves thin-bedded mudstones and theropod tracks. These suggest a change in the Sinemurian from a wet to a dry desert with large, down-wind and eastward migrating sand dunes. It also appears that in spite of climatic changes these Hettangian-Sinemurian ecosystems sustained a diverse biota.

Within the lowermost Drakensberg Group, interbedded with lava flows and pillow lavas, massive to cross-stratified sandstone units are common. These beds typically thin and fine upward and, at least locally, terminate in surfaces that are covered by symmetrical ripple marks. These suggest that by the Toarcian the land surface was again covered by temporary lakes and streams into which the lavas outpoured during the early stages of the Karoo volcanism. The study area is structurally deformed by ~ESE-WNW trending normal faults, some of which appear to have been active already during Clarens Formation times. This syn-sedimentary faulting is interpreted as part of the growing body of evidence for the changeover from a compressional to extensional tectonic regime during the Early Jurassic and may be the first signs of Gondwana break-up.

1 Introduction

Gondwana, the Southern Hemisphere supercontinent from the Early Palaeozoic to Middle Mesozoic, hosted several vast and dynamically evolving continental basins (Veervers et al., 1994). These basins received sediments from the highlands via glacial, aqueous, aeolian and mass movement processes, and experienced several marine incursions (Smith et al., 1993). One such basin of southern Gondwana is the main Karoo Basin (MKB), which contains strata of marine and continental origin (Smith et al., 1993; Catuneanu et al., 2005). The sedimentary succession in the MKB accumulated over ~ 120 million years and during this time the depositional environment shifted from glacial to fluvial/lacustrine and finally to an aeolian environment (Catuneanu et al., 1998; Bordy et al., 2004a). Changes in climate and tectonics throughout the evolution of the MKB were the main forcing mechanisms of the deposition and have been relatively well studied (Smith et al., 1993; Bordy et al., 2004a; Catuneanu et al., 2005). During the Early Jurassic, there was a major shift in the regional tectonics and climate within the MKB, and thus the palaeo-environmental change over this time period is what is of interest in the study. To find evidence for these changes and to reconstruct the palaeo-environment, the Lower Jurassic of the Karoo Supergroup, which includes the Stormberg and Drakensberg Groups, were studied. The study was conducted in southwestern Lesotho, in and around the town of Moyeni which is in the Quthing District (Figure 1.1). Not only does Moyeni expose high-quality outcrops of these upper Karoo rocks but the selection of the study site was also motivated by the rich palaeontological record of this region.

1.1 Rationale for undertaking research

This research forms part of an on-going multidisciplinary study on the geological changes (i.e. sedimentological, biological, structural/tectonic and climatic), which occurred during Late Triassic-Jurassic in southern Africa. The Early Jurassic, encompassing the Hettangian, Sinemurian, Pliensbachian, Toarcian stages, is an important interval in the history of southern

Africa both geologically and palaeontologically with an abundance of continental rocks and diverse body and trace fossil assemblages. During this time, the region also experienced a shift in the tectonic regime from compression to extension, which resulted in the deformation within the MKB. The stratigraphic units that preserve these events are the Stormberg Group and the Drakensberg Group and are associated with at least two global mass extinction events: 1) the end-Triassic and 2) end-Pliensbachian events (e.g., Sciscio and Bordy, 2016; Bordy et al., 2018). The end-Triassic mass extinction event is firmly linked to the outpouring of the continental flood basalts of the Central Atlantic Magmatic Province (e.g., Blackburn et al., 2013), however its impact on the continental ecosystems in southern Gondwana are still actively researched (e.g., Bordy et al., 2016; Sciscio and Bordy, 2016; Sciscio et al., 2016; Abrahams et al., 2017; McPhee et al., 2017; Sciscio et al., 2017a; Sciscio et al., 2017b; Sciscio et al., 2017c). The end-Pliensbachian mass extinction event is linked to the Toarcian biotic turnover that is particularly detected in the marine fossil record. The trigger of this mass extinction has been repeatedly shown to have been the massive volcanic event that took place in the Karoo-Ferrar Large Igneous Province (LIP) in the Pliensbachian-Toarcian (Sell et al., 2014; Burgess et al., 2015; Percival et al., 2015). The continental flood basalts and associated intrusive rocks of the Karoo-Ferrar LIP covered and impacted most of the southern Gondwana and are best exposed within the central MKB. However, not much is known about the environmental conditions prior, during and shortly after this huge volcanic event. Specifically, the main question that remains unanswered is what impact the volcanism had on the palaeoecology of the region in the late Early Jurassic (e.g., Moulin et al., 2017). Because of the global importance of the end-Triassic and end-Pliensbachian mass extinction events, establishing the climatic and ecological changes that occurred over 20 million years, from ~ 200 to ~ 180 million years ago, has the potential to give insights to and better understand of the history of southern Gondwana on both a regional and global scale.

This study, therefore aims to gain evidence and synthesize them to: 1) establish the nature of the Early Jurassic palaeoclimatic changes in southwestern Lesotho; 2) refine the

palaeoecological dynamics in southern Africa during this interval and 3) understand the structural elements which controlled deformation of the study area in the late Early Jurassic. This is accomplished by applying an interdisciplinary approach rooted in sedimentology, structural geology and ichnology. This study focusses on the geological processes of the upper Stromberg Group (the upper Elliot and Clarens Formations), and lowermost Drakensberg Group (the Barkly East Formation). In addition, the research also addresses the interactions between the organisms and the environment in which they lived. More specifically, the objectives are to:

1. Examine the sedimentology of the uppermost Stormberg and lowermost Drakensberg Group through high-resolution geological methods, with a view to: a) refine and reconstruct the dynamics of the palaeoenvironmental setting; and b) interpret the nature of the climatic changes in the Early Jurassic.
2. Describe and interpret the trace fossils that occur in the area to aid the palaeoenvironmental reconstruction.
3. Using transmitted light microscopy, analyse the petrography of representative sandstone samples from the upper Elliot, Clarens and Barkly East Formations for their classification and comparison.
4. Map the regional geology and produce a detailed geological map of the study area. The mapping includes assessment and illustration the spatial distribution of the upper Elliot, Clarens and Barkly East Formations, their structural elements and their stratigraphic contacts. The mapping of the stratigraphic contacts is important to understand the nature of the transition from the fluvial-lacustrine to aeolian deposition to dominantly igneous rocks higher up in the succession.

1.2 Geological Background

The Late Carboniferous to Early Jurassic MKB is described as a retroarc foreland basin, which underlies well over half of South Africa and all of Lesotho (Figure 1.1; Catuneanu et al., 1998). The basin contains siliciclastic rocks that are marine and continental in origin and form the Karoo Supergroup (Figure 1.1A; e.g., Johnson et al., 1997; Johnson et al., 2006; Catuneanu et al., 1998). These deposits reflect geological events which occurred over the ~120 Ma period, from the glacial deposition in the Late Palaeozoic (latest Carboniferous) to extrusion of lavas in the early Middle Mesozoic (Toarcian in the Early Jurassic). Deposits of the Karoo Supergroup are not limited to South Africa and Lesotho and extend into sedimentary basins of other southern African countries (e.g., Namibia, Botswana, Swaziland, Zimbabwe, Zambia, Mozambique; Johnson et al., 1996). The MKB (Figure 1.1A), which is limited to South Africa and Lesotho, contains one of the thickest and most complete Carboniferous to Jurassic succession in south-western Gondwana, with a maximum thickness of 6 km in the south-eastern part of the basin (e.g., Catuneanu et al., 1998; Lindeque et al., 2011; Scheiber-Enslin et al., 2015).

The youngest rocks of the Karoo Supergroup, namely the Stormberg Group (Molteno, Elliot and Clarens Formations) as well as the Drakensberg Group (Figure 1.1B) show a transition from fluvio-lacustrine to an aeolian and finally volcanic conditions (Lock et al., 1974; Bordy et al., 2004a, b; Catuneanu et al., 2005). These upper Karoo rocks are described in detail in the second half of Section 1.4.

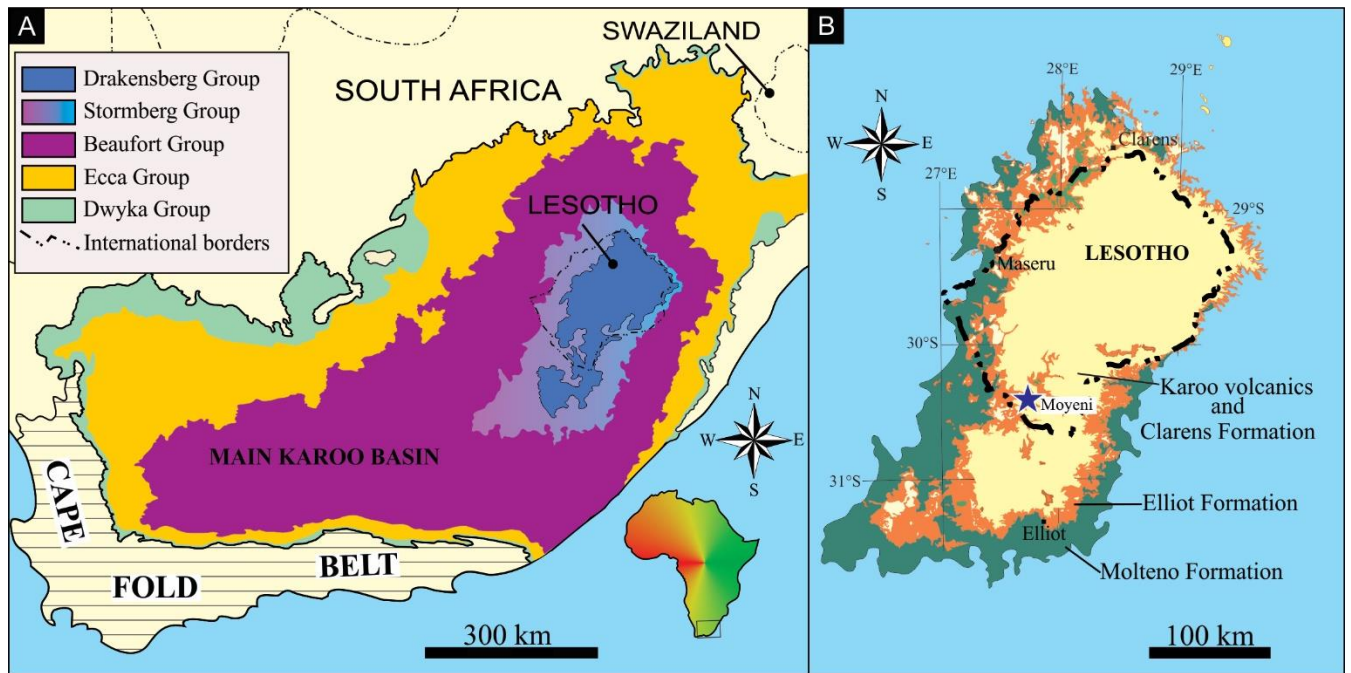


Figure 1.1: (A) Simplified geological map of the main Karoo Basin in South Africa and Lesotho, outlining the spatial distribution of the Dwyka, Ecca, Beaufort, Stormberg and Drakensberg Groups of the Karoo Supergroup. (B) Simplified geological map in the north-eastern part of the MKB), indicating the spatial distribution of the Molteno, Elliot, Clarens formations within the Stormberg Group, and the extrusive rocks of the Drakensberg Group. The study area near Moyeni (Quthing District in SW Lesotho) is marked with a blue star.

1.3 Tectonic setting of the main Karoo Basin

The sedimentary fill of the MKB records the change in stress regimes in SW Gondwana from extensional to compressional and back to extensional during Palaeozoic and Early to Middle Mesozoic (Veervers et al., 1994; Catuneanu et al., 1998). Many basin models have been proposed with regards to the formation and evolution of the MKB (e.g., Cole 1992; Turner, 1999; Tankard et al., 2009; Lindeque et al., 2011), however, its most accepted formation and development model, which has been repeatedly justified by various independent studies (e.g., Pysklywec and Mitrovica, 1999; Bordy et al., 2004a, b; Rubidge et al., 2013), is the retroarc foreland basin model that is most eloquently summarized in Catuneanu et al. (1998). This model suggests that in the southern African portion of Gondwana, the Karoo retro-arc basin formed in front of the Cape Fold Belt due to the subduction of the Palaeo-Pacific plate beneath the southern margin of Gondwana (Figure 1.2A). The Cape Orogeny formed part of the

Gondwanan Mobile Belt (or Gondwanides) and developed along Late Proterozoic structural trends in southern Africa (Catuneanu et al., 1998). The foreland basin itself has been fragmented due to Gondwana break-up (i.e., due to tensional tectonics and crustal thinning) in the Middle Jurassic, the remnants of which are found in South Africa (Karoo Basin), South America (Parana Basin), Australia (Bowen Basin) and Antarctica (Beacon Basin) (e.g., Lock, 1980; Catuneanu et al., 1998; Turner, 1999). The Karoo foreland basin developed within this compressional tectonic setting in response to mainly but not only supralithospheric loading, which was essentially from the thickening and shortening of the rocks of the Palaeozoic Cape Supergroup and lower Karoo during the Permo-Triassic Cape Orogeny (e.g., Catuneanu et al., 1998; Hansma et al., 2016).

The sedimentation within the Karoo foreland basin was controlled by the loading and unloading events of the Cape Fold Belt during the Permian, Triassic and earliest Jurassic (Figure 1.2B & C; Catuneanu et al., 1998; Hansma et al., 2016). In short, a loading event, which is a mountain building phase, results in subsidence near the orogen, which allows for the increase in accommodation space and preservation of sediments next to the orogen (in the foredeep). This in turn correlates to episodes of uplift in the distal part of the foreland system, causing erosion and formation of regional unconformities. The opposite, i.e., uplift near the orogen and subsidence in the distal part, occurs during unloading events when the proximal regional slopes become increasingly steeper (Figure 1.2B & C; Catuneanu et al., 1998). The alternation between the supracrustal loading and unloading events of the Cape Fold Belt had a strong influence on the basin evolution, and among others, determined the lateral movement and rate of subsidence in the depocenter (i.e. the area of maximum deposition) within the foreland system. As a result, the depocentre of the basin alternated between the proximal region during orogenic loading and distal region during orogenic unloading phases, respectively (Figure 1.2; Catuneanu et al., 1998).

The flexural tectonism of the foreland basin ended during the first order unloading event in the Late Triassic (e.g., Cole 1992; Hancox, 1998; Catuneanu et al., 1998; Bordy et al., 2004a).

This final first order tectonic unloading event in the Cape Fold Belt commenced by the early Late Triassic (possibly in the Ladinian; e.g., Catuneanu et al., 1998; Hancox and Rubidge, 2018), and caused not only the erosion, reworking and northward transport of the older foredeep sediments in the south but also the development of a foresag in the distal region (Figure 1.2C; Bordy et al., 2004b). The reworked foredeep sediments that were transported into the foresag setting were preserved as the Stormberg Group (see next section; Bordy et al., 2004a). The flood basalts of the Drakensberg Group subsequently filled the most depressed region of the foresag region, thus allowing for the building up of a ~1.8 km thick pile of basaltic lavas. The Stormberg Group as well as the Drakensberg Group are situated further away from the CFB in the distal part of the MKB (see foresag region in Figure 1.2; Catuneanu et al., 1998).

Finally, for sake of completeness, hereby is a brief mention of the alternative basin models that were suggested for the formation and evolution of the MKB in order of acceptance gained in the literature:

- 1) Tankard et al. (2012) proposed that the MKB formed due the vertical displacement of rigid basement blocks related to crustal faulting and argues that the influences of the Cape Fold Belt on the basin fill only commenced during the Early Triassic.
- 2) Turner (1999), while accepting the foreland basin dynamics for the lower Karoo, suggested an extensional tectonic regime for the upper Karoo, which he argued to be the result of a mantle plume induced thermal anomaly, which in turn generated deformation of the crust and the Triassic onset of the volcanic activity.
- 3) Lindeque et al. (2011) speculated that the basin evolution is linked to collisional tectonics (arc-continent collision), which resulted in the formation of the thick CFB and subduction taking place in the distant south.

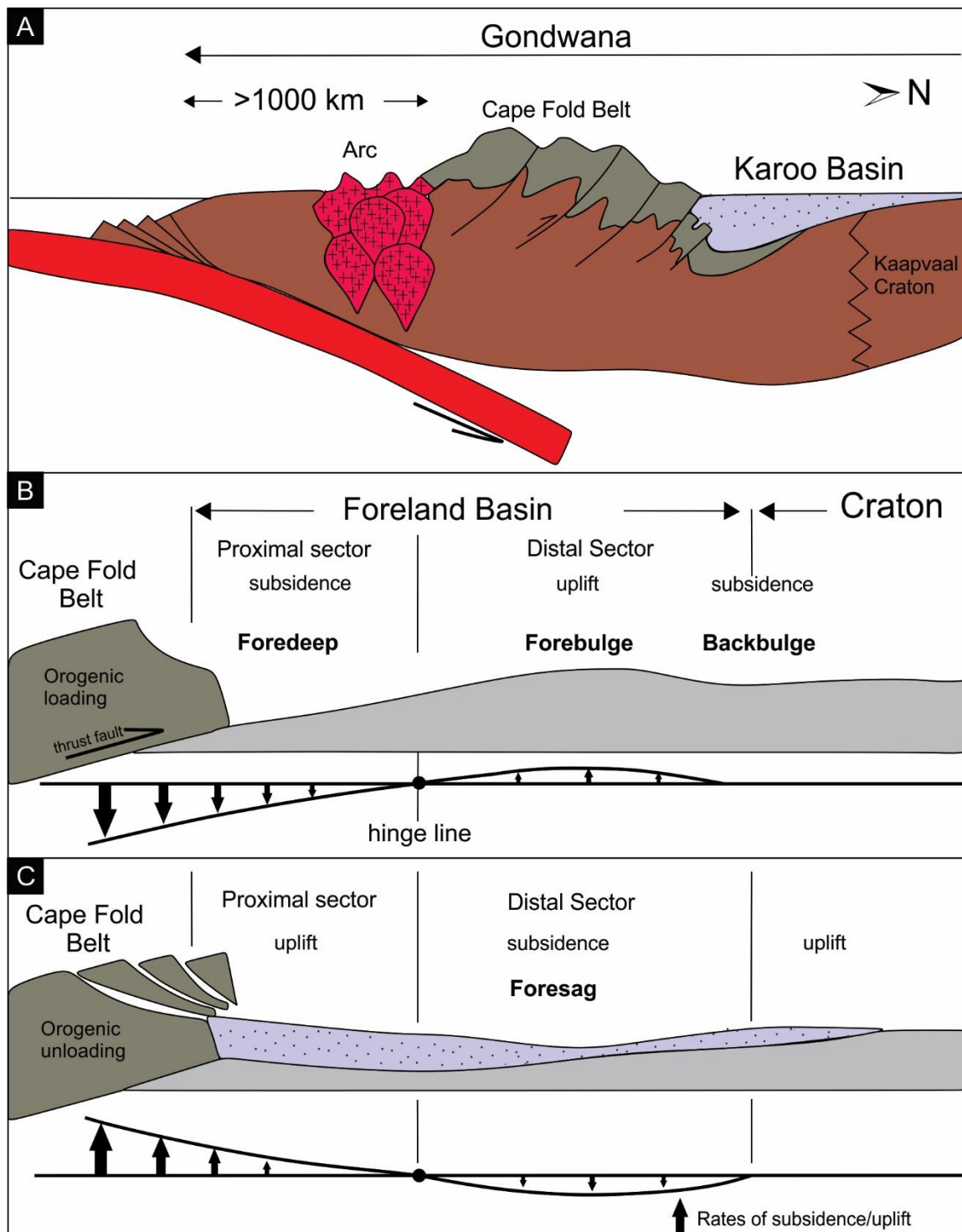


Figure 1.2: Tectonic setting and evolution of the Karoo retro-arc foreland basin illustrating: (A) the subduction of the Palaeo-Pacific plate underneath the southern margin of Gondwana; (B) Orogenic loading event of the Cape Fold Belt which results in the different flexural provinces (i.e. foredeep and forebulge) within the foreland system. (C) Orogenic unloading which results in the uplift and erosion of the Cape Fold Belt and the development of the foresag in the distal sector in which reworked sediments deposited. Figure adapted from Catuneanu et al. (1998).

1.4 Stratigraphy of the Karoo Supergroup

The Karoo Supergroup is subdivided into five lithostratigraphic groups, namely (from oldest to youngest) the Dwyka, Ecca, Beaufort, Stormberg and Drakensberg Groups (Figure 1.3; Johnson, 1994). Except for the latter group, which comprises mostly igneous rocks, all other groups are dominated by siliciclastic rocks. Due to the foreland basin origin of the MKB (see previous section), the north-south thickness distribution of the Karoo Supergroup is highly asymmetrical and shows rapid thinning towards the north (Catuneanu et al., 1998). The succession contains numerous stratigraphic gaps, of which the most significant one is at the base of the Stormberg Group (e.g., Catuneanu et al., 1998; Hancox and Rubidge, 2018). This regional unconformity separates the Dwyka, Ecca and Beaufort Groups (i.e., lower Karoo Supergroup) from the Stormberg and Drakensberg Groups (i.e., upper Karoo Supergroup). The Karoo sedimentary rock units show evidence for a major climatic shift from glacial to cool and moist conditions during the deposition of the Dwyka and Ecca Groups to warm, semi-arid to finally to arid conditions during the formation of the Beaufort and Stormberg Groups, respectively (Smith, 1990; Smith et al., 1993; Catuneanu et al., 1998; Bordy et al., 2004a). The Karoo Supergroup holds an abundant fossil record, especially of Permo-Triassic and Jurassic vertebrates and plants, which allowed for the biostratigraphic subdivision of the Karoo (e.g., Kitching, 1977; Hancox and Rubidge, 2001; Rubidge, 2005; Rubidge et al., 2013).

According to radiometric ages obtained from the Karoo Supergroup, the sedimentation of the Dwyka Group in the MKB was already ongoing by ~ 302 Ma, and probably commenced earlier in the Late Carboniferous (Bangert et al., 1999; Isbell et al., 2008). The Dwyka Group, which formed during the Permo-Carboniferous glaciation of Gondwana (Johnson, 1996; Catuneanu et al., 1998; Isbell et al., 2008), is up to 800 m thick in the south and comprises glacial or glacial-related deposits (e.g., tillites, varvites, diamictites) and associated sedimentary rocks such as glaciofluvial conglomerates and sandstones on glaciated striated basement rocks, and glacio-lacustrine mudstones with dropstones (Visser, 1990; Johnson et al., 1996; de Wit,

2016). Deposition of the Dwyka Group concluded before 289.6 ± 3.8 Ma in the Early Permian (Bangert et al., 1999).

The overlying units of the Lower to Middle Permian Ecca Group lies conformably on the Dwyka Group, and consists of sandstones, siltstones, mudstones and coal seams (Catuneanu et al., 2005). These deposits, with maximum thickness of 3000 m in the southern MKB, are characterised by the overall large-scale upward coarsening succession, which formed initially in a deep marine setting, and later in a shallow marine to costal depositional environments (Johnson et al., 1996). The Ecca Group also contains marine invertebrate fossils and vertebrate body and a diverse ichnofauna. In addition, the Ecca Group is also well-known for its abundant *Glossopteris palaeoflora* and associated assemblages of insects and insect damage trace fossils (Smith et al., 1993; Prevec, et al., 2010; Prevec, 2011).

The Middle Permian to upper Middle Triassic Beaufort Group contains predominantly fluvio-lacustrine mudstones and siltstones, with secondary sandstones and the highest abundance and diversity of tetrapod fossils of all Karoo units (Catuneanu et al., 2005). These sedimentary rocks were deposited in both high-energy braided and highly sinuous meandering rivers with well-developed and vegetated floodplains (Smith, 1990). This succession of rocks lies conformably on the Ecca Group but there is a major unconformity between the Beaufort Group and overlying Stormberg Group, with the stratigraphic gap of several million years (Cole, 1992; Hancox and Rubidge, 2018).

The youngest sedimentary succession of the Karoo Supergroup, the Upper Triassic – Lower Jurassic Stormberg Group is made up of the fluvio-lacustrine Molteno and Elliot Formations, and predominantly aeolian Clarens Formation (Smith et al., 1993; Johnson et al., 1996). Cumulatively, these units are over 1500 m thick and records the final stages of the basin evolution (e.g., Catuneanu et al., 2005; Bordy et al., 2004 a, b).

The Stormberg Group started forming approximately 230 Ma ago with the accumulation of the sandstones, plant fossil-rich carbonaceous mudstones and coal seams of the Molteno

Formation. Deposition occurred in a braided river system and associated swamps on an alluvial plain fed mostly from the south (Turner, 1983).

The Norian to Sinemurian Elliot Formation, the middle unit of the Stromberg Group, was deposited from ~215 to ~190 million years ago (Sciscio et al., 2017) and consists of red, pink, purple and maroon mudstones, siltstones and medium to very fine-grained sandstones. The maximum thickness of the Elliot Formation is 480 m in the south of the basin but gradually thins towards the north where the maximum thickness is less than 30 m (Du Toit, 1954).

The formation has a sharp, unconformable basal contact with the underlying Molteno Formation, and a gradational, conformable contact with the overlying Clarens Formation (Bordy et al., 2004a, b; 2005; Bordy and Eriksson, 2015; Bordy and Head, 2018). The unconformable lower contact is distinguished by the following differences which occur across the boundary: architecture of the sandstone units, palaeocurrent directions, pedogenic indicators and fossil content (Bordy et al., 2005). Furthermore, there are several sedimentary characteristics (e.g., lithologies, palaeocurrents, associations of sedimentary structures) of the Elliot Formation which are significantly different in the upper and lower part of the formation, thus there is a regional, but informal lithostratigraphic subdivision of the unit into the lower Elliot (IEF) and the upper Elliot (uEF) Formations (Bordy et al., 2004a).

Climatic and tectonic changes in the Latest Triassic and at the turn of the Triassic and Jurassic, caused a major fluvial style change, not only at the start but also during the deposition of the Elliot Formation (Bordy et al., 2004a, b; Catuneanu et al., 2005). Within the Elliot Formation, this change in river styles is recorded by mainly meandering river and floodplain deposits in the IEF and ephemeral stream and lake deposits in the uEF, respectively. The switch in facies architecture at the IEF-uEF boundary is linked to a cryptic unconformity, which is interpreted as a second order sequence boundary in the upper Karoo (Bordy et al., 2004a, b).

In addition, the Elliot Formation is highly fossiliferous with major groups of vertebrate fossils ranging from dinosaurs, turtles, fish, amphibians and early mammals (Knoll, 2004; 2005; Bordy and Eriksson, 2015; Abrahams et al., 2017; Bordy et al., 2017; McPhee et al., 2017; Sciscio et al., 2017). Crustaceans such as conchostracans, fossilized wood and a diverse array of trace fossils such as tetrapod footprints and vertebrate burrows, are also common within the formation (Ellenberger, 1970, 1972; 1974; Kitching and Raath, 1984; Smith et al., 2009; Wilson et al., 2009; Sciscio et al., 2016; Abrahams et al., 2017, Bordy et al., 2016; 2017).

The main sediment source of the Elliot Formation was the Cape Fold Belt in the south, however sediment has also been supplied from the west as documented by Bordy et al. (2004 a, c). Furthermore, the upper Elliot Formation also contains the first evidence for the inversion in tectonic regime, from compressional to extensional in form of syn-sedimentary normal faults and purported seismites (Bordy et al., 2004 a,b).

The Sinemurian to Pliensbachian Clarens Formation is the youngest formation of the Stormberg Group. This formation outcrops over a large area in southern Africa, and is formerly known as the Cave Sandstone because of the many sandstone overhangs that form mainly at its lower contact with the less resistant Elliot Formation. The Clarens Formation generally consists of cream-yellow fine-, medium- to coarse-grained sandstones (mostly arenites) with subordinate mudstones especially in its lower part (Eriksson, 1981;1984; Bordy and Catuneanu, 2001; Bordy and Head, 2018). The common sedimentary structures in the sandstone beds include small to large-scale planar and trough cross-bedding, horizontal and ripple cross-laminations and desiccation cracks (Bordy and Catuneanu, 2001; Bordy, 2008; Bordy et al., 2009; Bordy and Head, 2018). The depositional environment was reconstructed as a desert with wind-blown dunes as well as wetter settings with shallow playa lakes and ephemeral streams (Beukes, 1970; Eriksson, 1981;1984; Bordy and Head, 2018). The contact between the Elliot and Clarens Formations is generally uneven and is marked by the first appearance of sandstones with large- to very large-scale cross-bedding. The Clarens Formation also contains fossils of vertebrates (e.g., dinosaurs, fish), invertebrates (e.g.,

conchostracans), plants as well as a diverse ichnofauna of both invertebrates (e.g., termites) and vertebrates (e.g., tetrapods) (Ellenberger, 1970; Tasch, 1984; Bordy, 2008; Bordy et al., 2009). This palaeontological diversity suggests that the palaeoenvironment was still capable of sustaining a rich ecosystem despite the overall desert conditions (Beukes, 1970).

The youngest rocks of the Karoo Supergroup are volcanic in origin, and according to radiometric dates, they extruded to the surface of the main Karoo Basin $\sim 183 \pm 1$ Ma ago (age range of 184 to 179 Ma) during the Late Pleinsbachian to Early Toarcian (Duncan et al., 1997; Moulin et al., 2017). The Pleinsbachian-Toarcian lavas of the Drakensberg Group forms part of the Karoo-Ferrar Large Igneous Province, and is subdivided into two main formations, namely the lower Barkly East Formation (~ 300 m thick) and the uppermost Lesotho Formation (Lock et al., 1974; Marsh et al., 1997; Hanson et al., 2009). The latter consists of mostly tholeiitic lavas that dominate in the highlands of Lesotho over a thickness of >1400 m, with majority of these lavas exposed in northern Lesotho (Duncan et al., 1997; Marsh et al., 1997). During the Jurassic, this previously continuous basalt plateau covered an area of approximately two and a half million square kilometres, one of the largest continental flood basalts (Lock et al., 1974). The contemporaneous intrusive rocks (i.e. the dolerite dykes and sills) are geochemically identical and are interpreted to have fed the volcanic eruptions on the surface. Evidence has shown that the main volcanic activity took place after the deposition of the last Stormberg sediments and the accumulation of lava flows occurred over a very short geological period (i.e., $< \sim 500\,000$; Marsh et al., 1997; Moulin et al., 2017). The volcanic activity was most likely sporadic during the generation of the Barkly East Formation and became widespread during the generation of the Lesotho Formation (e.g., Moulin et al., 2017). The most extensive outcrops of these volcanic rocks are found in Lesotho and parts of the adjoining highlands of the Drakensberg in eastern South Africa, however equivalent igneous rocks are found in most of southern Africa in subcrop or erosional remnants (Lock et al., 1974; Visser, 1984; Marsh et al., 1997).

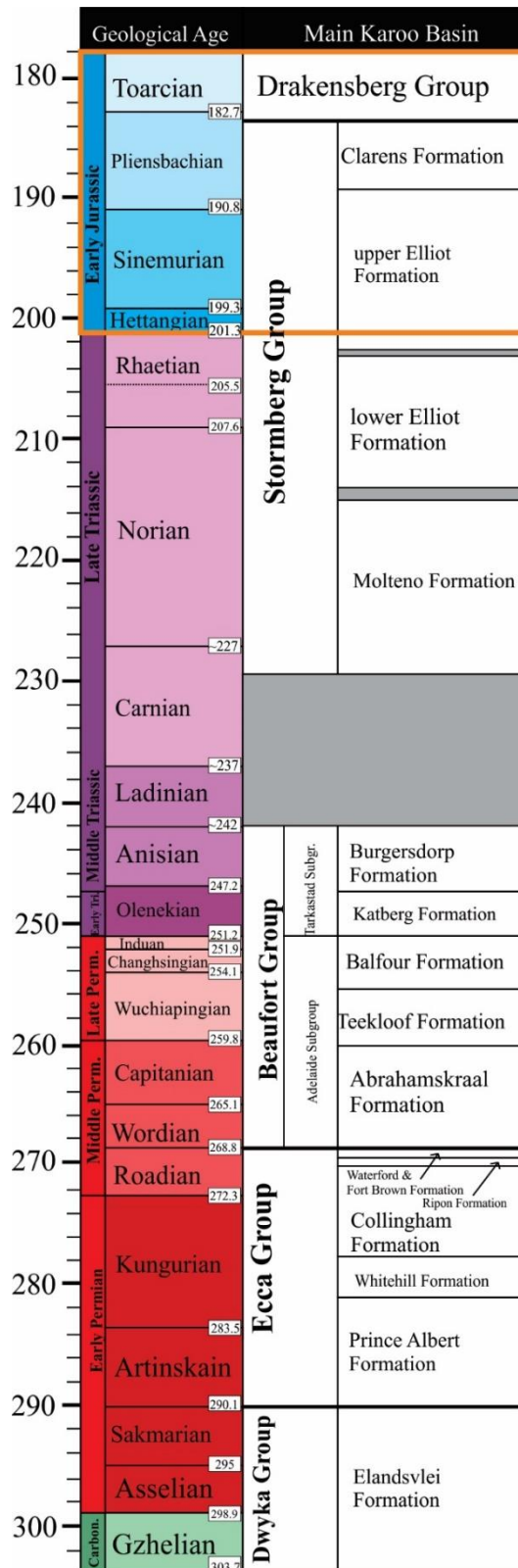


Figure 1.3: Litho- and chronostratigraphic chart illustrating and the main lithological groups of the Karoo Supergroup in the southern MKB. The Karoo rocks of the Early Jurassic (Hettangian -Toarcian), which are of importance for this study are highlighted with an orange box; the grey areas indicate a stratigraphic gap. Geological time scale after Gradstein et al. (2009). Figure adapted from Bordy et al., 2004a, b, 2005; Rubidge et al. (2013).

2 Methodology and study area

2.1 An Overview

The methodology applied in the study area was predominantly qualitative as most of the methods were field-based. The main method, sedimentary facies analysis was applied to aid the identification and interpretation of the different sedimentary units, and to reconstruct the changes in the depositional environments of the study area, through geological time. Geological mapping was also conducted to spatially separate the main stratigraphic units in the region (i.e., uEF, Clarens Formation and Barkly East Formation) and assess the nature of their contacts as well as the structural geology in the study area. Collectively, these methods aided the generation of the 1: 20 000 scale geological map of the Moyeni area, which in turn gives insight to the better understanding of the broader geological history of the region, including the deformational events that occurred in the Early Jurassic. Ichnological analysis was applied to identify and classify the trace fossils as well and interpret the possible fauna that made the trace fossils. Laboratory analysis involved petrographic studies of the samples taken from outcrops of the main rock units in the study area, in order to establish their mineralogical and textural characteristics.

The study area, located in and around Moyeni in the Quthing District of southwestern Lesotho (Figure 2.1) exposes in road cuttings, steep sided river valleys, hill sides and cliffs, the Lower Jurassic continental sedimentary rocks of the upper Elliot and Clarens Formations as well as the interbedded sedimentary and igneous rocks of the lowermost Drakensberg Group. The fieldwork entailed the detailed recording of the different rock units of each formation. The features of the outcrops were documented using photographs and sketches, as well as detailed descriptions in field notebooks. Photographs were taken to digitally capture the outcrops and ichnosites (lower Moyeni, upper Moyeni and Phahameng; Figure 2.1B), and photos were merged into panoramic view. Centimetre-scale sedimentary logs of the uEF at

upper Moyeni, lower Moyeni, the Clarens Formation and the lowermost Drakensberg formation were drawn and are illustrated in the results section.

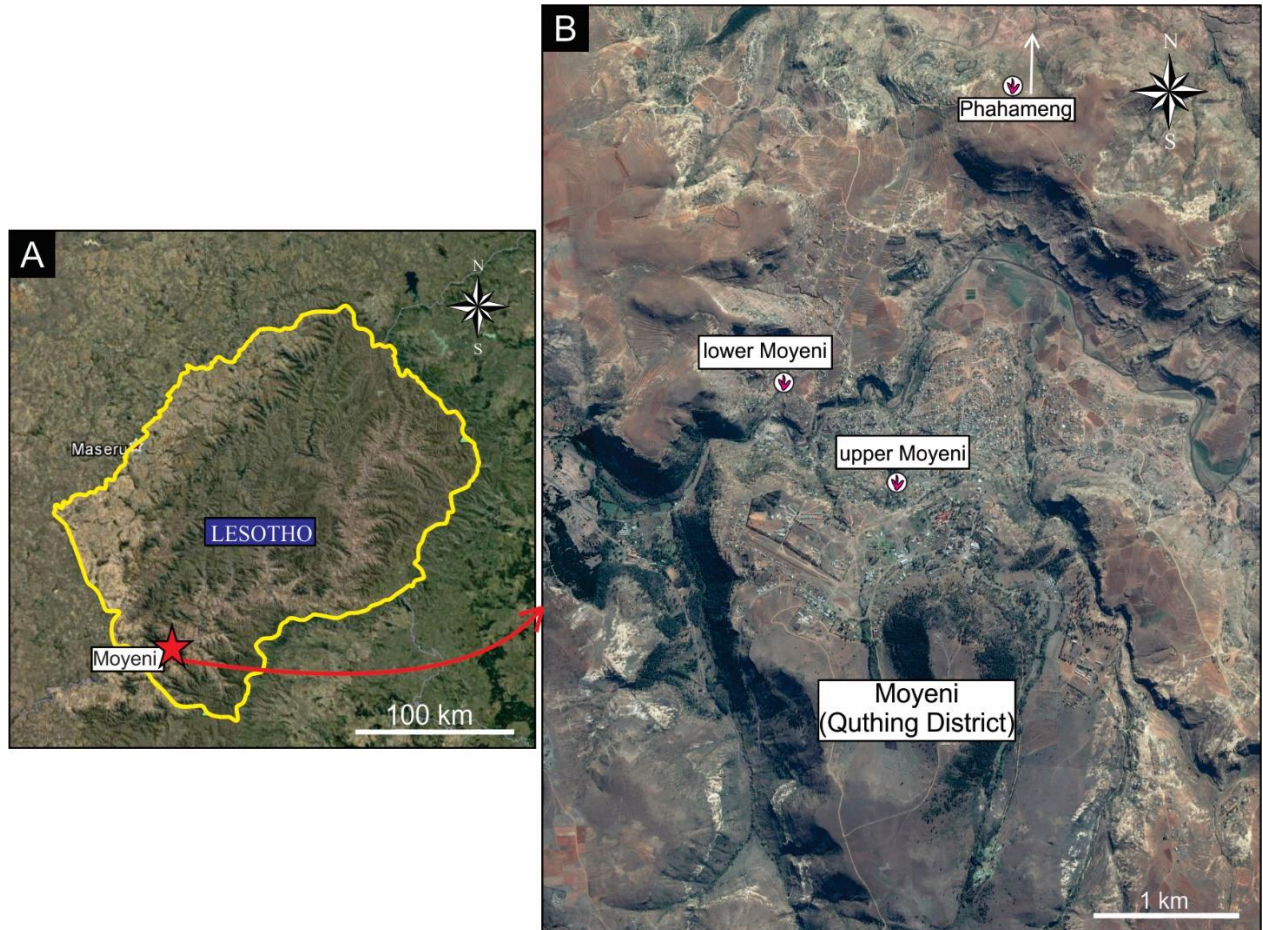


Figure 2.1: Google Earth satellite images showing: (A) the southern African Kingdom of Lesotho and the study site of Moyeni, located in the south western region (marked by a red star). (B) Higher resolution satellite image of Moyeni (Quthing District) with the locations of the 3 key ichnosites namely, lower Moyeni, upper Moyeni (labelled and marked by a dinosaur track) and Phahameng further north on the outskirts of Moyeni (direction of site is pointed by white arrow).

2.2 Sedimentary Facies Analysis

2.2.1 Sedimentary Facies

In order to provide a detailed sedimentological description and interpretation of the lithologies of the different formations in the study area, the method of sedimentary facies analysis was

applied to the outcrops of the uEF, Clarens Formation and the sandstone interbeds within the Barkly East Formation. This method forms the basis for the interpretation of sedimentary processes and depositional sub-environments, thus is fundamental for palaeoenvironmental interpretation (McIlroy, 2008; Walker, 1984).

The concept of sedimentary facies can be described as the product of a sedimentary process that occurs within a depositional environment (Boggs, 1995). It is implied in the concept that different facies represent different ancient depositional processes, thus the properties of the sedimentary rocks are in turn a reflection of the conditions of the ancient depositional sub-environments, that prevailed in each depositional setting (Boggs, 1995). These properties include texture, sedimentary structure and composition of the rock as well as geometry, palaeo-current patterns and fossil content. Thus, different rock units are distinguishable from the adjacent or associated rocks based on its sedimentary facies (Selley 1970; Boggs, 1995).

When conducting sedimentary facies analysis, a hierarchal approach is followed i.e. there is a classification of the sediments from micro- and meso-scale (individual facies of the rock units) to mega-scale (sedimentary successions) (Figure 2.2; Heinz and Aigner, 2003). Furthermore, the lithofacies is objectively described and clearly separated from interpretations (Walker, 1984). The classification of the lithofacies in this study is based on Miall (1978, 1985, 1996) in which the sedimentary features are described based on the grain size and sedimentary structures or features. The main lithofacies which were identified in this study are shown in Table 2.1. The grain size variations within the units of a section were determined for each lithology of the different formations. The sedimentary structures (i.e. horizontal laminations, cross bedding, ripple-cross laminations, trough cross-beds, massive etc.) and geometry of the individual units was also identified and described. These lithofacies are coded with specific facies codes (e.g., Sm “S” for “sand” and “m” for “massive”; Table 2.1). The sedimentary features give insight into the energy level, flow direction of the transportation medium and more specifically the mode of transport. In addition, post depositional features were also established such as desiccation cracks and carbonate nodules within palaeosols,

which can be used to deduce the climatic conditions. From these descriptions, lithofacies associations are produced by grouping together lithofacies which form together under particular conditions and represent the same sub-environment of the overall depositional setting. Finally, interpretations of the processes which operated together to form the particular facies and respective facies associations, are made (Figure 2.2).

2.2.2 Facies Models

The interpretations of the depositional environments are reconstructed with the use of facies models. These facies models are schematic block diagrams and/or visual representations and can provide the reference framework needed for the interpretation of depositional environments. Facies models are generally based on modern day sedimentary environments and sedimentary process, as it is assumed that natural laws remain constant in space and time, thus, processes which are observed in the present day can be used to explain features within the rock record (Boggs, 1995). However, it is important to note that sedimentology and sedimentary processes are highly variable, and very similar sedimentary facies can form in a range of different depositional environments. Therefore, facies models are generalisations of particular depositional settings and should not be strictly followed, hence such facies models only aid the palaeoenvironment interpretation (Walker 1992; Boggs, 1995). Palaeoenvironmental interpretations are improved if facies associations are accurately studied in conjunction with the individual sedimentary facies (Boggs, 1995). Therefore, the study of the entire stratigraphic succession as well as the lateral variation of the facies can contribute as abundantly to the palaeoenvironment interpretation as the characteristics of the individual facies themselves (Boggs, 1995).

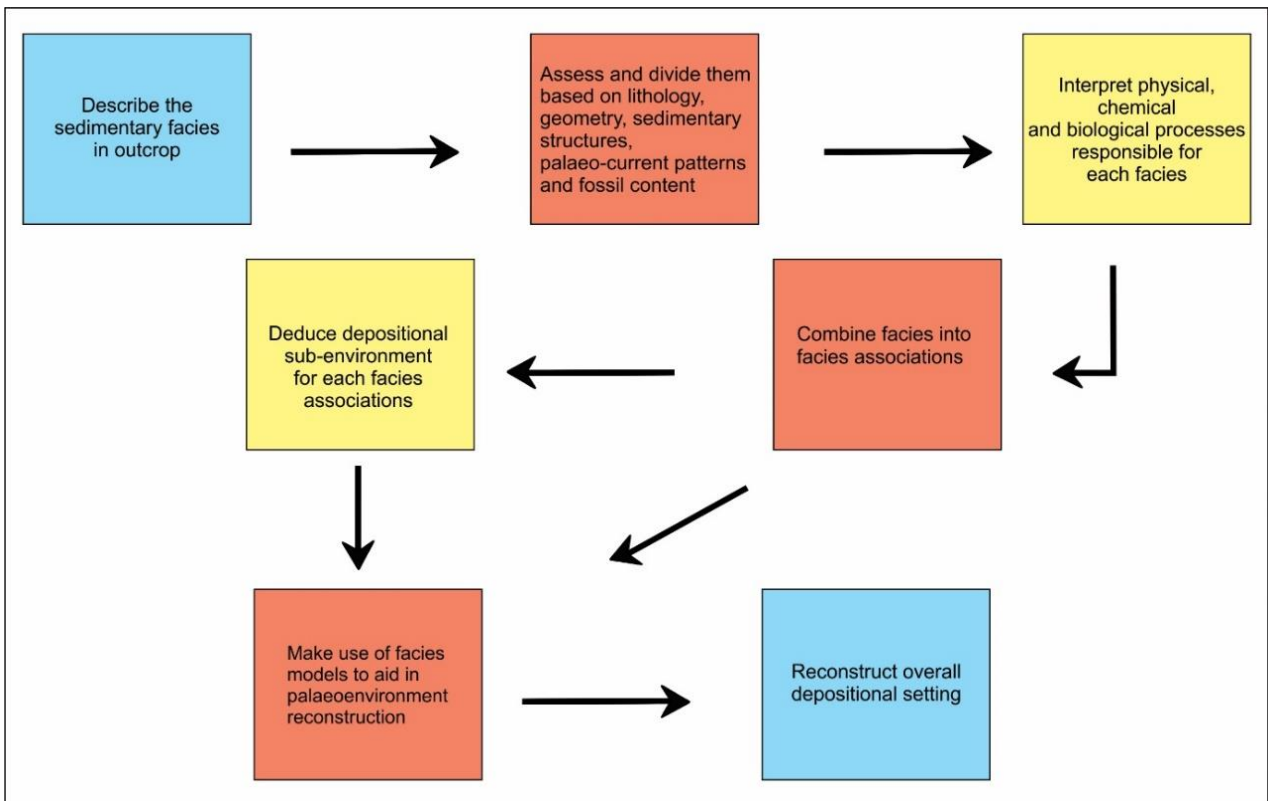


Figure 2.2: Flow diagram illustrating the hierarchical approach in the steps followed systematically for facies analysis. From describing the individual facies to interpretation of the facies associations and finally the overall depositional setting (modified after Walker, 1984).

Table 2.1: Lithofacies applied in this study for sedimentary facies analysis (modified after Miall, 1978, 1985, 1996).

Facies Code	Lithofacies	Sedimentary structures	Interpretation
Gmm	massive, matrix-supported gravel (breccias)	none	debris flow deposits
Gcm	massive, clast-supported gravel (conglomerates)	none	gravel bars, debris flow deposits
Gt	massive or crudely bedded gravel	trough cross-beds	minor channel
Gp	gravel, stratified	planar cross-beds	linguoid bars or deltaic growths from older bar remnants
St	gravel, stratified	solitary or grouped trough cross-beds	sinuous-crested dunes (lower flow regime)
Sp	sand, medium to very coarse, may be pebbly	solitary or grouped planar cross-beds	transverse bars, straight-crested dunes (lower flow regime)
Sr	sand, very fine to coarse	ripple-cross laminations	ripples (lower flow regime)
Sh	sand, very fine to very coarse	horizontal laminations	planar bed from fast, shallow flow (upper flow regime)
Sl	sand, fine	low angle (<10°) cross-beds	wash-out dunes, antidunes
Sm	sand, very fine to medium	massive	deposition in hyperconcentrated flows and/or destruction by bioturbation etc.
Fl	sand, silt, mud	fine laminations, very small ripples	overbank or waning flood deposits in standing bodies of water or abandoned channels
Fm	mud, silt, clay-sized particles	massive, desiccation cracks, pedogenically altered.	overbank, waning flood deposits or drape deposits

2.3 Ichnological Analysis

Ichnological studies (i.e. the study of trace fossils) is regarded as the interface between sedimentology and palaeontology. The method used in ichnological analysis is similar to that of sedimentary facies analysis which involves the identification and descriptions of ichnofacies i.e. the assemblage of trace fossils. The ichnofacies model, which was proposed by Seilacher (1964, 1967) and has subsequently been refined over the years in a series of studies (e.g., Bromley and Asgaard, 1993; Gibert et al., 1998; Buatois et al., 2002) is vital to majority of the palaeoenvironmental studies of trace fossils, especially in marine environments (McIlroy, 2008; Buatois and Mangano, 2007). It is built upon the premise that organisms will produce a similar range of traces in response to the environmental conditions (McIlroy, 2008).

Ichnofacies can be used to understand the parameters needed in a specific depositional environment to produce particular ichnofacies but are not necessarily direct indicators of sedimentary settings (Buatois and Mangano, 2007; MacEachern et al., 2012). Thus, the main objective is the collection of detailed palaeoenvironmental data through the integration of sedimentological and ichnological studies. As in the case of sedimentary facies analysis, ichnofacies models are also produced and serve as a framework for interpretation or for purposes of comparison (Buatois and Mangano, 2007). When combining sedimentological and ichnological data the ichnofacies can be used to understand the general character of the depositional environment as well as discern the palaeoecology. Since these trace fossils are found *in-situ*, integration of identifying particular track assemblages and sedimentary facies also offers understanding into the trackmaker and habitat relationship (Lockley, 1998). Ichnofossils, specifically fossilised tracks and trackways can also give insight into the behaviour and locomotion style of the ancient fauna. In the study however, the latter is not the main focus; here tracks are used for their palaeoecological messages, which can aid in palaeoenvironmental analysis and reconstruction.

In this study the three key ichnosites were recognised, the different ichnotaxa at each site were documented, categorised and all sites were put into sedimentological and stratigraphic context. The data collected include but are not limited to:

- Description of the lithologies and sedimentary structures at the ichnosites.
- Measuring the dimensions of the ichnofossils (i.e. length, width and pace of the tracks and trackways using a tape measure). The track length is measured from the base of the heel to the tip of digit III whereas the track width is measured from the furthest point on digit II to the furthest point on digit IV (Figure 2.3).
- The relative abundance of the various ichnofossil.
- The relationship between the different trace fossils.
- Classification of the trace fossils.

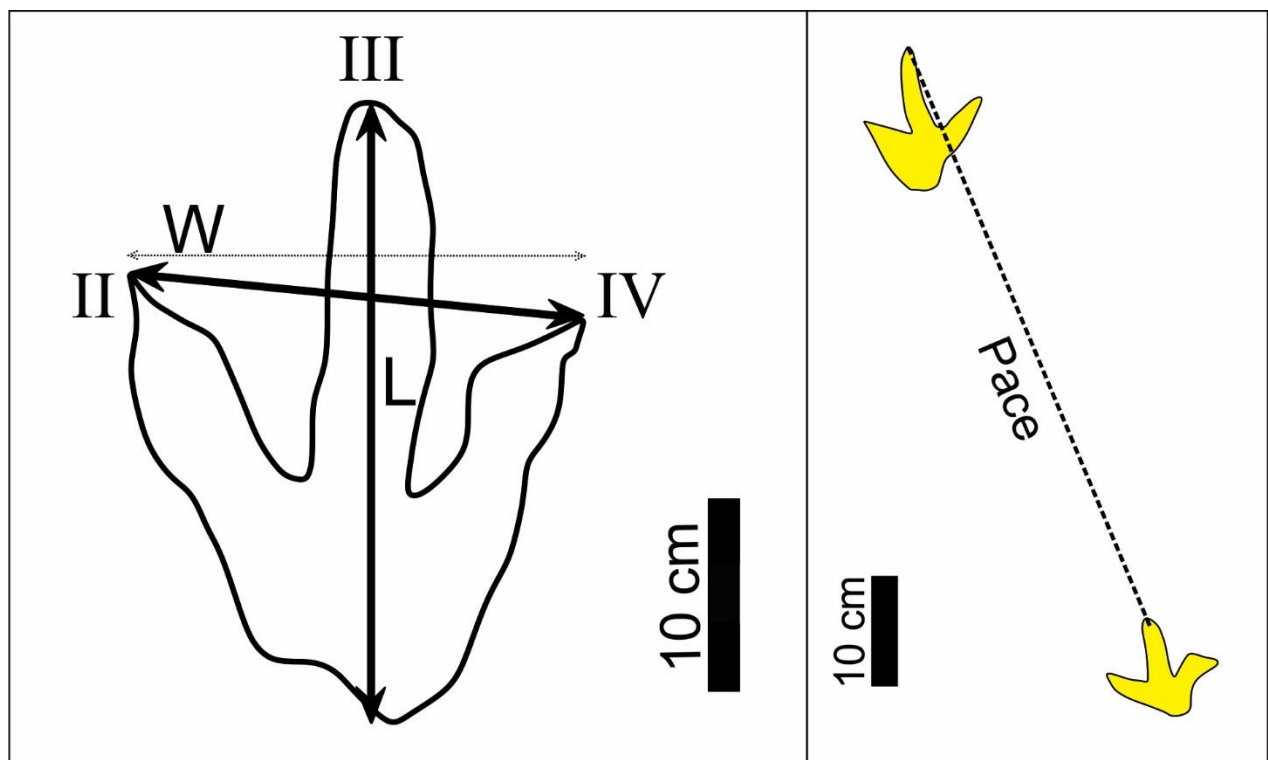


Figure 2.3: Measurements taken on a tridactyl (3-toed) track. L- foot length measured from digit III to heel and W- foot width measured from digit II to digit III. Pace measured between digits III of respective tracks. Note the Roman Numerals II, III, IV depict the digits 2, 3 and 4 respectively of the track.

2.4 Geological mapping

The main approach to geological mapping is highly practical and is done to obtain and provide insight about the geology by showing the distribution of the rock units and the geological structures across the study area. This is done through direct observations and in some cases also by collecting rock samples. Geological mapping involves geological reconnaissance which refers to the process of getting acquainted with the basic geological features of the study area prior to the field mapping. This was done by consulting available literature as well as older geological maps of the region (Quthing, 3027B). Geological maps form part of the foundation for explaining various geological formations and structures, thus certain parameters also need to be taken into consideration such as the scale of the mapping, which will ultimately impact the detail of the map.

The study region of Moyeni (Quthing District) was mapped across an area of 6 km x 5 km to a scale of 1: 20 000. The units mappable are those characterised as geological formations, are mappable over a large area and are distinguishable from one another based on their sedimentary features. The geological units and structural features were mapped in the field using traditional geological mapping techniques, which involved the traversing along a predetermined profile line and documenting on a base map the key stratigraphic and structural contacts. The base map is essential for geological mapping and thus is used as a reference. The main structural elements of the area were mapped and documented by traversing along the faults, documenting and quantifying the faults in terms of the strike, approximate length, direction trend and displacement.

To assess the thickness variation of the different formations, specifically in the Clarens Formation, GPS co-ordinates and the elevation above sea level at various points in the study area were also documented using a hand-held GPS (Geographical Positioning System) specifically a Garmin GPSmap 62s which uses a barometric altimeter. The field data was combined with both CNES/Airbus satellite imagery obtained from Google Earth as well as the

georeferenced topographical map of Quthing (3027BC27; scale 1: 100 000). Ultimately the produced geological map, a composite map of the Google Earth image, georeferenced topographic map and the traced over outcrops, contacts and structural elements of the uEF, Clarens Formation and the lowermost Drakensberg Group, illustrates the key geological features of the Quthing area and documents the spatial and temporal relationships of the major stratigraphic units and their key structural elements. Each formation is identified and a code or abbreviation for the name of the rock unit is used e.g. “CF” for “Clarens Formation”. Structural symbols are also plotted onto the map which highlight the strike and direction trend of the faults.

2.5 Petrographic analysis

Petrography was the only method used to further investigate the samples collected from the field. All sample preparation (e.g., cutting hand specimens into thin sections) and laboratory analysis for the petrographic analysis were conducted in the Department of Geological Sciences at the University of Cape Town. Six samples were collected for petrographic analysis: one from the uEF, three from the Clarens Formation, and two from the sandstone interbeds within the Barkly East Formation. These specific samples were collected in order to see the textural variation on a microscopic scale of the different sandstones beds within the study area. The rocks were cut into standard thin sections that are 75 mm in length, 25 mm in width and 30 μm thick. Petrographic analysis was performed using transmitted light microscopy on the sections and were examined under a Leica transmitted light microscope which has a 20 mm field of view, with 02.5x/0.10, 10x/0.25 and 40x/0.65 objectives. This was done to gain insight into the mineralogical composition as well as the textural properties of the samples. These include but are not limited to the grain size, sorting, roundness, sphericity and matrix content of the sandstone (for raw data, see Appendix Table 1A). The thin section descriptions of the sedimentary rocks were based on semi-quantitative visual estimates such as comparison charts for the roundness, sorting, sphericity, etc (Figure 2.4). Petro-

micrographs were also taken of each sample at 10x magnification. Comparisons were made between the sections in the study area as well as to previously published datasets from the upper Karoo Supergroup (e.g., Hanson et al., 2009). These comparisons not only help distinguish the sandstones from the different formations, but also allow for a better understanding of the dynamics of the sedimentation as well as the nature of the source rocks that supplied sediment to the study area.

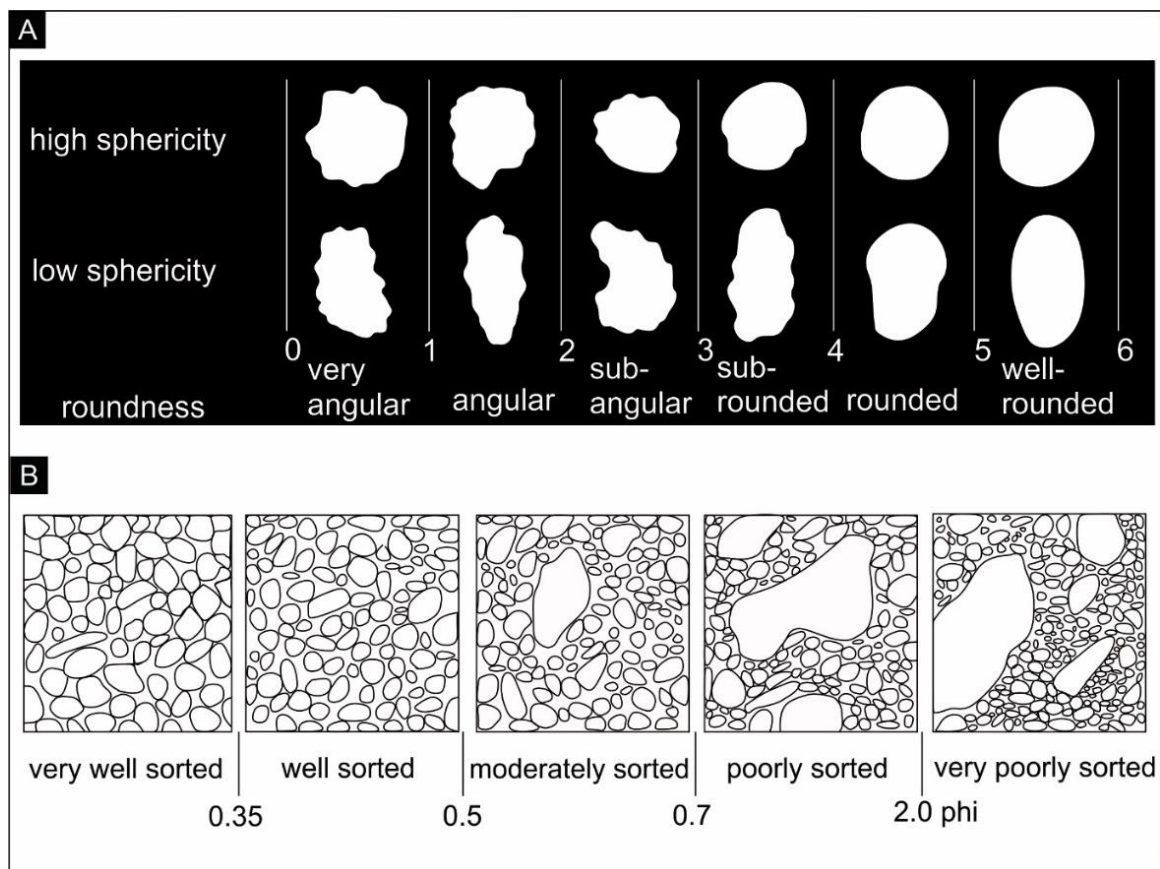


Figure 2.4: Comparison charts used for the visual estimates of (A) roundness, sphericity and (B) sorting of each sample (modified after Terry and Chilingar, 1955).

3 Results

3.1 Geological Map of Moyeni

The geological map of Moyeni, illustrated in Figure 3.1 and in Appendix Figure 1A, covers an area of ~ 5 x 6 km. The map shows the spatial distribution of the uEF, Clarens Formation and the lowermost Drakensberg Group, which are also displayed in the general sedimentary log (Figure 3.2). It is important to note that these units have significant lateral thickness variation in the study area. This is especially pronounced for the Clarens Formation, which varies in thickness from ~ 10 to 90 m. All Moyeni strata have gently north-dipping to horizontal attitude, and limited and localized deformation. The main structural features of interest are ~ENE-WSW trending normal faults and a breccia facies, which are discussed below in section 3.5 “Structural geology near Moyeni” of this chapter.

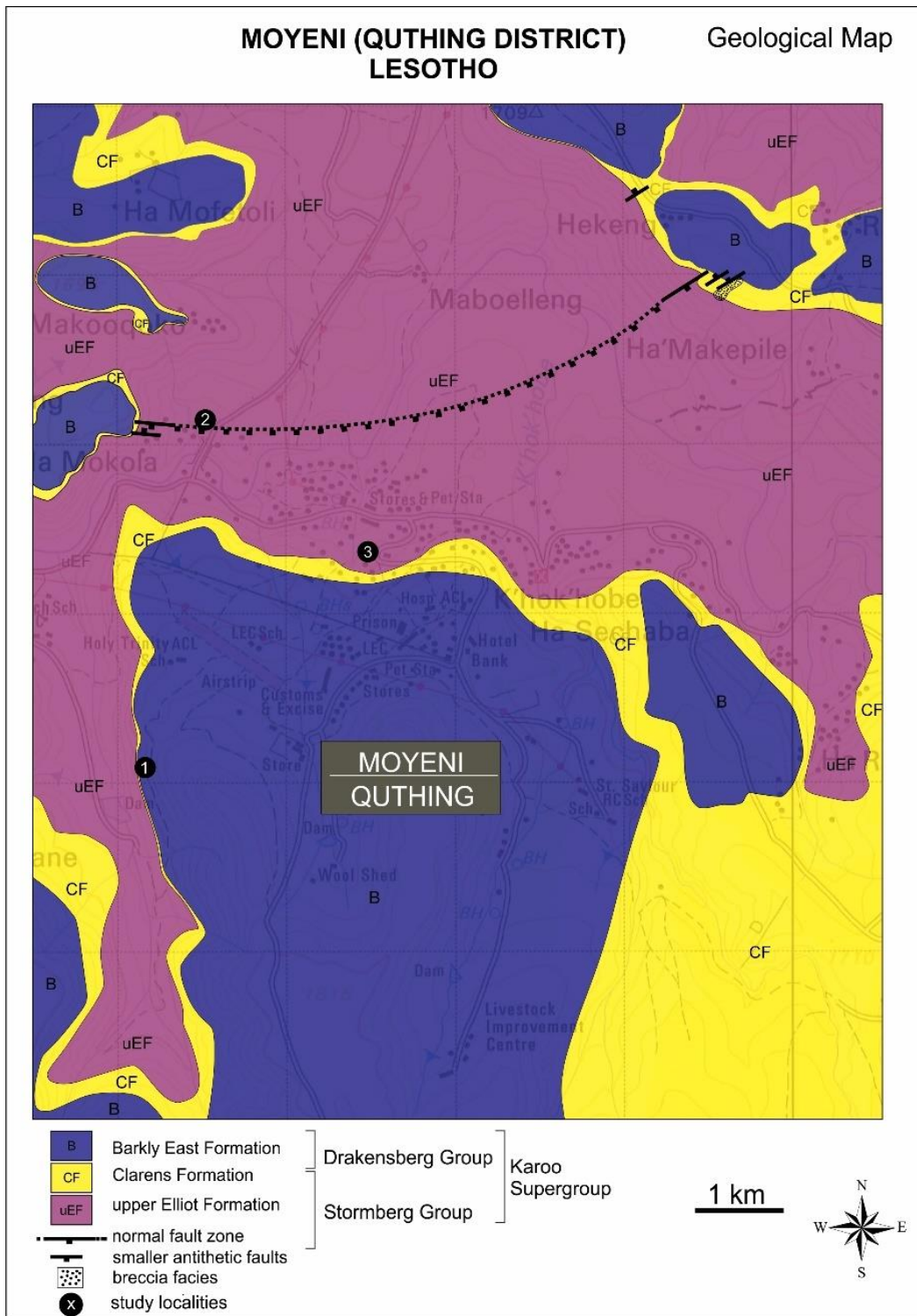


Figure 3.1: Geological map of Moyeni (Quthing district) in southwestern Lesotho. See Appendix Figure 1A for the A3 size version of the map. The main study localities are also labelled; (1) pillow lava succession, (2) lower Moyeni ichnosite and (3) upper Moyeni ichnosite.

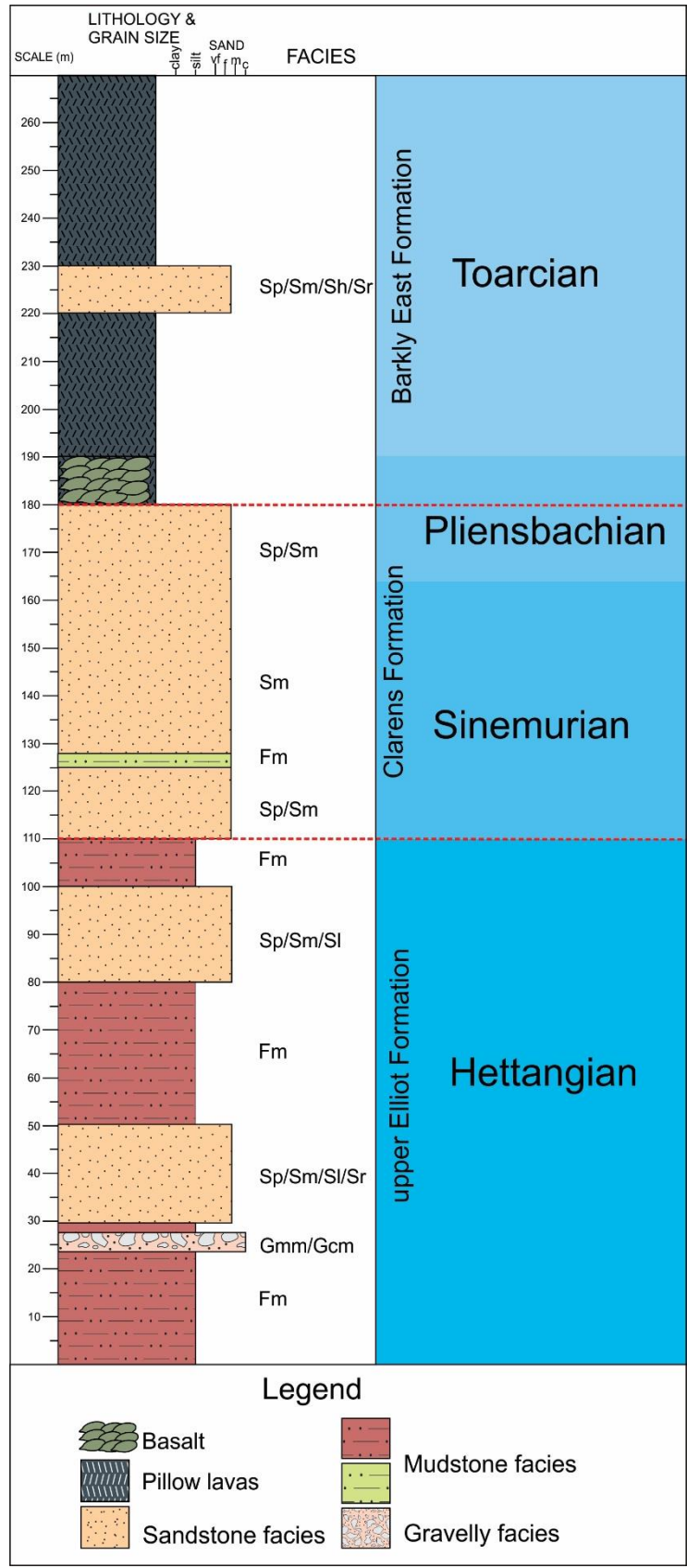


Figure 3.2: General sedimentary log illustrating the lithologies of the upper Stormberg Group (upper Elliot Formation and Clarens Formation) and the lowermost Drakensberg Group (Barkly East Formation) in Moyeni. See Table 2.1, for facies codes.

3.2 Description of the main stratigraphic units and their lithofacies assemblages

The study area in and around Moyeni exposes relatively high-quality outcrops of the upper Elliot (uEF), Clarens and Barkly East Formations. The former two comprises sedimentary rocks and belong to the Stormberg Group, whereas the latter contains igneous rocks as well, which are mostly basaltic lava flows, dolerite dykes and sills, and belong to the lowermost Drakensberg Group. Sedimentological, ichnological, stratigraphic and structural features identified within these Karoo rocks are presented in the following sections and in Figures 3.3-3.25.

3.2.1 The upper Elliot Formation (uEF)

In the immediate vicinity of Moyeni, the uEF is well exposed. These rocks are laterally extensive for tens of kms and can be studied in natural outcrops in the valley as well as the mountain slopes around the town. The uEF is the oldest exposed rock formation in Moyeni and is stratigraphically below the Clarens Formation. The general regional thickness of the uEF is not possible to determine due to the fact that both the upper and lower boundaries need to be recognised, and at Moyeni the lower contact of the uEF is not exposed. The succession of the uEF rocks consists of red-maroon or green-grey mudstone, light-red to dark-purple sandy siltstone and pale-brown to beige sheet-like sandstone bodies as well as rare gravelly deposits occurring as breccias and conglomerates (Figures 3.3- 3.6). These sedimentary facies were assessed in detail and are described and discussed below.

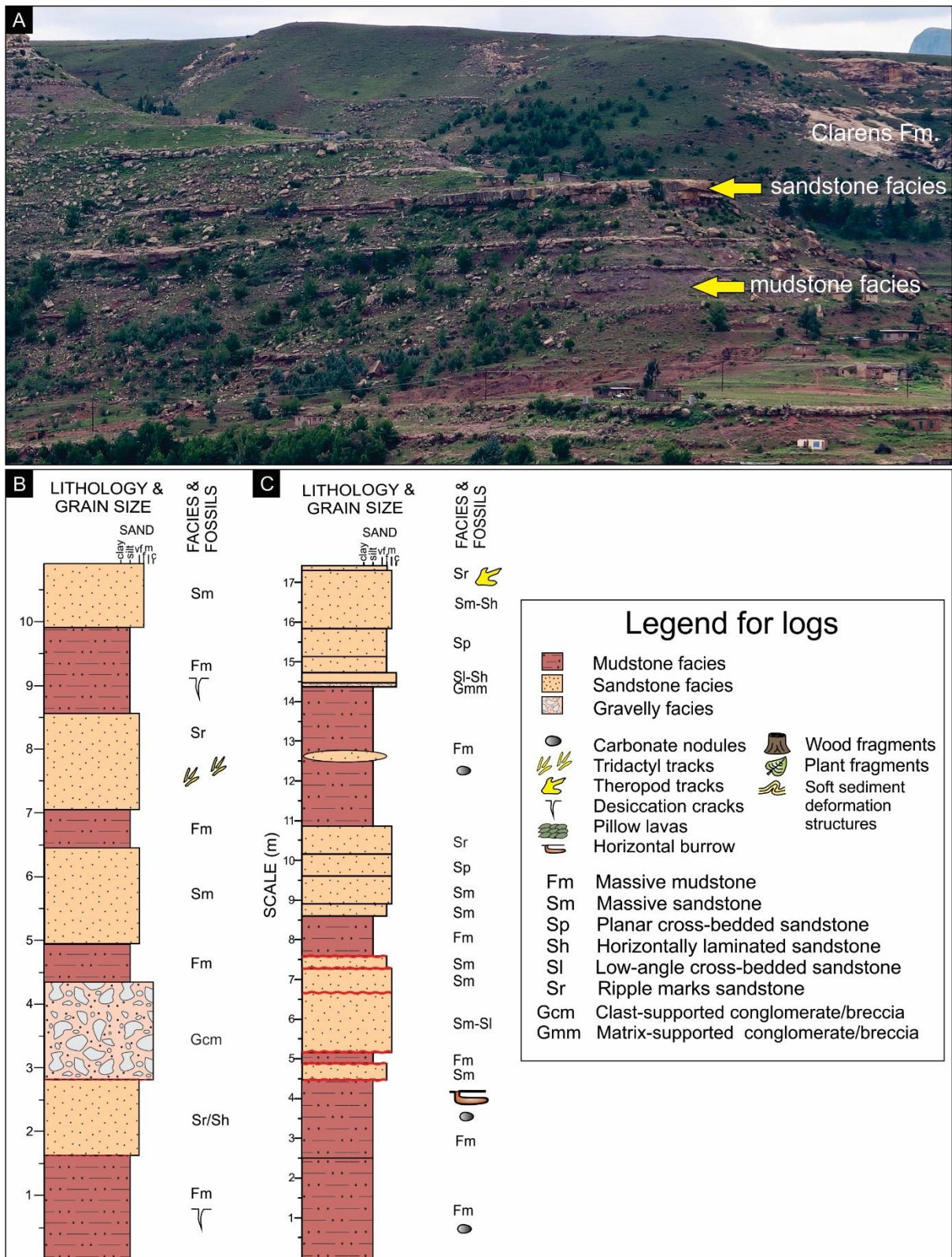


Figure 3.3: (A) Outcrop view of the uEF in central Moyeni illustrating the laterally continuous brown-beige sandstone benches and the purple-red mudstone facies (pointed out by yellow arrows). Sedimentary logs of two sections of the uEF at lower Moyeni (B) and upper Moyeni (C), which are stratigraphically 65 m apart. The logs display the main sedimentary facies characteristics of mudstone, sandstone and rare gravelly facies of the uEF.

3.2.1.1 Mudstone Facies Assemblage

One of the striking features of the uEF are the prominent red-maroon mudstones as well as the dark purple sandy siltstones, which make up most of the basal units of the uEF (Figure 3.3B & C). The mudrocks are intercalated with the fine-grained sandstone units that are >10 m in length and 1.5 m thick. The thickness of the mudstone units range between 0.4 m and >10 m, and are laterally continuous for tens of km. The lower and upper bounding surfaces of the mudstones appear to be relatively sharp with occasional irregular surfaces.

The predominant lithofacies are the massive (Fm) or faintly horizontally laminated (Fl) mudstones (Figure 3.4). Post-depositional features such as desiccation cracks appear frequently within the mudstones (Figure 3.4C & D). The largest desiccation cracks noted in the field have a width and depth of 20 cm and >150 cm, respectively (Figure 3.4C). The fine-grained sandy siltstone (Fm facies) are also massive and contain numerous *in-situ* pedogenic carbonate nodules (Figure 3.4E & F), which are 2-10 cm in diameter and are generally less abundant towards the base of the uEF. The siltstones also host fine-grained sandstone lenses, which have a maximum thickness of 50 cm and are 2 m in length. Furthermore, the relatively coarser grained sandy siltstone hosts various bone fossils, bioturbation and ichnofossils such as horizontal burrows. The latter is described in detail in the 'Ichnology of Moyeni' section.

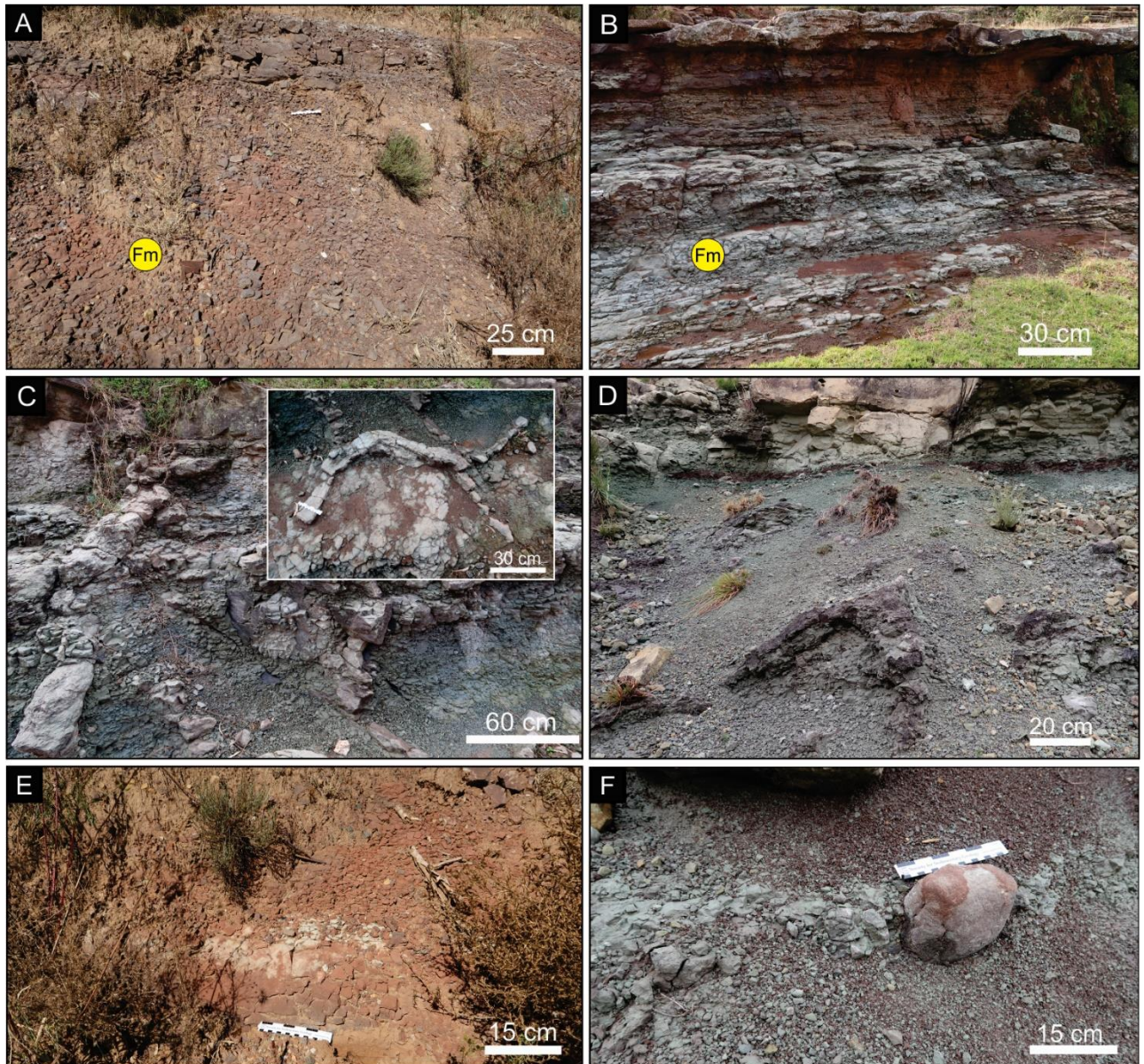


Figure 3.4: Mudstone facies of the uEF displaying: (A) red to maroon-purple, massive mudstones forming the basal units of the uEF. (B) Massive green-grey mudstone layers, outcropping in the western part of Moyeni (Fm – massive mudstone). Desiccation cracks found in western (C) and eastern (D) region, respectively. The giant desiccation cracks in C are 20 cm wide (inset image) and > 150 cm deep. (E & F) Calcareous siltstone with *in-situ* carbonate nodules.

3.2.1.2 Sandstone Facies Assemblage

The sandstone facies assemblage of the uEF is characterized by sandstone bodies, which are either very fine- to fine-grained or fine- to medium-grained and brown-yellow to beige-white in colour (Figure 3.5). These sandstone units outcrop as prominent benches within the uEF and range in thickness between 1 m to 1.5 m, with thinner sandstone bodies of 30 cm to 70 cm also occurring locally (Figure 3.5A-C). The sandstone bodies become more prominent with increasing stratigraphic height, closer to the Elliot-Clarens contact and are lateral extensive for tens of metres with some localised isolated units. The geometry of the sandstones appears to be either as sheet-like or channel-shaped. Lenticular shaped bodies with a maximum thickness of 0.5 m and length of 2 m, also occur locally (Figure 3.5A inset image).

The lower and upper bounding surfaces of the sandstone bodies are irregular in some regions of the uEF and are relatively sharp in other parts of the valley. The sandstones show a variation of sedimentary structures. Majority of the sandstone bodies are massive (Sm) while some have ripple-cross laminations, ripples marks (Sr), low-angle planar cross-bedding (Sl) (Figure 3.5D & E) and rare trough cross-bedding (St).

Ichnofossils within the sandstone facies assemblage are vertebrate tracks and trackways as well as invertebrate trace fossils. Associated with the ichnofossils, microbial matted textures are also present on upper bedding planes of sandstone units. Detailed descriptions of these ichnofossils and associated sedimentary structures are discussed in the 'Ichnology of Moyeni' section.

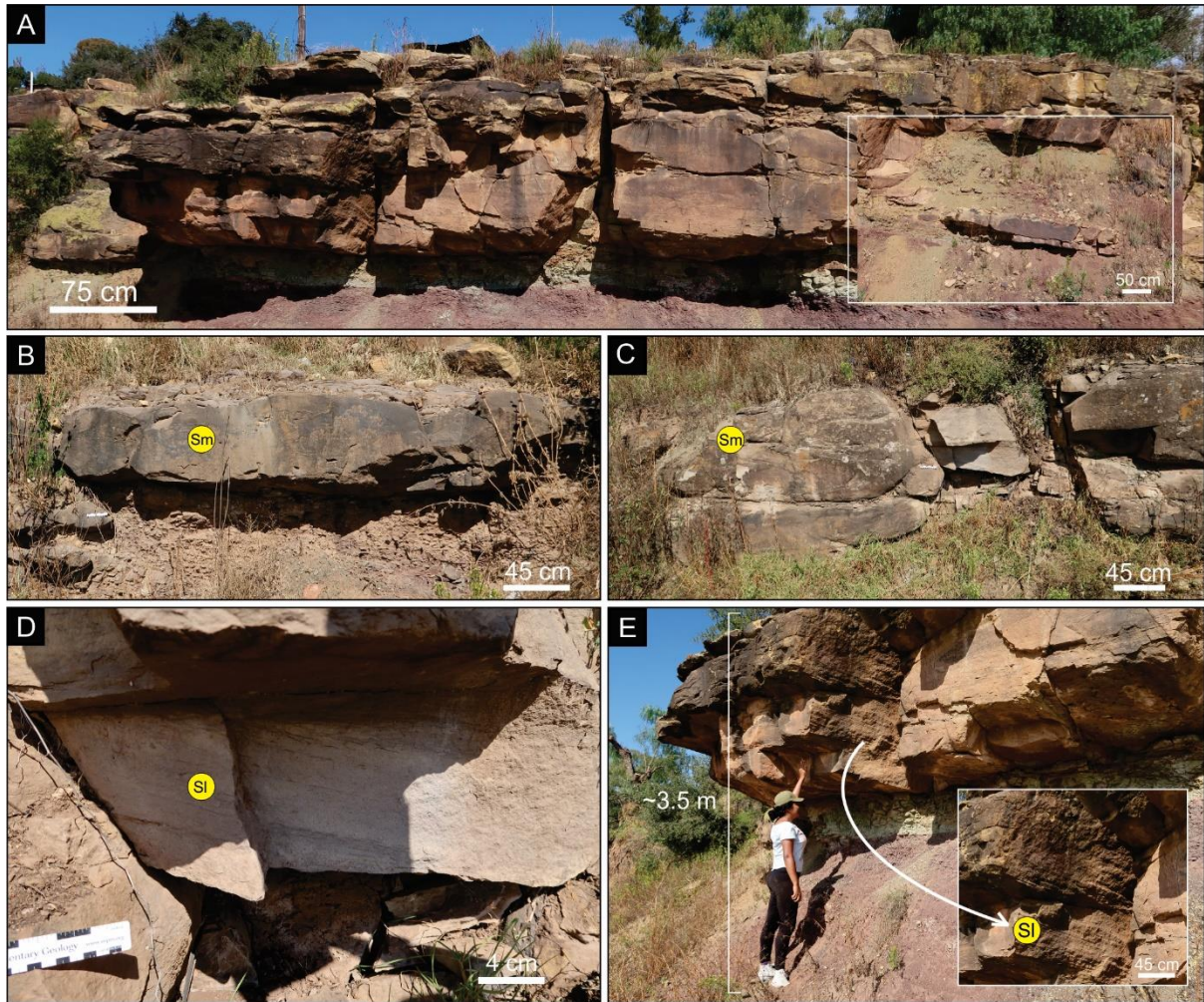


Figure 3.5: Sandstone facies assemblage of the uEF showing: (A) very fine- to fine-grained and fine- to medium-grained sandstone layers, which show an upward-thinning and fining trend, and terminate into ripple marked surfaces (also see sedimentary log, Figure 1.3B). Inset shows a sandstone lens that is up to 0.5 m thick. (B & C) Massive fine- to medium-grained tabular sandstone units. (D & E) Low-angle planar cross-bedding within a fine- to medium-grained sandstones. See Table 2.1 for facies codes.

3.2.1.3 Gravelly Facies Assemblage

Gravelly facies assemblage (Figure 3.6), including conglomerates and breccias, is a minor component of the uEF at Moyeni. The conglomerates (Gmm) are generally poorly sorted and matrix-supported. In the eastern region, an oligomictic paraconglomerate shows sub-rounded sand- and mudstone clasts within the abundant green mudstone matrix (Figure 3.6A). The clasts diameters range from <1 cm to a maximum of 8 cm. Vertically, the concentration of the clasts is variable with bands of high-clast-concentration alternating with bands of more

scattered clasts (Figure 3.6B). This banding defines a crude bedding in these paraconglomerates.

In the western region, breccias (Gcm) also occur and are mainly clast-supported with sub-rounded to sub-angular mudstones chips as well as very fine-grained sandstone clasts, with diameters ranging from 1 to 5 cm (Figure 3.6C and D). Some of the sandstone clasts also preserve rare mm-scale ripple cross-laminations (Sr).

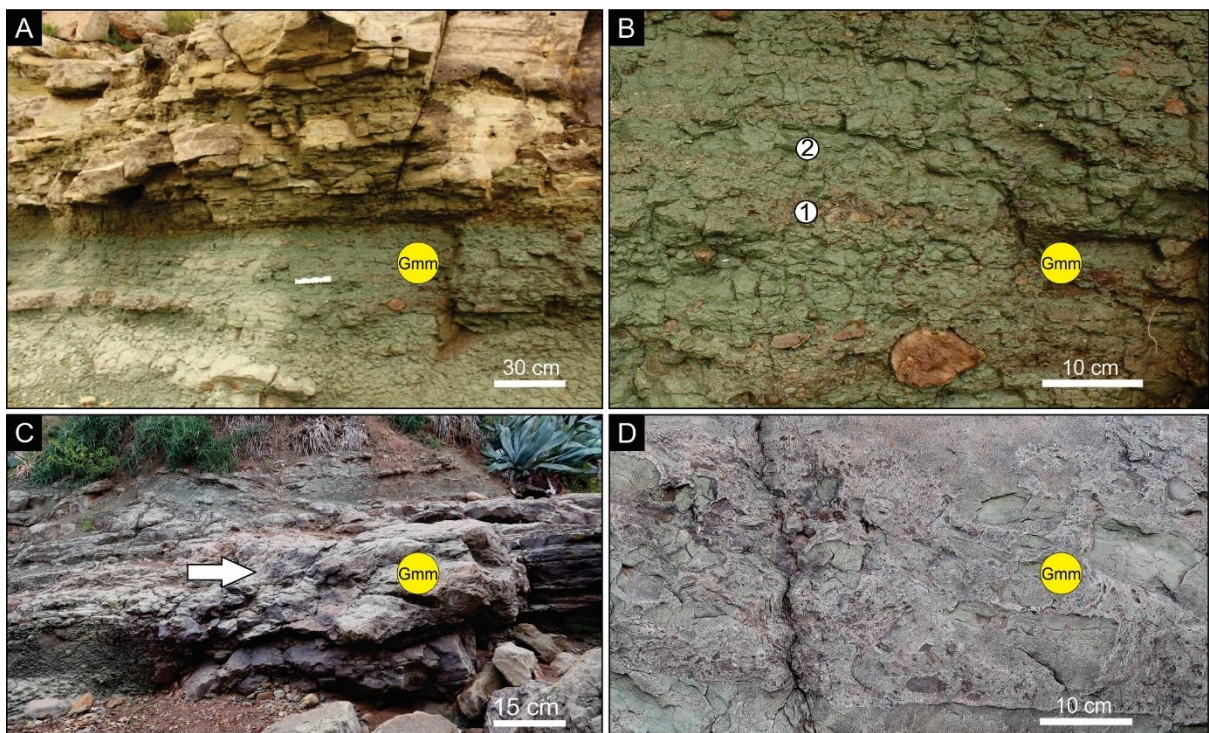


Figure 3.6: Gravelly facies assemblage of the uEF from east (A & B) and west (C & D) of Moyeni, showing variation of facies Gmm: (A) oligomictic paraconglomerate with (B) rounded to sub-rounded clasts, ranging between 1 and 8 cm and the alternating “bands” of concentrated clasts and scattered clasts, marked by numbers 1 and 2, respectively. (C) Massive oligomictic orthobreccia with (D) sub-rounded to sub-angular mud- and sandstone clasts.

3.2.2 The Clarens Formation

The Clarens Formation in and near Moyeni is dominated by fine- to medium and medium- to coarse-grained sandstone units, which are commonly cliff forming and can be traced regionally (Figure 3.7B & C). Intercalated with the lowermost sandstone units, mudstone layers are also present. The thickness of the Clarens Formation varies throughout the region from ~ 5 to 90 m (Figure 3.7). Overall there is an upward-coarsening trend in the vertical profile represented by the transition from the uEF to the Clarens Formation (Figure 3.7A), which is largely due to the presence of more mudstones in the uEF than the Clarens Formation. This trend is clearly evident in Moyeni, with the mudstones and finer-grained sandstones of the uEF, grading into the relatively more arenaceous Clarens Formation. This transition marks the gradational contact between the uEF and the Clarens Formation which occurs at irregular elevations throughout the study area (Figure 3.7A).

The vertical facies variation in the Clarens Formation allows the subdivision of the unit into three distinct lithofacies zones. The first distinct facies zone consists of sandstones that are fine-grained with subordinate interbeds of thinly-bedded mudstones. This facies is mostly within the lower part of the Clarens Formation as well as in some localised regions above the large-scale cross-bedded sandstones that are in upper part of the Clarens Formation (Figure 3.7D & E). The fine- to medium-grained sandstones appear to be cross-bedded (Sp) and are mostly channel-shaped or less frequently wedge-shaped. The upper and lower bounding surfaces of the sandstone bodies are relatively sharp with some undulatory surfaces. The second facies occur as fine- to medium and rare medium- to coarse-grained, beige-brown massive sandstones (Sm; Figure 3.7F). The uppermost, third facies zone in the Clarens Formation consists of sandstones with a thickness ranging between ~ 30 and 90 m. These cliff-forming sandstones are pale- white to cream- brown in colour, well-sorted and fine- to medium-grained (Figure 3.7G). The sandstones show a tabular geometry and are massive (Sm) or large-scale cross-bedded (Sp) (Figure 3.7G). The very large-scale cross beds have a set thickness of ~2 m with forests inclined at angles > 30° (Figure 3.7G). A detailed description of the uppermost Clarens strata and the Clarens-Barkly East contact is presented in the next section of this chapter. Similarly, to the uEF, the Clarens Formation also hosts ichnofossils (vertebrate tracks) as well as plant fossils, which are discussed in the sections below.

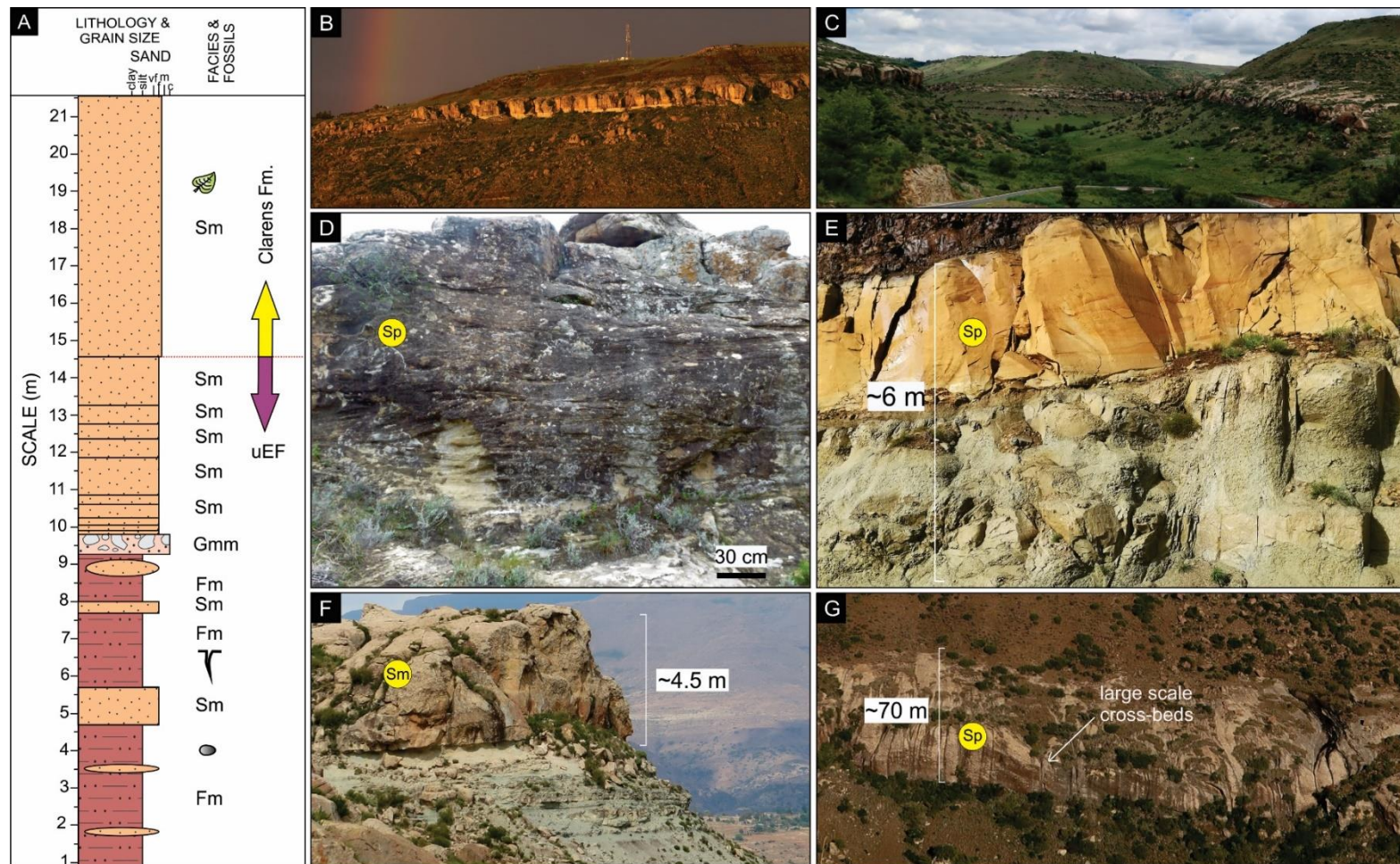


Figure 3.7: Overview of the Clarens Formation and its sedimentary features at Moyeni. (A) Sedimentary log capturing the gradual contact of the Clarens- Elliot Formations in eastern Moyeni. (B) Outcrop view of the prominent massive fine- to medium-grained cliff-forming sandstone units in the east. (C) Outcrop view of the lateral continuity of the Clarens Formation in southern Moyeni. (D) Medium-grained, planar cross bedding sandstone. (E) Outcrop of the tabular, fine- to medium-grained, planar cross-bedded sandstone overlying a finer grained, silty sandstone. (F) Massive fine- to medium-grained sandstone overlying the uEF mudstones. (G) Large-scale cross bedded sandstone. See Table 2.1 for facies codes.

3.2.3 The Drakensberg Group

In general, the Drakensberg Group in SW Lesotho consists of basaltic and subordinate andesitic volcanic rocks (Marsh and Eales, 1984). The Barkly East Formation is the lowermost unit in the Drakensberg Group and is well-exposed in the Moyeni region. It comprises basaltic lava flows and pillow lavas that are interbedded with sandstone layers. These rocks outcrop on the highest mountain tops and cap the uneven uppermost surface of the Clarens Formation near Moyeni (Figure 3.8). Overlying the Barkly East Formation, the Lesotho Formation of the Drakensberg Group, is not prominent within the Quthing valley but constitute the highlands that surround the study area further to the SE and E.

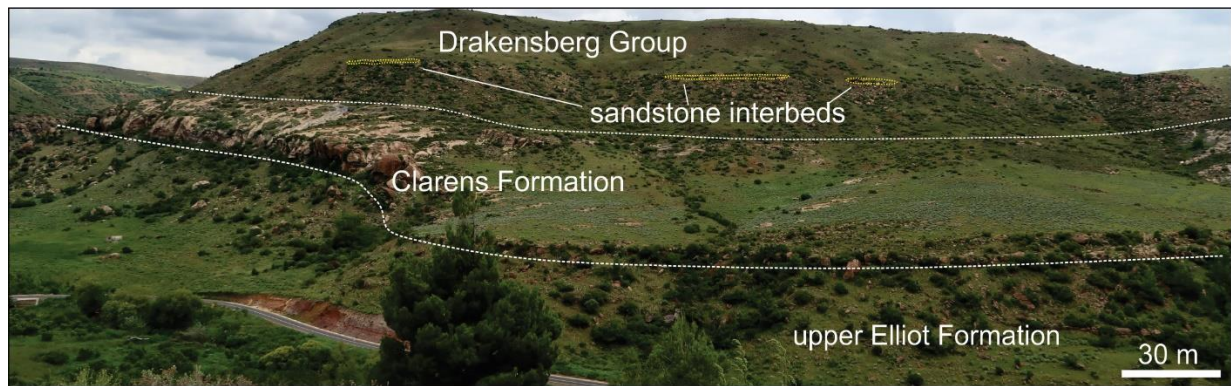


Figure 3.8: Overview of the lowermost Drakensberg Group (Barkly East Formation) and underlying formations of the upper Stromberg Group (uEF and Clarens Formation) in south-western Moyeni. Note the several sandstone interbeds within the Barkly East Formation.

3.2.3.1 Sandstone interbeds

Isolated by basaltic lava flows, the sandstone interbeds of the Barkly East Formation are up to 10 m in thickness, and < 400 m in length (Figures 3.8-3.10). These laterally discontinuous sandstone interbeds are easily accessible in the south-western region of Moyeni and are described in detail in this section (Figure 3.10).

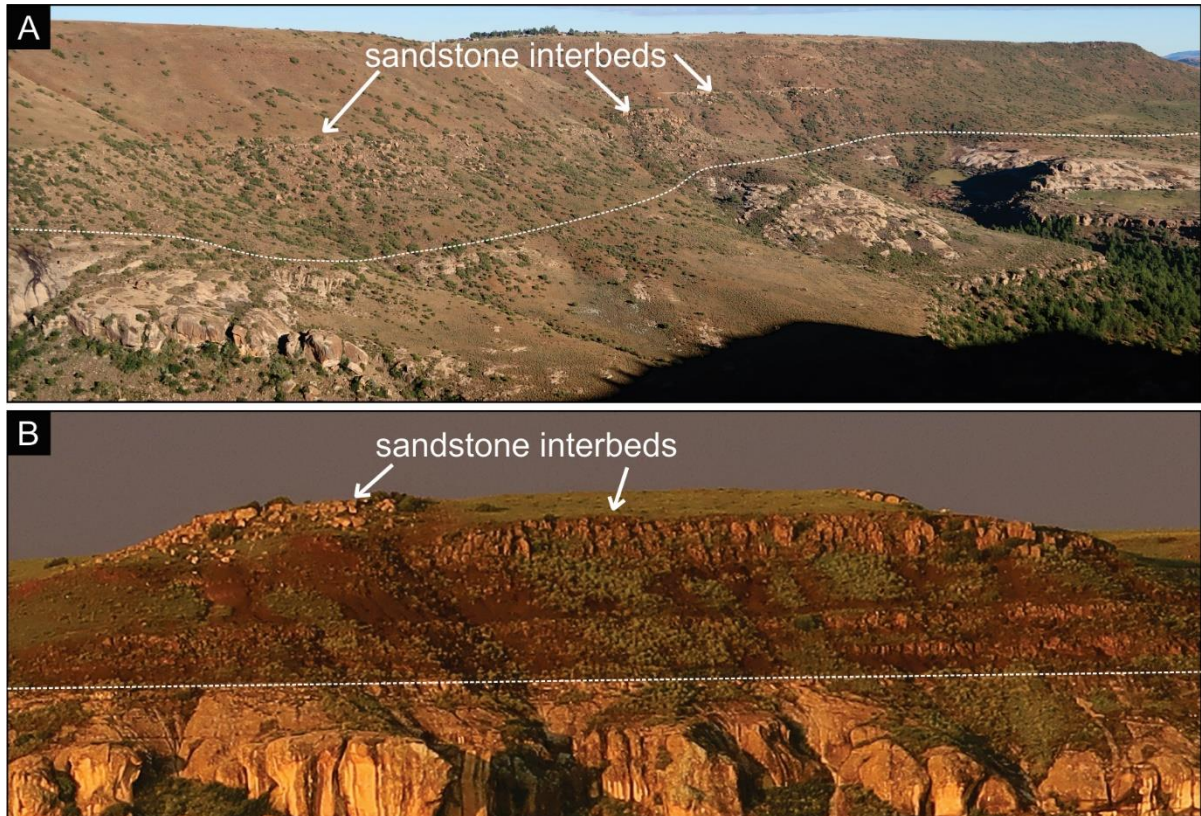


Figure 3.9: Overview of the sandstone interbeds within Barkly East Formation of the lower Drakensberg Group near Moyeni. (A) Photograph taken in the south-western region of Moyeni displaying discontinuous sandstone units. (B) Sandstone interbeds in the east of Moyeni. The contact between the Drakensberg Group and the underlying Clarens Formation is marked by a white dotted line for clarity.

These sandstone interbeds are fine- to medium-grained and vary in thickness from 40 cm to ~10 m (Figure 3.10). The sandstones also preserve a variety of primary sedimentary structures, which are illustrated in the sedimentary log shown in Figure 3.10A. The beds commonly display horizontal lamination (Sh) (Figure 3.10C), low angle cross-bedding (Sl) and planar cross-bedding with foresets of up to ~1m (Sp) (Figure 3.10B). Massive (Sm) layers are also common. The interbeds fine upward (Figure 3.10A) and at least locally, terminate in surfaces that are covered by symmetrical ripple marks (Sr) (Figure 3.10D & E). The sandstones also contain rare matrix-supported conglomerates (Gmm) (Figure 3.10A), which are made up of ripped up, sub-rounded mud chip clasts that are 2- 3 cm in diameter (Figure 3.10F). Desiccation cracks are also present (Figure 3.10G)

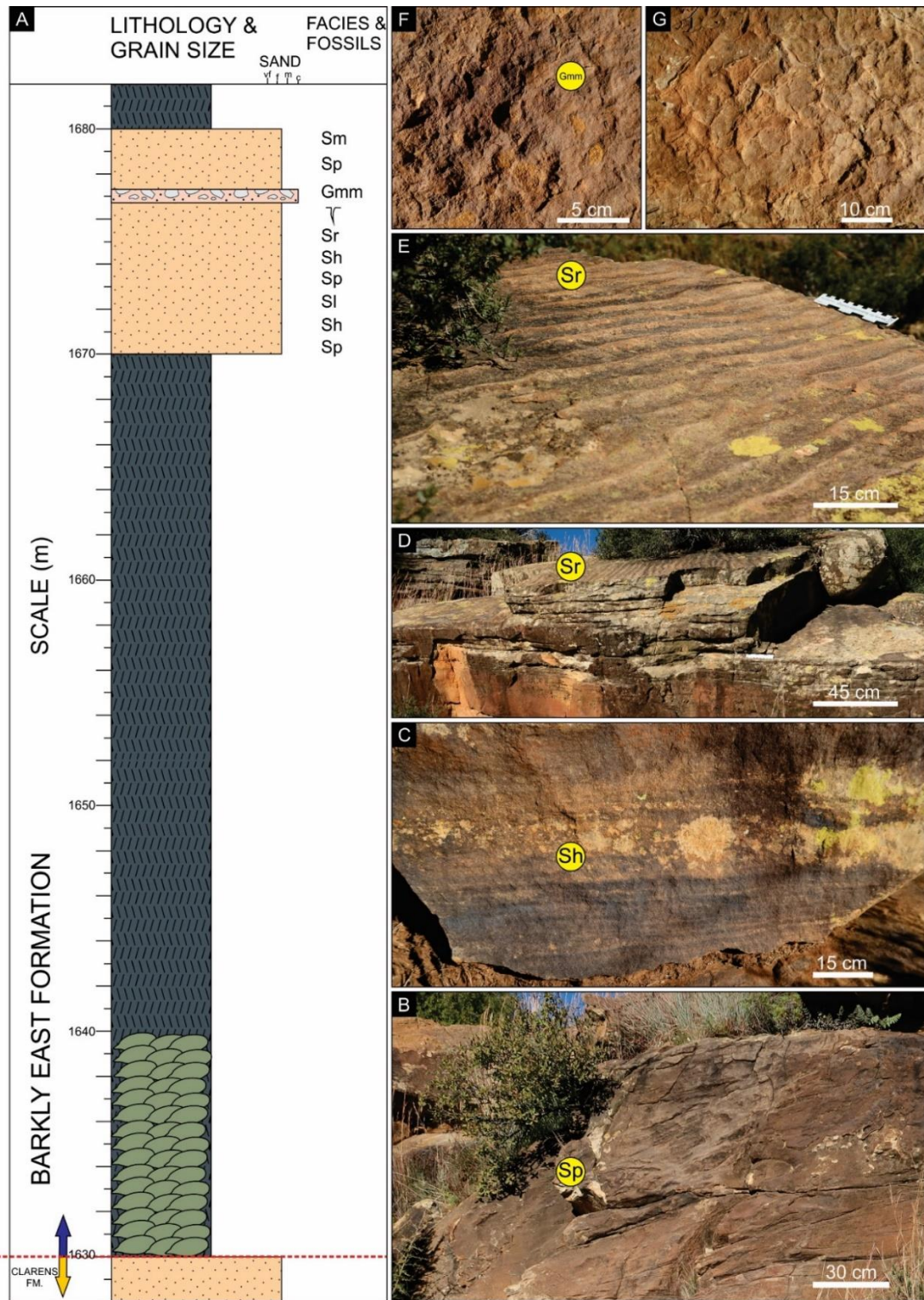


Figure 3.10: (A) Stratigraphic log of the lowermost Barkly East Formation (Drakensberg Group) in the south-western region of Moyeni showing the details of the lowermost, ~10 m thick sandstone interbed unit within the basalts. (B) Planar cross-bedded sandstone in the lower part of the sandstone interbed unit. (C) Fine-grained sandstone with horizontal laminations. (D & E) Sandstone layer within an interbed package that is ripple cross-laminated and terminates in symmetrical ripple marks. (F) Matrix-supported conglomerate with sub-rounded, rip-up mud chip clasts. (G) Desiccation cracks within sandstone package. See Table 2.1 for facies codes.

3.2.3.2 Pillow lavas

In southwestern Moyeni (Site 1; Appendix- Figure 1A), within the lowermost Barkly East Formation, massive sheet-like lava flows transition laterally into a 9.5-m-thick package of pillow lavas that extends laterally for ~ 120 m (Figure 3.12). Some pillows are ellipsoidal and spherical, however, most of the pillows are tube-like, elongate cylinders (Figure 3.11A-D), and show distinct layering or foreset beds, which dip to the south at ~35° (Figures 3.11A). The lava pillows are closely packed and vary in diameter from ~ 20 to ~ 50 cm. The longer lava tubes display maximum exposed length of ~4 m (Figure 3.11B). The pillow lavas also display a coarse-grained volcanoclastic sediment matrix (Figure 3.11B-D).

In this outcrop (Figure 3.13), the pillow lavas have a transitional contact with the underlying Clarens Formation and a sharp contact with the overlying massive sheet-like basalts (Figure 3.13A & B). The uppermost Clarens Formation underlying the pillow lavas at this locality shows some unique features, which justifies their detailed description in this section. The uppermost layers of the Clarens Formation comprise beige fine- to medium-grained massive (Sm) to cross-bedded (Sp; Figure 3.13E), mud-rich sandstone layers. The sandstones are overlain by a green-grey, locally laminated, mostly massive mudstone layer (Fm/FI) that is 10-50 cm thick (Figure 3.13A). This layer is followed by a ~2-3-m-thick, very fine- to fine-grained, orange-yellow, cross-bedded (Sp; Figure 3.13D) sandstone (Figure 3.13A & C) with localized soft sediment deformation structures (Figures 3.13A & 3.14C) and rare plant fragments (Figure 3.14). The latter sandstone layer is channel-shaped and has a gradational contact with sandstone matrix of the overlying pillow lavas and a sharp, erosive lower contact with the underlying mudstone (Figure 3.13C). Overlying this cross-bedded, channel-shaped layer, there is a localized, pod-shaped, 1.5-m-thick and 2-m-wide massive sandstone (Sm; Figure 3.13A) that preserves clusters of rounded to angular, poorly sorted mudstone clasts, fragmentary wood and plant fossils (Figure 3.14). The diameter of mudstone clasts ranges from 0.25 to 1 cm (Figure 3.14D), whereas the fossil wood and plant fragments range in length from 2 to 8 cm (Figure 3.14). The sandstone is overlain by a few-cm-thick mudstone layer that

is cut by polygonal network of sandstone-filled desiccation cracks (Figure 3.13A- inset image). The oldest pillow lavas either rest on this desiccated mudstone layer or are deeply imbedded into the cross-bedded sandstone with soft sediment deformation (Figures 3.13A-C & 3.14C).

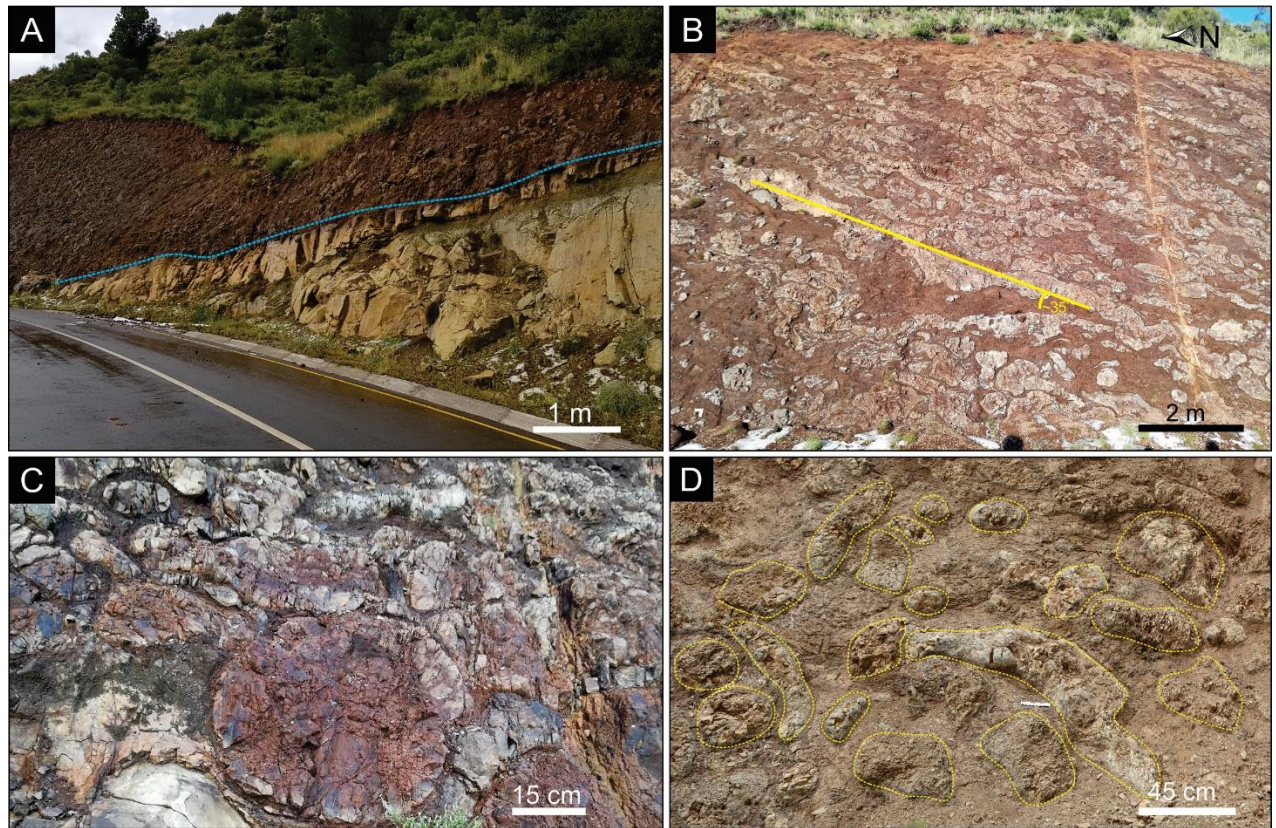


Figure 3.11: (A) Stratigraphic contact (blue dotted line) between the pillow lavas of the Barkly East Formation and the underlying sandstones and mudstones of the Clarens Formation. (B) Outcrop showing the oblique layering or foreset beds of the pillow lavas dipping $\sim 35^\circ$ to the south. (C, D) Tightly packed pillow lavas with cross-sections that are circular (C) to elongate, ellipsoidal (D).

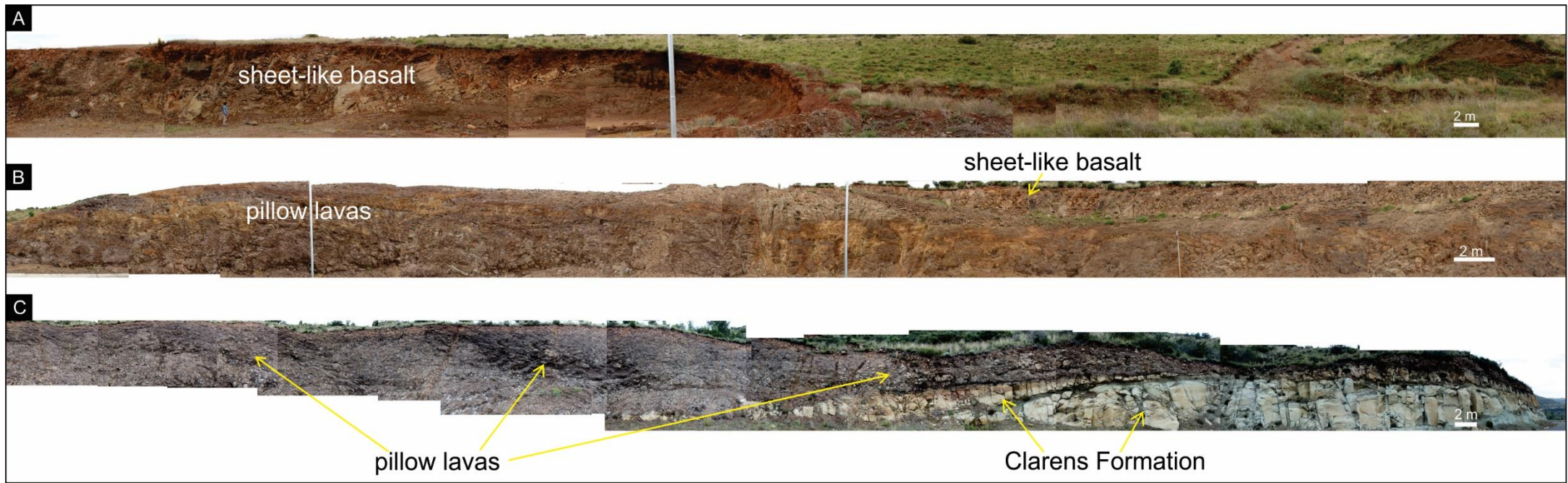


Figure 3.12: Panoramic view from north (A) to south (C) along the road-cutting in southern Moyeni showing: (A) The massive, sheet-like lava flows which transitions laterally to (B) the underlying pillow lavas succession. (C) The southern section of the road-cutting which exposes the pillow lavas as well as the underlying sandstone and mudstone package of the Clarens Formation.

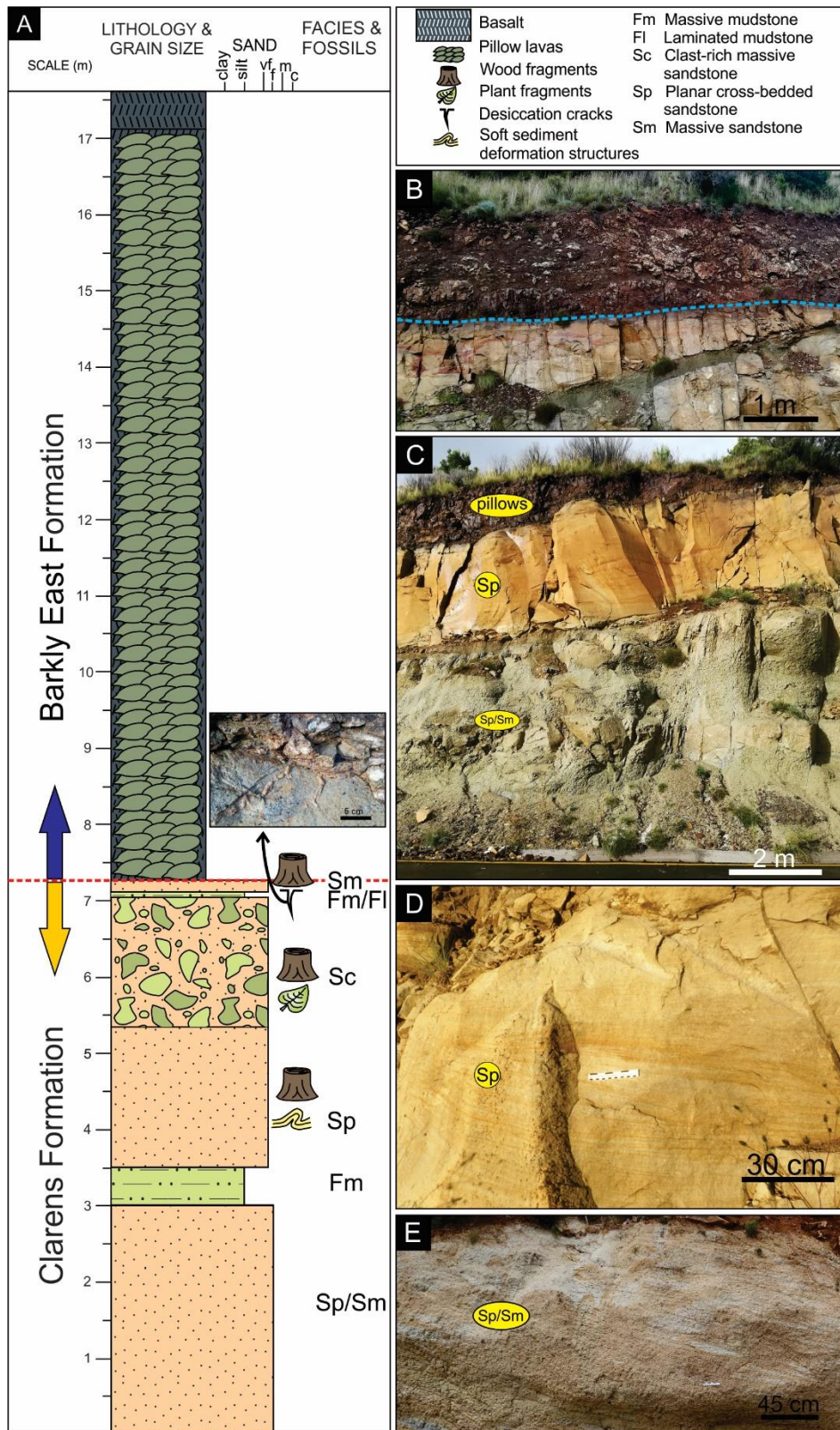


Figure 3.13: (A) Sedimentary log south of Moyeni along the road cutting, which exposes the 9.5 m pillow lava package as well as the underlying Clarens Formation. Inset shows the very thin mudstone layer with desiccation cracks near the contact. (B) Outcrop of the Clarens-Barkly East contact (blue dotted line). (C) Outcrop view of the channel-shaped sandstone with the overlying pillow lavas. (D) Close-up of the cross-bedded fine- to medium-grained yellow-orange sandstone and (E) the lowermost massive to cross-bedded, beige sandstone.

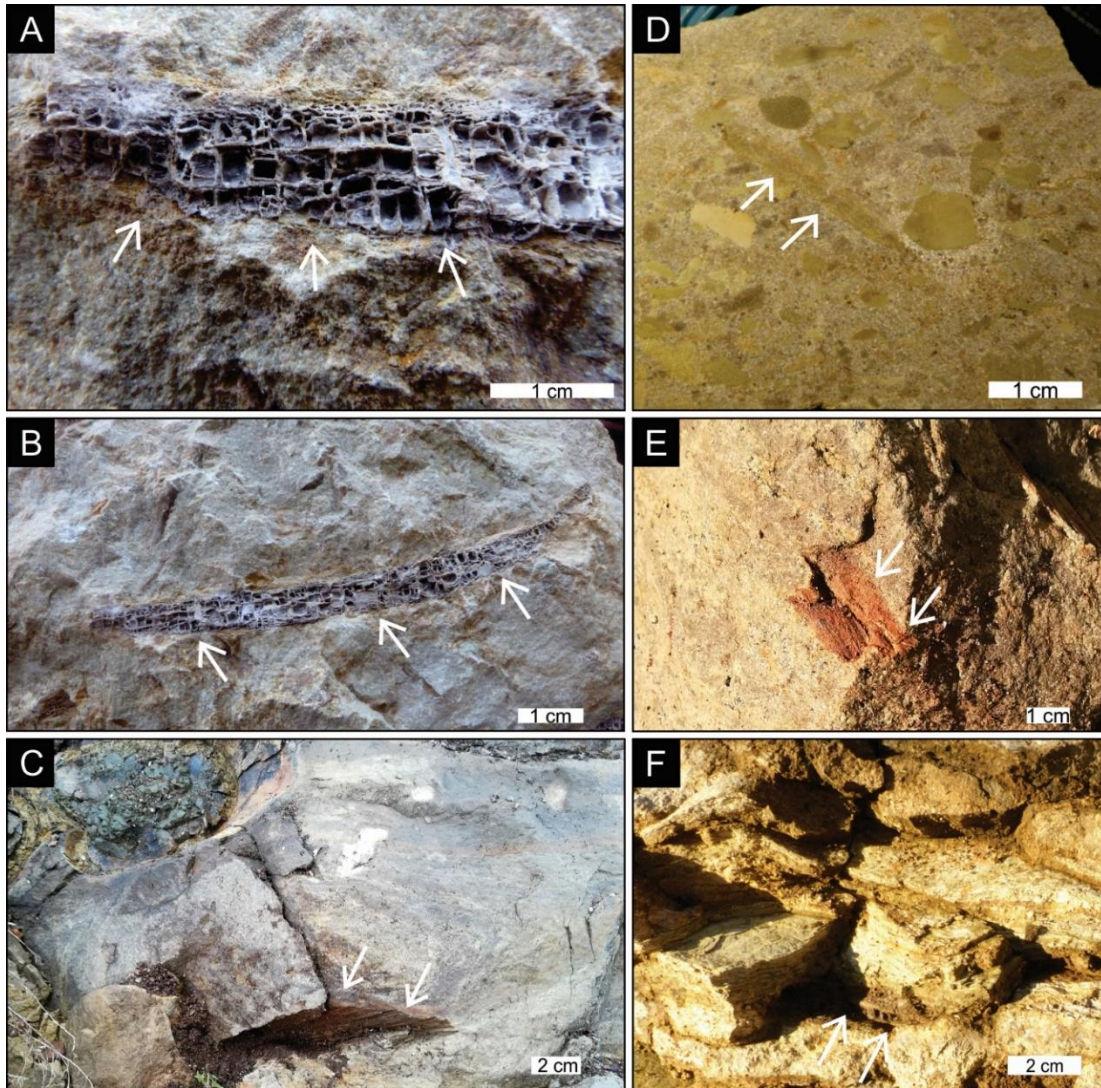


Figure 3.14: Fossilised wood fragments (marked with white arrows) in sandstones near the Clarens-Barkly East contact. These medium-grained sandstone beds are either massive (A, B, E, F), and locally can display soft sediment deformation structures (C) or contain clusters of sub-rounded to angular mudstone clasts (D; facies Sc in the log). Note the deeply imbedded pillow lava in C.

3.2.3.3 Igneous intrusions

In addition to the extrusive igneous rocks, dolerite intrusions in the form of dykes and sills are also present at Moyeni. Large sills occur within the lower beds of the uEF and are well-exposed along road cuttings in the western region of the study area (Figure 3.15). Here, the thickness of the sills vary between 50 cm to a maximum of 4 m, are fine- to medium-grained and more resistant to weathering than the sedimentary rocks away from the contact metamorphosed country rock. The sills intrude mostly along the bedding planes of the uEF sandstone layers, and locally deform the strata (Figure 3.15).



Figure 3.15: Panoramic view of the dolerite sills (outlined with a yellow dotted line) that intruded into the lower uEF in the western part of Moyeni. Note the displacement and deformation of the sandstone strata in the uEF (highlighted in pink).

3.2.4 Breccia Facies

The eastern part of the mapped area exposes a breccia facies (Figures 3.16; Appendix- Figure 1A), which is the youngest geological unit in Moyeni, because it contains fragments from all the lithostratigraphic units of Moyeni, including the amygdaloidal basalts clasts from the Barkly East Formation. The outcrops of breccia facies are situated near the southernmost normal fault (see subchapter 3.5) and extend intermittently in the N-S direction for ~45 -50 m (Figure 3.16A)

The breccia facies unit is located to the south, further from the fault, and can be described as a polymictic parabreccia (Gmm) (Figure 3.16B). This matrix-supported breccia has clasts ranging between grains of 0.5 mm to cobble-sized clasts of 60 cm in diameter (Figure 3.16D-G). The clasts are very angular to sub-rounded, and comprise of green mudstone, fine-grained sandstones, fine- to medium-grained sandstone and basalts with amygdales (Figure 3.16D-G). The sandstone clasts are consistent with the regional textural properties of Clarens Formation. The matrix of the breccia is fine-grained sandstone. The lower breccia beds appear to be massive, whilst the upper beds show very crude bedding, often marked by flat clasts (Figure 3.16B). The brecciated area also contains a large (tens of meters in diameter) block of basaltic lava that lies below the Clarens-Barkly East contact (Figure 3.16C). In addition, a breccia with fragmented clasts of Clarens sandstone was also observed within the breccia zone (Figure 3.16A) which may be fault related.

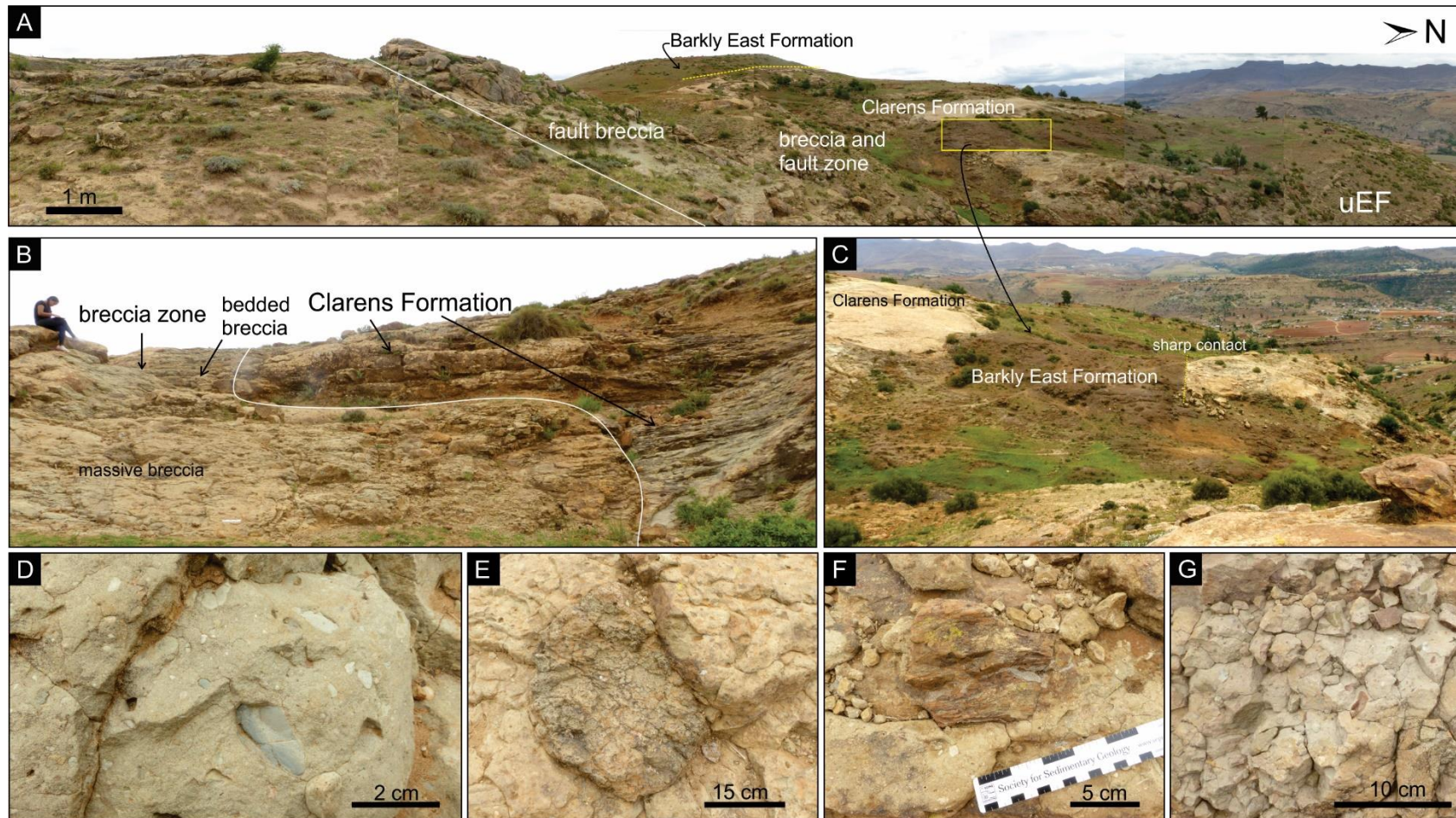


Figure 3.16: (A) Panoramic view of the spatial relationship of the breccia facies and the uEF, Clarens and Barkly East Formations. Note the block of the Barkly East Formation (marked with yellow rectangle) within the first breccia facies and fault zone (~ 15 m below the Clarens-Drakensberg contact), close up is seen in (F). (B) Polymictic parabreccia (first breccia facies unit) with massive to crudely bedded units. (C) Brecciated area containing block of basaltic lava note the sharp contact with the Clarens Formation. Clasts in this coarse, poorly sorted breccia comprise of (D) white sandstone and green-grey mudstone fragments, (E) basalt with amygdales, (F) Large sandstone clast with horizontal laminations and (H) sandstone and mudstone chips.

3.3 Petrographic analysis

Petrographic observations of the samples collected from the Elliot, Clarens and Barkly East Formations are summarized in the following sections. The full petrographic descriptions of these samples, focusing on mineral composition and textures, are presented in Appendix Table 1A. All samples are dominated by monocrystalline quartz grains, and the sandstones show a general increase in maturity with decreasing stratigraphic age (from the uEF to the Barkly East Formation).

3.3.1 Upper Elliot Formation

This medium-grained uEF sandstone sample (labelled A) comprises ~ 65 % quartz, ~ 25 % lithic fragments, 10% of feldspar and traces of micas and opaque minerals (Figure 3.17A; Appendix Table 1A). The grain size ranges between 0.2 and 0.5 mm, and the dominant grain size is ~0.4 mm (medium sand). The grains are angular to sub-rounded with moderate sorting and low sphericity. Overall, this sandstone is sub-mature with a moderate matrix content of ~ 12%.

3.3.2 Clarens Formation

Three samples, 2 sandstones and 1 mudstone, were taken from the Clarens Formation. Sample B, taken in the lower part of Clarens Formation, is moderately to well-sorted, medium-grained sandstone (Figure 3.17B; Appendix Table 1A). Quartz makes up 65% of the grains, whilst feldspar 20 %, lithic fragments (10 %) and micas and opaque minerals constituting the remaining mineral composition (5 %). Grains in this sample are angular to sub-rounded and show low sphericity. The sandstone is immature with a matrix content of <10 %.

Sample C was taken from the uppermost Clarens Formation layer (Figure 3.17C; Appendix Table 1A), below the contact with the overlying pillow lavas of the Barkly East Formation. It comprises ~ 55 % quartz, 25 % feldspars, 15 % lithic fragments and 5 % opaques and

accessory minerals. The quartz grains are ~ 0.5 mm in diameter (medium-grained), however the grain size of feldspars seems to be coarser with an average diameter of ~ 0.75 mm. The grains are sub-rounded to sub-angular, relatively poorly sorted and shows high sphericity. About 10 % of the sample is matrix that is made up of a very fine-grained material, possibly fragments. Similarly, to the Sample B of the Clarens Formation, this sandstone is also texturally immature.

Sample D was taken from a thin, mudstone layer in the uppermost Clarens Formation near the Clarens-Barkly East contact (near sample C; Figure 3.17D; Appendix Table 1A). The mudstone is dominated by clay-size particles (well over ~70 %) that display a slight laminated fabric. Sample D also contains relatively coarser grains (~ 0.25 mm) of very angular to angular quartz.

3.3.3 Barkly East Formation

Two sandstone samples were taken from the lower and upper part of a sandstone interbed unit from Barkly East Formation (lower Drakensberg Group) in southern Moyeni. The lower sandstone sample (labelled E; Figure 3.17E, Appendix Table 1A) contains ~ 60 % quartz, 20 % feldspar (plagioclase and alkali feldspar), 15 % lithic fragments, and other minerals which include opaque (possibly oxides) and micaceous minerals make up 5 %. The grains are mostly medium-grained sand, moderately sorted, and sub-rounded to angular with moderate sphericity. The sample is texturally mature to sub-mature with a matrix content of < 15%.

The upper sandstone sample (labelled F; Figure 3.17F, Appendix Table 1A) contains fine- to medium-grained quartz and feldspar grains with a dominant grain size of ~ 0.25 mm. In comparison to sample E, this specimen is finer grained and contains relatively fewer lithic fragments (~ 10 %), but more quartz (~ 70 %), feldspar (20 %) and opaque minerals (< 1 %, trace amounts). Similarly, to sample E, the grains in F are sub-angular to sub-rounded with moderate sphericity. The very low matrix content (< 10 %) makes specimen F texturally more mature than sample E.

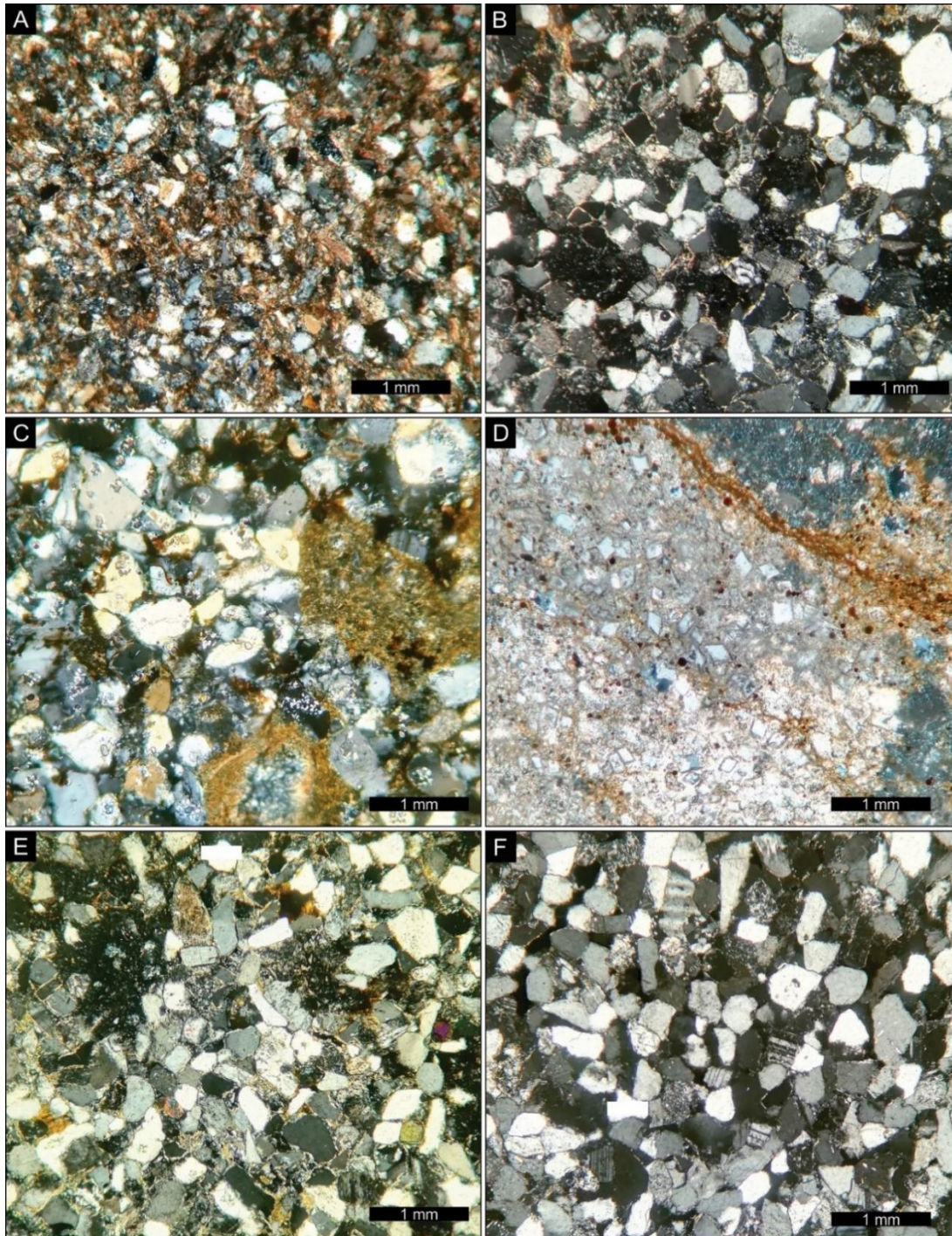


Figure 3.17: Petro-micrographs showing: (A) Upper Elliot sandstone with sub-rounded to angular quartz grains and lithic fragments. (B) Lower Clarens sandstone comprising of well-sorted, sub-angular to sub-rounded quartz, feldspar and opaque minerals. (C) Uppermost Clarens sandstone from the Clarens-Barkly East contact displaying quartz grains and fine-grained lithic fragments. (D) Uppermost Clarens mudstone with very angular to angular quartz grains in a clay-rich matrix. (E) Sandstone from the lower part of a sandstone interbed unit (Barkly East Formation) showing moderately sorted, sub-rounded to angular grains. (F) Sandstone from the upper part of a sandstone interbed unit (Barkly East Formation) containing quartz and feldspars grains that are fine-grained and moderate to well-sorted. All images were taken in cross-polarized light.

3.4 Ichnology of Moyeni

Vertebrate ichnofossils are found in the uEF at lower Moyeni (Figures 3.18 & 3.19) and upper Moyeni (Figures 3.20 & 3.21) as well as in the Clarens Formation at Phahameng (Figure 3.22).

3.4.1 Lower Moyeni ichnosite

The lower Moyeni uEF ichnosite is at ~1500 m elevation (Site 2; Appendix- Figure 1A), some 65 m below upper Moyeni uEF ichnosite. It was discovered and extensively studied by Ellenberger and co-workers (see Ellenberger et al., 1963; Ellenberger 1970, 1974), and restudied in detail using modern techniques by Smith et al. (2009), Wilson et al. (2009) and Marsicano et al. (2014). Originally, this ichnosite exposed more than 450 tracks, but about 200 tracks were obliterated during conservation efforts (e.g., building of a protective shelter and visitors centre) in the past few decades, which were mainly triggered by the construction of the national road that runs adjacent to it.

This uEF palaeosurface is preserved within a thinly bedded medium- to fine-grained sandstone succession, which is sandwiched between mudstones (Figure 3.18A) The palaeosurface is ripple marked and preserves pitted, algal mat textures (Figure 3.19A & C). In addition to the vertebrate tracks (described below; Figure 3.18), the surface also preserves invertebrate traces (Figure 3.18B; e.g. feeding trails of nematodes, beaded trails created by foraging organisms and backfilled meniscate burrows; Smith et al., 2009).

The palaeosurface host distinct tridactyl tracks and trackways. The first is characterised by its robust rounded or blunt digits (Figure 3.18B & C). These tracks are subequal widths and lengths (10- 16 cm), with the central digit (digit III) projecting further forward (relative to digits II and IV; Figure 3.18B). Additional morphologies of these tracks show preservation of the five-digit manus (front foot) and elongated metatarsal impressions. More exotically, drag marks

extending from digits or found between/across tracks are found with some of these track types and have been interpreted as tail or toe drag marks (see e.g., Ellenberger 1974).

The second trackway is made up of 25 tracks and show narrow tridactyl tracks with elongate pointed digits with the central digit projection accounting for ~30 % of the track length (Figure 3.18D), and in some cases preserve claw marks (Figure 3.18D). These tracks are ~ 27 cm in length and ~ 18 cm wide with a L/W ratio of 1.5.

Pentadactyl (five-digits) trackways are also preserved, purely as round digit impressions, present as manus-pes (front and hind feet respectively) pairs of equal length and width (average 13 cm; Figure 3.18E). Drag marks extending from the digits of both the manus and pes are observed. Additional, smaller pentadactyl tracks are found within the sandstone and show a five-digit pes and four-digit manus of ~2 cm- 3 cm in length, respectively (Figure 3.18F).

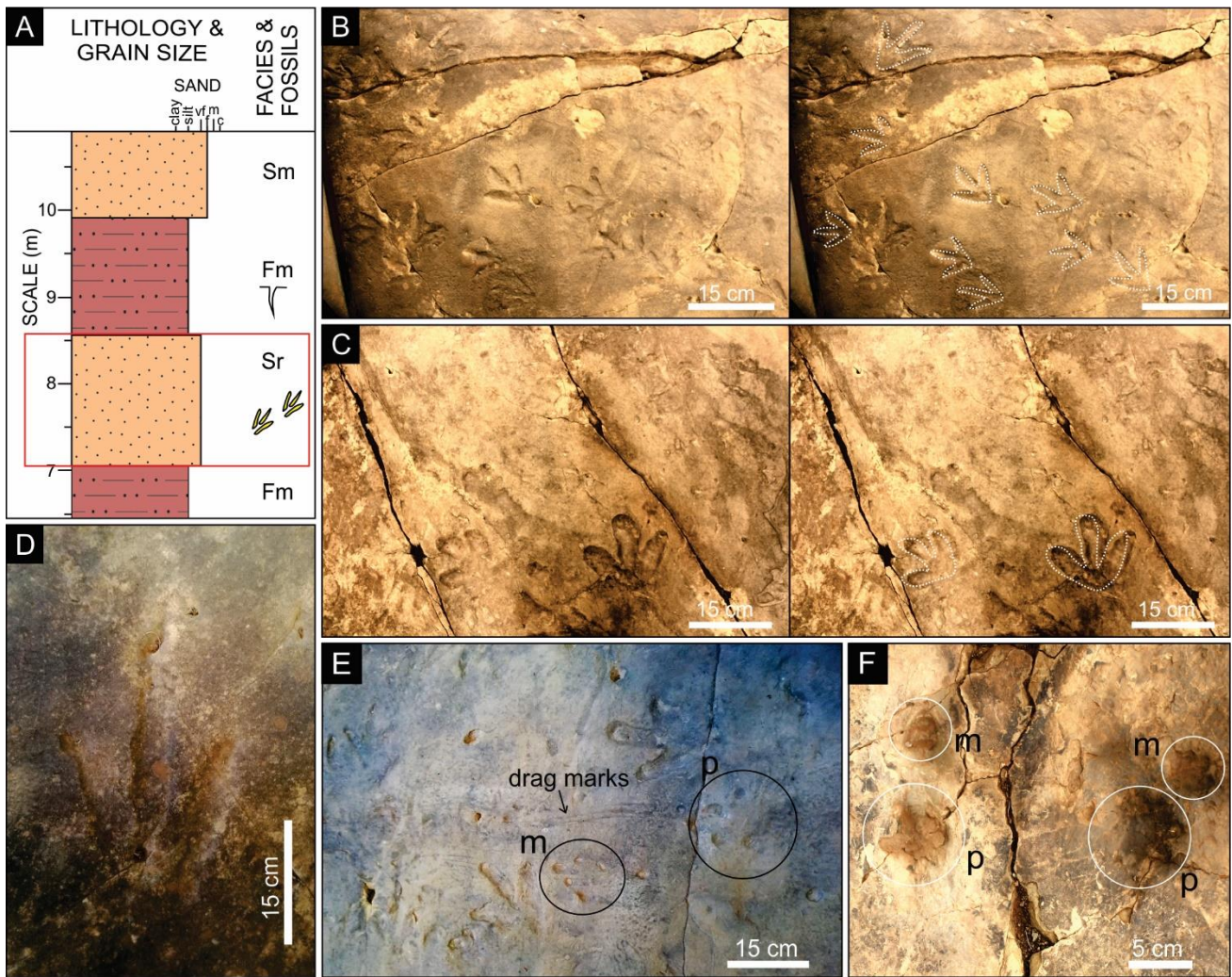


Figure 3.18: (A) Sedimentary log, illustrating the stratigraphic position of the Lower Moyeni ichnosite (this is part of the log shown Figure 1.3C). Tracks preserved within a medium- to fine-grained, thinly bedded sandstone are: (B) tridactyl tracks with elongate digit III and (C) rounded digit impressions. (D) Larger tridactyl tracks with claw marks. (E) Four-toed manus and five-toed pes pairs of a pentadactyl vertebrate and associated drag marks. (F) Smaller 2-3 cm tracks comprising manus and pes pairs (marked by white circles and labelled with M and P, respectively). See Table 2.1 for facies codes.

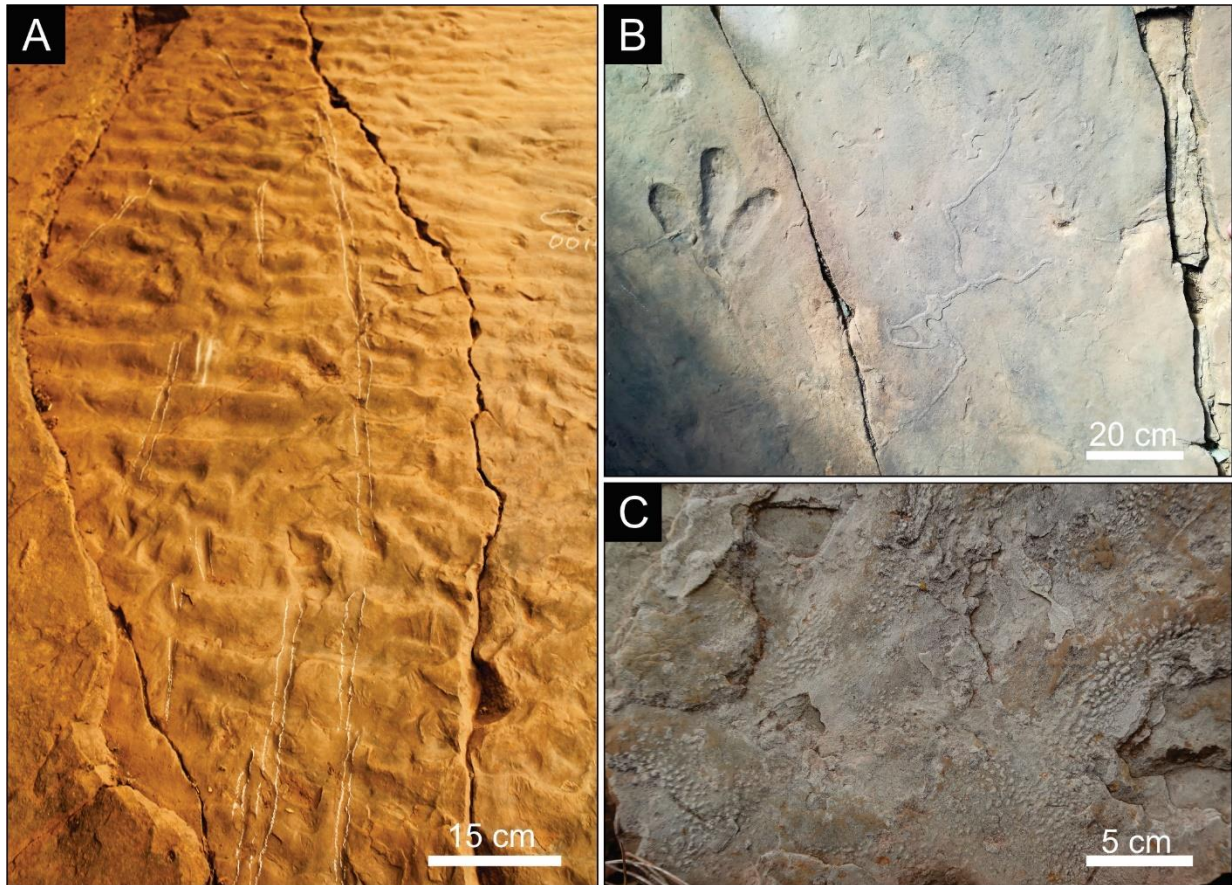


Figure 3.19: (A) Ripple marks and drag marks along the sandstone palaeosurface. (B) Invertebrate traces (right of image) and alongside a tridactyl track (left of image). (C) Pitted texture characteristic of a preserved algal mat within the sandstone.

3.4.2 Upper Moyeni ichnosite

The upper Moyeni ichnosite (Site 3; Appendix- Figure 1A) is ~ 35 m below the Elliot-Clarens contact, and ~ 65 m above the lower Moyeni ichnosite (Figure 3.20). This is a newly discovered site and preserves ichnofossils in a fine- to medium-grained sandstone unit of the uEF. The sandstone surface is ~ 130 m long, 2-2.25 m wide and is the last layer of a 1.5 m thick, fine- to medium-grained, upward-thinning and upward-fining sandstone package (Figure 3.20A). The palaeosurface preserves ripple marks (Sr) and > 60 tridactyl vertebrate tracks, of which 18 make up 4 trackways. The lengths of these tracks range between 17.5 and 48 cm. The track measurements also show that track lengths are greater than the track widths (average L/W ratio of 1.3) and the length of digit III is greater than digit II and IV lengths (Figure 3.20B). The tracks also show varying degrees of preservation and morphological detail i.e. shallow

vs. deep impressions as well as incomplete vs. complete tracks with digital pad impressions, claw marks and expulsion rims (Figure 3.20B). The smaller tracks (i.e. foot length of ~ 20 cm) are characterised by long and pointy toes and rare claw marks (Figure 3.20B-2). The larger of the tridactyl tracks (i.e. foot length of > 40 cm) show elongate but slightly outward-curving digits that terminate in sharp claw marks (Figure 3.20B-3). These larger tracks also make up one of the trackways, made up of 9 tracks, whilst each of the other trackways comprise of 3 tracks.

In addition to the preserved vertebrate tracks, an isolated vertebrate burrow cast with a bilobate cross-sectional shape is located within the purple-red silty mudstone, which is ~ 13 m below the track bearing upper Moyeni palaeosurface (Figures 3.21A). This semi-horizontal burrow cast shows a maximum diameter of 23 cm and a maximum height and exposed length of 10 and 45 cm, respectively (Figure 3.21B & C). Scratch marks in a chevron pattern are on the side of the burrow cast and dissipate towards the top of the burrow cast, which is a smooth surface. The fill of the burrow is massive, fine-grained sandstone with mm-scale bioturbation that is visible on the topside of the cast (Figure 3.21D & E).

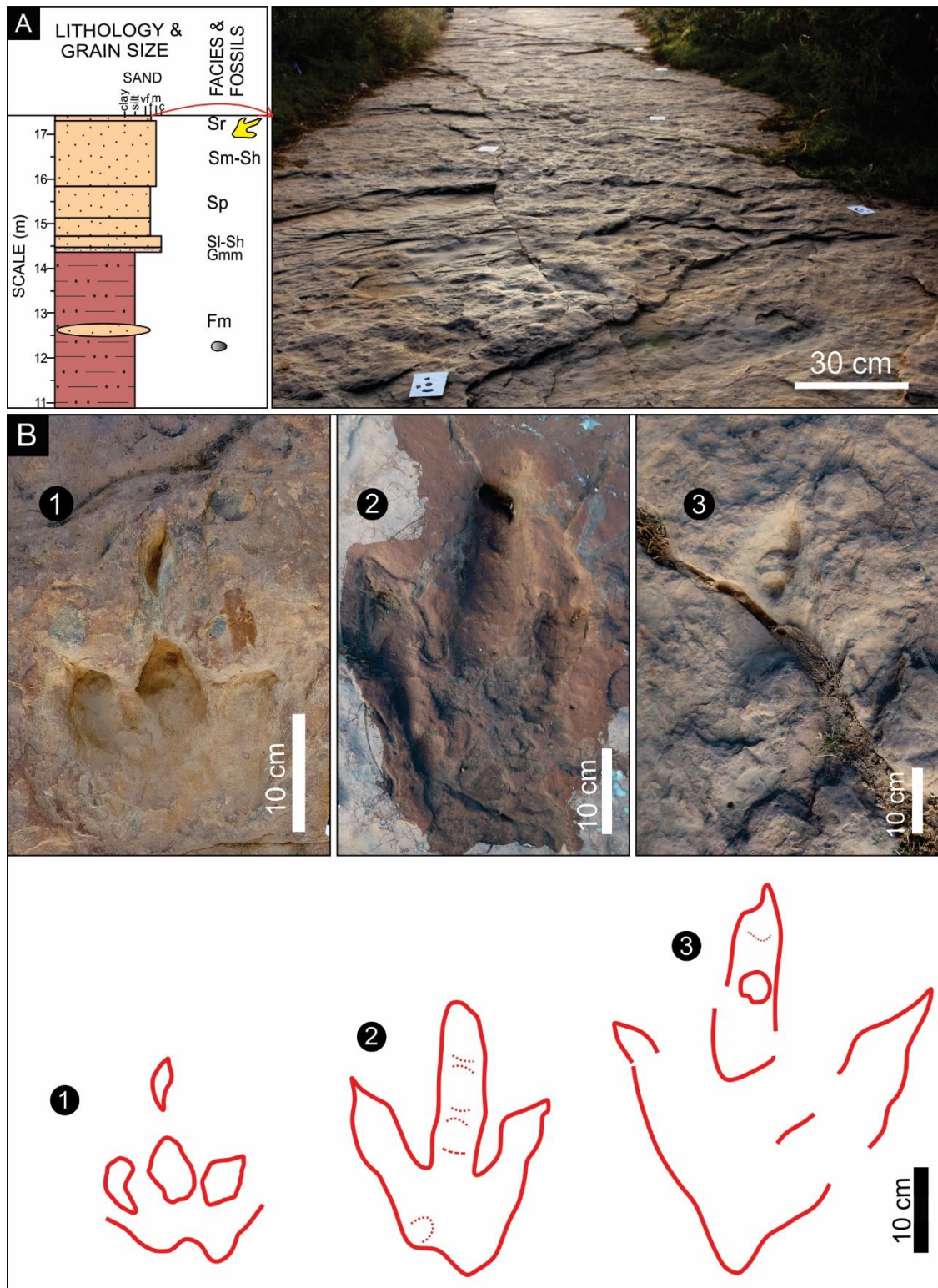


Figure 3.20: (A) Sedimentary log showing the stratigraphic position of the upper Moyeni ichnosite, which is preserved on the upper bedding plane of the last sandstone layer in the log (highlighted by the red arrow) as well as the outcrop view of the 130-m-long surface (which is a busy suburban road). (B) Representative photographs and interpreted outlines of the tridactyl tracks to illustrate: i) size variations in track length ranging from 17.5 cm (track 1) to 48 cm (track 3), ii) expulsion rims (track 1), iii) claws marks (tracks 1, 2) and, iv) digital pad impressions (tracks 2, 3). See Table 2.1 for facies codes.

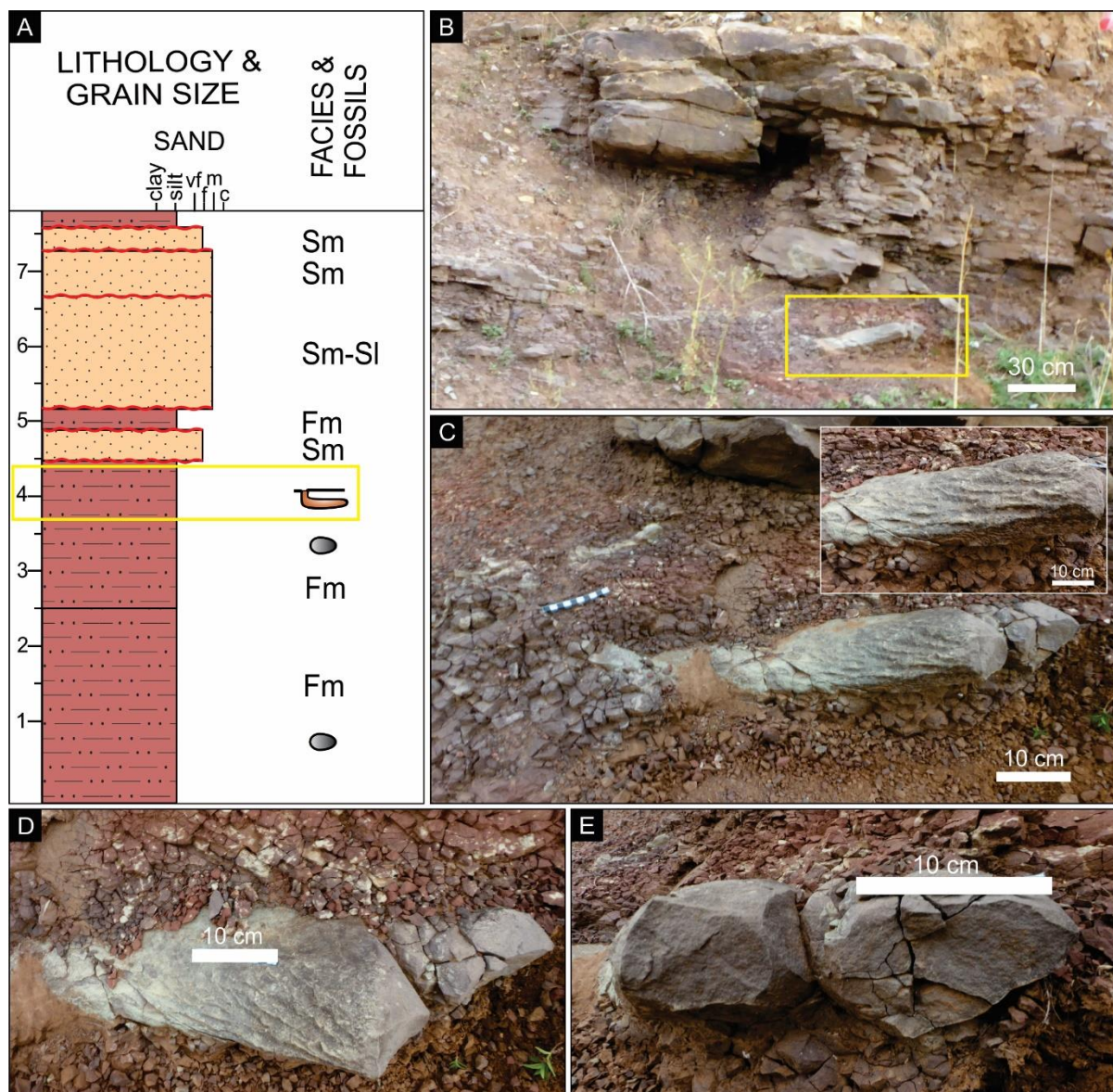


Figure 3.21: (A) Sedimentary log and (B) outcrop view showing the semi-horizontal vertebrate burrow cast and its stratigraphic position within a pedogenically altered uEF mudstone unit at upper Moyeni. (C) External geometry of the burrow cast displaying scratch marks along the side (inset image). Note the pedogenic alteration (carbonate nodules) in the host mudstone. (D) Close-up of the burrow cast from the top showing the scratch marks in oblique view and mm-scale bioturbation on the top of the burrow cast (white specs). (E) Cross-sectional view of the burrow cast displaying its kidney-shape and massive, fine-grained sandstone burrow fill. See Table 2.1 for facies codes.

3.4.3 Phahameng ichnosite

On the outskirts of Moyeni (site outside of mapped area), at a village called Phahameng (loosely translated as “Lift up” from Sesotho), the lower Clarens Formation preserves a two-step tridactyl trackway. The tracks are hosted within a fine- to medium-grained massive sandstone along with desiccation cracks (Figure 3.22). The tracks labelled 1 and 2 have slender digits with claws marks (most elongated is digit III), are 32 and 35 cm long, respectively, have a L/W ratio of 1.2, and show a pace of 87 cm (Figure 3.22).

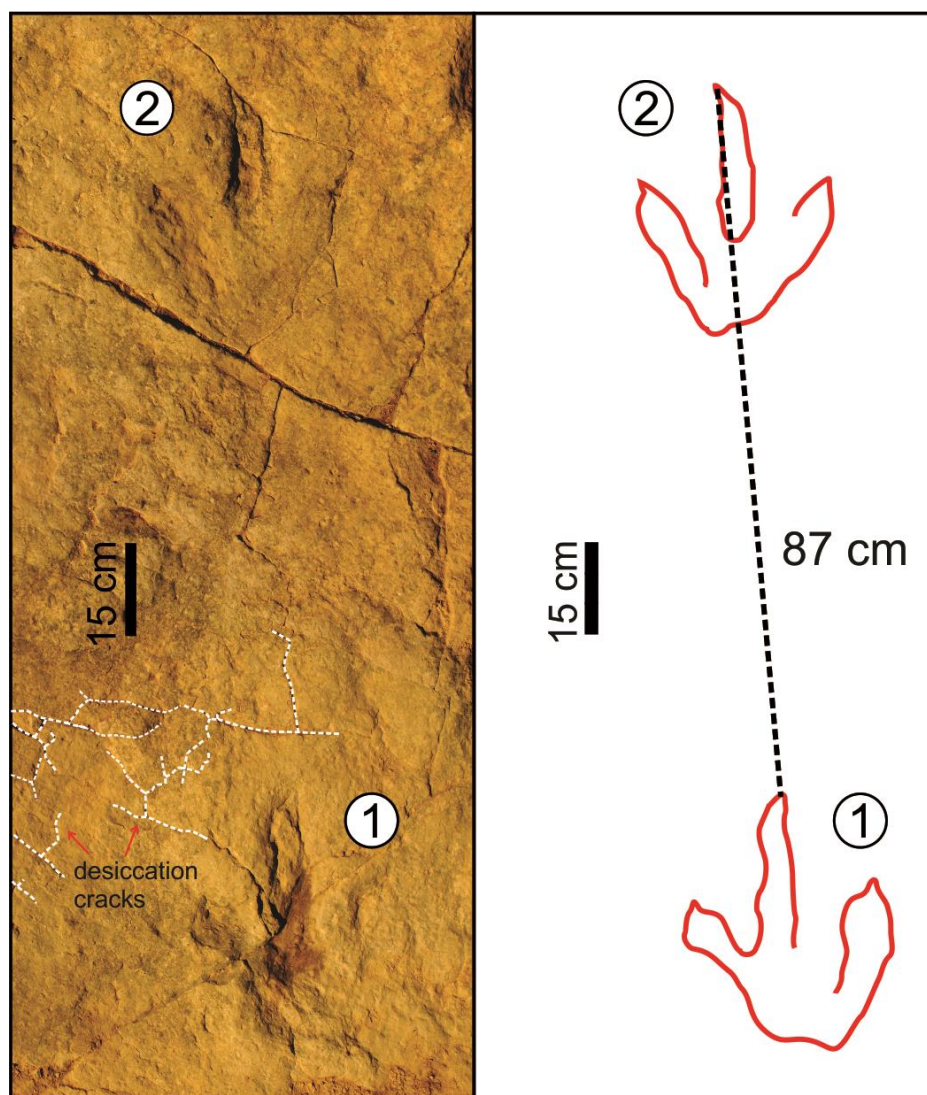


Figure 3.22: Two-step tridactyl trackway with preserved claw marks preserved within a fine- to medium-grained desiccated sandstone (a few marked with white dotted line) of the lower Clarens Formation at Phahameng, ~2.3 km from the lower Moyeni ichnosite in the uEF.

3.5 Structural geology near Moyeni

The area contains significant surface relief. The valley of the Qomongqomong River and its tributaries incise ~ 500 m into the local geology and carve out the surrounding hills, which reach a maximum elevation of 1836 m in the southernmost region. These hills contain prominent cliffs composed of the sandstone that belong to the uEF and Clarens Formation. Regionally, the strata have been gently folded in a series of small folds and Moyeni is situated in one of the smaller troughs of the fold. The strata at Moyeni have been deformed by steeply-dipping normal faults, as shown in the geological map (Figure 3.1 & Appendix Figure 1A) and explained in the next sections. Deformation is concentrated along a fault zone with a width of tens of meters, containing a series of associated synthetic and antithetic faults. The trend of the faults in the fault zone are ENE-WSW, with a strike of $\sim 286^\circ$ (Figures 3.23- 3.25). The full length of the fault zone has not been determined, but it extends beyond the borders of the mapped area. The faults outcrops in the hillsides on both the eastern (Figures 3.23 & 3.24) and western part (Figure 3.25) of the area but is difficult to follow in between, within central Moyeni, due to poor exposure. Overall the fault zone downthrows the southern side relative to the northern side; the dominant dip of the strata is to the north.

3.5.1 Faults in eastern Moyeni

The stratigraphic succession in eastern part of Moyeni is modified by a fault zone consisting of at least three normal faults trending in the ENE-WSW direction and an associated breccia facies (Figures 3.23, 3.24 and 3.16; Appendix- Figure 1A). The normal fault 1 is shown in Figures 3.23 and 3.24 and is marked on the geological map (Appendix- Figure 1A). The vertical displacement of ~10-15 m along fault 1 is particularly prominently shown by the offset of the lower contact of the Clarens Formation, which here comprises a lower, coarser-grained sandstone unit and an upper, finer-grained sandstone unit (Figure 3.23). The latter shows significant and abrupt thickness variation across the fault, as this finer-grained unit is ~2 m

thick north of the fault and ~15 m thick south of the fault (Figure 3.23). Importantly, there is no visible displacement of the Clarens-Barkly East contact at fault 1 and the uppermost beds of the Clarens Formation are continuous across this fault strand. Faults 2 and 3 (Appendix-Figure 1A), which outcrop further south of fault 1, offset the Clarens-Barkly East contact (Figure 3.24C). In addition, fault 3 is associated with a breccia facies (Figure 3.24D), which was discussed in the “Breccia facies” section of this chapter (Figure 3.16).

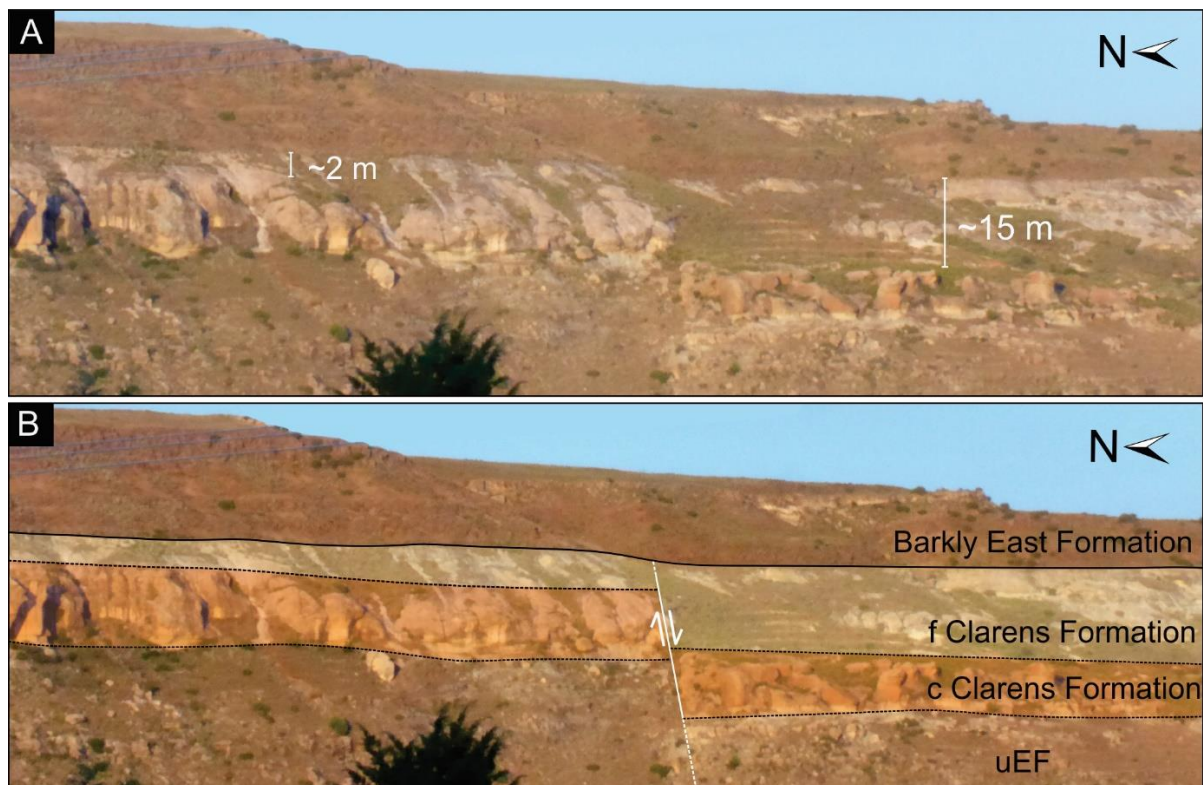


Figure 3.23: (A) Photographic panorama of the eastern region of Moyeni showing displacement along the ENE-WSW trending normal fault 1. The fault does not affect the upper contact of the Clarens Formation but offsets the lower contact by ~10 m and brings the relatively coarser-grained sandstone cliff in the lower Clarens Formation in direct vertical contact with the uEF. (B) Annotation of the normal fault illustrating the direction of movement as well as the thickness change across the fault in the fine-grained sandstone unit in the upper Clarens Formation. Abbreviations: c = relatively coarse-grained sandstone unit; f = relatively fine-grained sandstone unit in the Clarens Formation.

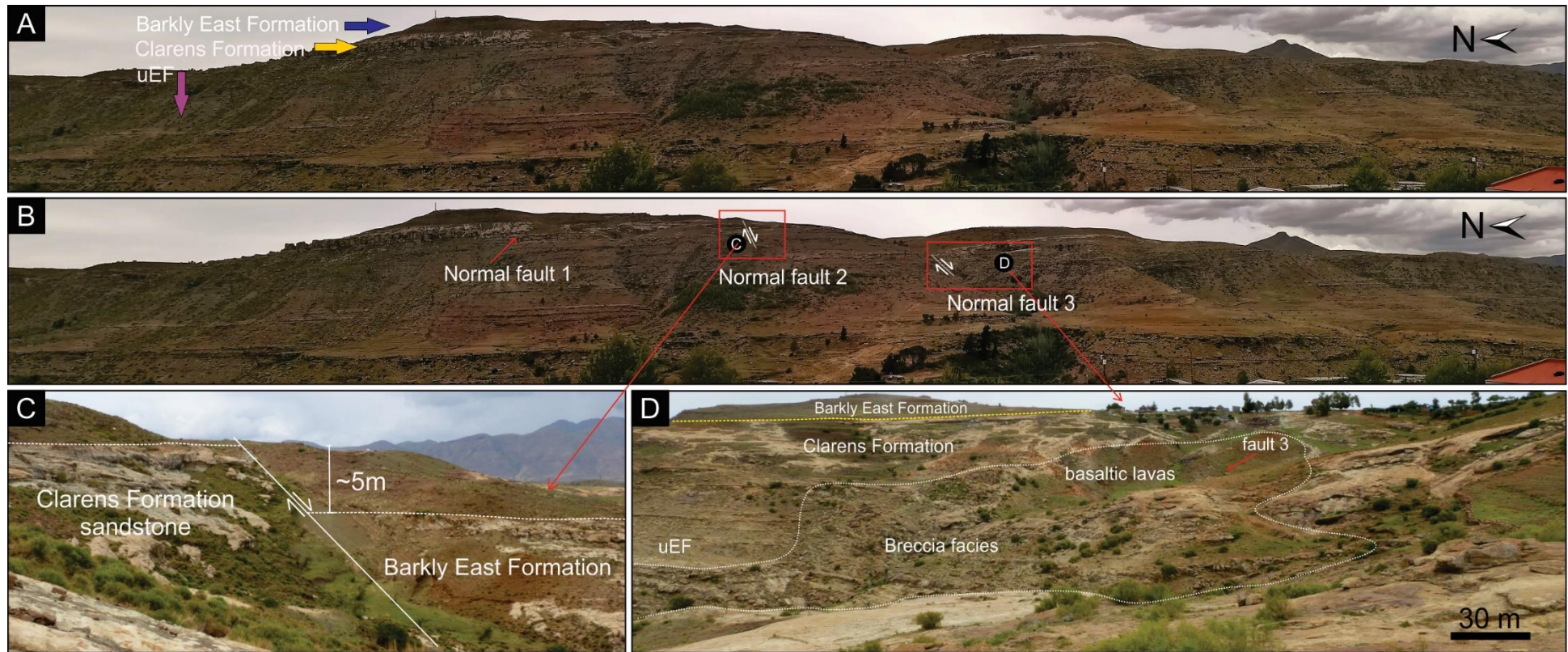


Figure 3.24: (A) Photographic panorama of the eastern region of Moyeni showing the stratigraphy northeast of the town and (B) annotation of A to show the eastern normal faults: fault 1 (also seen in Figure 3.23), the trend and direction of movement of fault 2 and 3. (C) Close up of fault 2 showing the vertical displacement of ~ 5 m of the Clarens Formation and Drakensberg basalts. (D) Close up of fault 3 showing the breccia facies (mapped with white dotted line) that is nested in uEF and Clarens Formation and a down-thrown sliver of basaltic lavas. The latter is ~ 15 m below the local level of the Clarens-Barkly East contact (marked by the yellow dotted line).

3.5.2 Faults in western Moyeni

The fault zone outcrops along strike from the eastern fault zone in the western region of Moyeni, where it appears as a single main fault (Appendix- Figure 1A) associated with an antithetic fault that is poorly exposed (Figures 3.25). The antithetic fault outcrops to the south of the main fault and dips towards it, and thus forming a small graben structure (Figure 3.25B). The abrupt change in lithology on either side of the fault is visible from afar, among others from central Moyeni. The fault caused an offset of ~ 30 m and a distinct and abrupt altitude change in the position of the Clarens-Barkly East contact (Figures 3.25). The antithetic fault caused a further displacement of ~ 5 m (Figure 3.25), which is confirmed by direct field measurements and elevation readings from the GPS used in this study. Preliminary mapping to the south of the western fault zone (Figure 3.25A) shows that the Clarens Formation is up to ~ 50 m thick, thus seems to get thicker to the south, outside the study region.



Figure 3.25: (A) Photographic panorama of the western region of Moyeni showing the area southwest of the town. (B) Closer panoramic image of the western region and (C) annotation of B to show the western normal fault, the faulted stratigraphic units and the displacement of ~30 m as well as the antithetic fault, which caused further ~5 m of displacement. This fault is dipping north and resulted in a small graben structure.

4 Discussion

4.1 Interpretation of the facies analysis results

4.1.1 The upper Elliot formation (uEF)

The facies associations of the uEF in Moyeni are common in the rest of the basin and have been previously characterised by Visser and Botha (1980); Eriksson (1984, 1985); Smith et al. (1993); Bordy et al. (2004b). The red-purple and green mudstones and very fine to fine grained silty sandstones (Figures 3.3 & 3.4), which are laterally continuous throughout the uEF exposures are interpreted as sediments that have accumulated in a low energy fluvial to lacustrine depositional environment (Bordy et al., 2004b). Specifically, the mudstones are seen as sediments that accumulated over low gradient floodplain areas with standing bodies of water or abandoned water channels. The red to maroon-purple colour pigmentation of the mudstones (Figure 3.4A) can be attributed to the presence of iron oxide associated with minerals such as haematite, which forms a coating around the grains (Blodgett, 1988; Eriksson et al., 1994; Xiuman et al., 2006).

The presence of the carbonate nodules hosted by the mud- and siltstones (Figure 3.4E & F) serve as evidence for the climatic conditions during the deposition of the mudstones. These post-depositional features are characteristic of palaeosols (ancient soils or soil horizons) in semi-arid environments where calcareous pedogenic alteration and calcretes are common (Blodgett, 1988; Smith 1990). The fluctuations from wet to dry, in a semi-arid environment causes the drying up of calcium rich groundwater resulting in the precipitation of evaporites, which results in the formation of calcretes (Wright and Tucker, 1991; Goudie, 1996). The carbonate nodules record the initial stages of the pedogenic carbonate accumulation therefore their presence is common in depositional environments in which sedimentation rate came to

a halt or was low enough for the palaeosol horizons to develop (Blodgett, 1988). The latter can be explained with regional basin tectonics in the late evolution of the MKB in conjunction with the regional change in climatic conditions. According to Bordy et al. (2004a, b), during the deposition of the Elliot Formation, particularly the lower Elliot Formation, the floodplain aggradation rates were high due to the relatively higher tectonic subsidence rates, this in turn resulted in lower soil profile maturity. In contrast, the decreasing subsidence rates in the terminal phase of foreland basin evolution led to lower clastic sediment supply (and more time for soil maturation) during the deposition of the uEF and allowed for pedogenic development to occur on the abandoned surfaces of the floodplains (Bordy et al., 2004b). The transition from a wetter climate (with perennial rivers) in the IEF to a hotter and drier climate in the uppermost uEF resulted in the decrease in the flash flooding and thus sediment supply, which further contributed to the pedogenic maturity that is especially common in the upper parts of the uEF (Bordy et al., 2004b).

The sandstone-filled casts of desiccation cracks in continental mudstones indicate episodic wetting and drying up of the clayey sediment and subsequently infilling by fine-grained sand, a process that is particularly common in semi-arid regions (Allen, 1984; Martins and Pfefferkorn, 1988; Ghosh et al., 2006). The cracking of mud is linked to the swelling properties of clay minerals within the sediments: swelling up occurs due to the absorption of water in wetter periods, whereas shrinking and cracking take place due to moisture loss via evaporation during the drier periods (Gustavson, 1991). Overall the presence of the desiccation cracks in floodplain mudstones demonstrates the seasonal variability in water content in the sediment substrates, the temporary nature of the water bodies as well as the high rate of evaporation (Allen, 1984; Retallack, 2005). The very wide and deeply penetrating desiccation cracks in the mudstones (Figure 3.4C & D) imply longer and possibly repeated drying out events (Rayhani et al., 2008; Shi et al., 2008). The desiccation cracks with widths up to 20 cm width (Figure 3.4C) indicate that the wet mud was relatively thick prior to drying up.

The fine- to coarse-grained tabular sandstones units (Figure 3.5) are indicative of fluvial deposits (Bordy et al., 2004b). These laterally continuous sheets of sandstone beds are interpreted as products of short-lived, high-energy depositional events such as flash floods which distributed sandy sediments not only in shallow, wide ephemeral channels but also as sheet washes over the low gradient floodplains (e.g., Visser and Botha, 1980; Bordy and Catuneanu, 2002; Bordy et al., 2004a, b, c). These energetic but short-lived events are confirmed by the sedimentary structures present within the sandstone such as the horizontal laminations and low-angle cross bedding (Figure 3.5D & E) which are interpreted as products of upper flow regime sedimentary processes (Bordy et al., 2004b). The ripple marks and ripple-cross laminations sandstones (Figures 3.1B & C) are indicative of the gentle currents which would form due to the waning of flash floods (Bordy et al., 2004b). The more localised medium- to coarse-grained channel-shaped sandstone units either formed in single flash flood events or several short-lived flooding events which were separated by periods of non-deposition and drying up (Hogg, 1982; Bordy et al., 2004b). The thickness of the channel filling, upward-fining sandstone units (1 -1.5 m; Figure 3.5A) may also give insight into the size of the channels, which on a regional scale range from small channels or streams of a water depth of >1 m to deeper channels with depths of at least 2 to 3 m (Bordy et al., 2004b). These channelized sandstone bodies in the uEF are interpreted as ephemeral anastomosing rivers (e.g., Visser and Botha, 1980; Eriksson, 1984,1985; Bordy and Eriksson, 2015).

The gravelly facies assemblage of the uEF (Figure 3.6) are products of highest energy depositional events in the river system of the uEF (e.g., Nemeč and Steel, 1984; Bordy et al., 2004b). The polymictic paraconglomerate in eastern Moyeni (Figure 3.6A & B) indicates the energetic transportation and deposition of poorly sorted, sub-rounded clasts. The alternating bands of concentrated and scattered clasts indicate the relatively rapidly alternating energy levels of the transporting media. The oligomictic orthobreccia, found in western Moyeni only (Figure 3.6C & D), is a product of a major flood event. The ripple-cross laminated sandstone clasts within the orthobreccia suggests that: 1) during the severe storms the floods were

vigorous enough erode and rip-up clasts from the older uEF strata (Figure 3.6D) and 2) the host sandstone layer was competent enough to survive complete obliteration during the flood. The latter also implies that the uEF contains several stratigraphic gaps of unknown duration (but long enough for sand layer to consolidate).

The transitional nature of the uEF-Clarens contact seen within the study area is corroborated by the facies description of this transition on a regional scale by previous authors (for reviews see Bordy and Eriksson, 2015; Bordy and Head, 2018).

4.1.2 The Clarens Formation

The different sedimentary facies of the Clarens Formation sediments indicate that different but related subaqueous and subaerial sedimentary processes occurred that are common in dry regions with spatiotemporally intermittent water supply.

The common fine- to medium-grained and medium- to coarse-grained massive sandstones (Figure 3.7F) can be interpreted as primary or secondary massive sandstones. In the case of the Clarens Formation, the latter is considered more plausible (e.g., Eriksson, 1981; 1986; Bordy and Catuneanu, 2002), and the common explanation is that the original structures of the massive sandstones may have been destroyed by rainfall or the rising of ground water, which occurred subsequent to deposition of the sediments (e.g., Chakraborty and Chaudhuri, 1993). However, it is possible the sedimentary structures within the Clarens Formation are not always visible on a macroscale or that the massive sandstone is indeed structureless (Eriksson, 1981; Bordy and Catuneanu, 2002). It has also been suggested that these massive sandstones formed due to deformation processes caused by pressure loading of sediment overburden which occurred soon after deposition (e.g., Bordy, 2008), or due to the slumping of sediments in mass movements along over-steepened foresets especially after desert storms saturated the unconsolidated sediments (cf. Cook and Warren, 1973; Pye and Tsaoar, 1990).

The thick packages of the large-scale cross bedded sandstones in the uppermost Clarens Formation (Figure 3.7G) are characteristic of aeolian influenced deposits and formed by blowing wind (Eriksson, 1981). The large-scale cross beds with set thicknesses of over ~2 m and the highly inclined foresets ($> 25^\circ$) (Figure 3.7G) are considered here as evidence for these aeolian processes. Steep foresets form due to the absence of water, which allows for a high angle of repose in large aeolian dunes (e.g., Hunter, 1977; Brookfield, 1992; Bordy and Catuneanu, 2002). These large-scale cross-bedded sandstone layers were thus generated as eastward migrating wind-blown sand dunes across the Moyeni and the rest of southern Africa (e.g., Beukes 1970; Eriksson, 1981; Visser, 1984; Bordy and Catuneanu, 2002; Holzförster, 2007).

The channel shaped, fine- to medium-grained, cross-bedded sandstone (Figure 3.7D) in eastern Moyeni is interpreted here as slightly channelized sheet-flood deposits that resulted from heavy by short-lived rainstorms (cf. Eriksson, 1981; 1986). In contrast, the subordinate mudstones indicate a change in energy conditions, with the muddy beds having been deposited from suspension, possibly in shallow lakes (playas). The channel-shaped geometry of the sandstone beds suggests that the temporary river channel in which the strata accumulated was incised. While data is insufficient to determine the fluvial style of this channel, similar deposits in the Clarens Formations have been previously associated with low-sinuosity single or braided wadi channels by Eriksson (1981; 1986) and Bordy and Catuneanu (2002).

The localised pod-shaped, massive sandstone in the uppermost Clarens Formation (close proximity to the Clarens-Barkly East contact), which bears fossilised wood and plant fragments as well as sandstone clasts (Figures 3.13A & 3.14), is a reliable indication of debris flow processes. To account for the rip up clasts and plant debris, the debris flow is explained as a having been triggered by an episode of flash flooding during the final stages of deposition of the Clarens Formation and swept up the riparian trees and plants in addition to the sandstone clasts. It is postulated that these palaeofloods may have occurred contemporaneously with

fires, which are not uncommon in the relatively dry environments (Bordy et al., 2018). The soft sediment deformation structures displayed in the underlying, channelized sandstone (Figures 3.13A & 3.14C) indicates that the deposition of the debris flow sediments occurred rapidly, before complete consolidation of the underlying water-laid sandstone unit.

In summary, the uppermost Clarens section observed along the road cutting in the south of Moyeni (e.g., Figure 3.13A) shows a relatively rapid depositional environment change in the terminal Clarens times. The thick ~ 3.5 m of sandstone with the large cross-bed foresets indicates an aeolian setting dominated by sand dunes at this level (Figure 3.13E). The transition from these thick, large cross-bedded sandstone to the overlying mudstone and channel sandstone deposits (Figure 3.13A and D) with soft sediment deformation structures (Figures 3.13A & 3.14C), however suggests that the Clarens environment was increasingly wetter and also occupied by ephemeral rivers/streams and lakes/ponds. A very thin mudstone layer deposited subsequent to the debris flow (mentioned above; Figure 3.13A), but, as indicated by the desiccation cracks (Figure 3.13A- inset image), dried out rapidly before the deposition of the overlying sandstone (Figure 3.13A). The latter units deposited in a low energy lacustrine environment, which also captured the debris flow sediments (discussed above) as well as the pillow lavas (see next section). The presence of the fossilised wood in the rocks straddling the contact of the Clarens-Barkly East Formations indicates that the environment sustained plants and trees, and is a further indication for the increasing wetness. Consequently, in the terminal Clarens times, the palaeoenvironment at Moyeni was more a fluvio-lacustrine rather than a dry sand sea setting. This interpretation resonates with the regional-scale wet desert reconstruction of the Clarens depositional environment (e.g., Beukes, 1970; Lock et al., 1974; Eriksson, 1981; Bordy and Catuneanu, 2002).

4.1.3 The Barkly East Formation (lowermost Drakensberg Group)

The basaltic lavas and the interbedded sandstones (Figures 3.8-3.10) are evidence that volcanic activity in the Moyeni region occurred without a stratigraphic break, immediately after the bulk of the Clarens sandstones were deposited. The lateral extent of tens of kilometres of these Karoo basaltic lava flows throughout Lesotho suggest that the lavas were probably very mobile and that eruption events occurred frequently over a large surface area (Marsh and Eales, 1984). The succession of the lava flows, especially in the upper part of the lava pile (i.e., Lesotho Formation), is also seen as evidence for the rapid outpouring typical of continental flood basalts, because indicators of long term weathering between the flows are absent (Lock et al., 1974).

The fine- to medium-grained sandstone interbeds (Figures 3.9 & 3.10) in the lower part of the Barkly East Formation suggest that the outpouring of the lavas was more intermittent initially, and when lava supply temporarily seized, various sedimentary processes could occur on the lava covered land surface. The sedimentary facies characteristics of the sandstone interbeds suggest that the sediments were deposited through fluvio-lacustrine processes. The change in sedimentary structures from the lower to the upper part of the interbed units (i.e. Sp to Sh to Sr; Figure 3.10B-D) shows the general energy level decrease within the deposition of a single interbed package. For example, cross-stratification with low to moderate foreset inclination (Figure 3.10B) suggests moderate energy levels of the running water in streams. The larger cross-beds, with foreset thicknesses of ~1 m, indicate that the subaqueous dunes were at least 1 m in height, and thus the fluvial channel was at least 2 m deep (Miall, 2006). Horizontal lamination in the fine-grained sandstones (Figure 3.10C) is indicative of upper flow regime conditions, whilst the desiccation cracks (Figure 3.10G) are evidence for drying out of the stream bed and thus of the ephemeral nature of these streams. The symmetrical ripple marks (Figure 3.10D & E) on the top of the sandstone surface points not only to the overall decrease in energy level but also a transition in deposition from running water to standing water. This is because symmetrical ripples represent bidirectional, oscillatory flow commonly

induced by wave action in a predominantly low energy depositional settings like a lake or pool (cf. Boggs, 1995). The energy level fluctuation within the stream is also recorded by the rare matrix-supported conglomerates (Gmm facies; Figure 3.10F). The Gmm facies suggests a short-lived yet high energy event that resulted in the deposition of the mud chip conglomerate. Based on these sedimentary features and facies associations, the sandstone interbeds are evidence for the transition of fast flowing but short-lived streams with pulsing energy levels (i.e., moderate to upper flow regime conditions to complete dry out) into standing water bodies like pools or shallow playas. In addition to the above proposed fluvio-lacustrine origin of the interbeds, Beukes (1970) mentioned that the interbeds were also wind deposited, but evidence for aeolian processes within the interbeds was not observed in the Moyeni region.

The presence of the thick ~ 9.5 succession of pillows lavas (Figures 3.11-3.13) are the most distinctive feature of the interaction between lava and water during the formation of the lowermost Karoo lava flows. Pillow lavas are pillow-shaped volcanic rocks that are mostly basaltic composition and form when lava flows into standing bodies of water (lake, sea) or extrudes subaqueously. The rapid lava cooling is linked to the generation of spherical and cylindrical masses that resemble “pillows” with a solid, quenched crust around them, which can easily fragment forming glass-fragment-rich volcanoclastic sediments (i.e., hyaloclastites) between the pillows (Figure 3.9B-D; Cas and Wright, 1987; Jones and Nelson, 1970).

The foreset bedded pillows in Moyeni (Figure 3.11B) can be interpreted as products of an expanding lava delta that was fed by subaerial basaltic lavas that flowed into a standing body of water. The pillow lavas were deposited subaqueously on the inclined front of a lava delta within a lake, which are informally here named as 'Moyeni lava delta' and 'Lake Quthing', respectively (Figures 4.1 and 4.2). The diameter variation of the pillows, as see in the Moyeni outcrop, is dependent on the shape of the pillow and orientation relative of the plane of the outcrop, i.e. tube-like pillows show greater diameters in outcrops that intersect their longest axis at acute angles (Figures 3.11B-D & 4.2B). Similar foreset bedded pillow lavas have also been mentioned by Lock et al. (1974) from the type area of the Barkly East Formation.

However, because pillow lavas occurrences are scattered within the Karoo lava pile, their formation is linked to several isolated standing water bodies (i.e. ephemeral lakes) that were more common during the early stages of Karoo lava effusion.

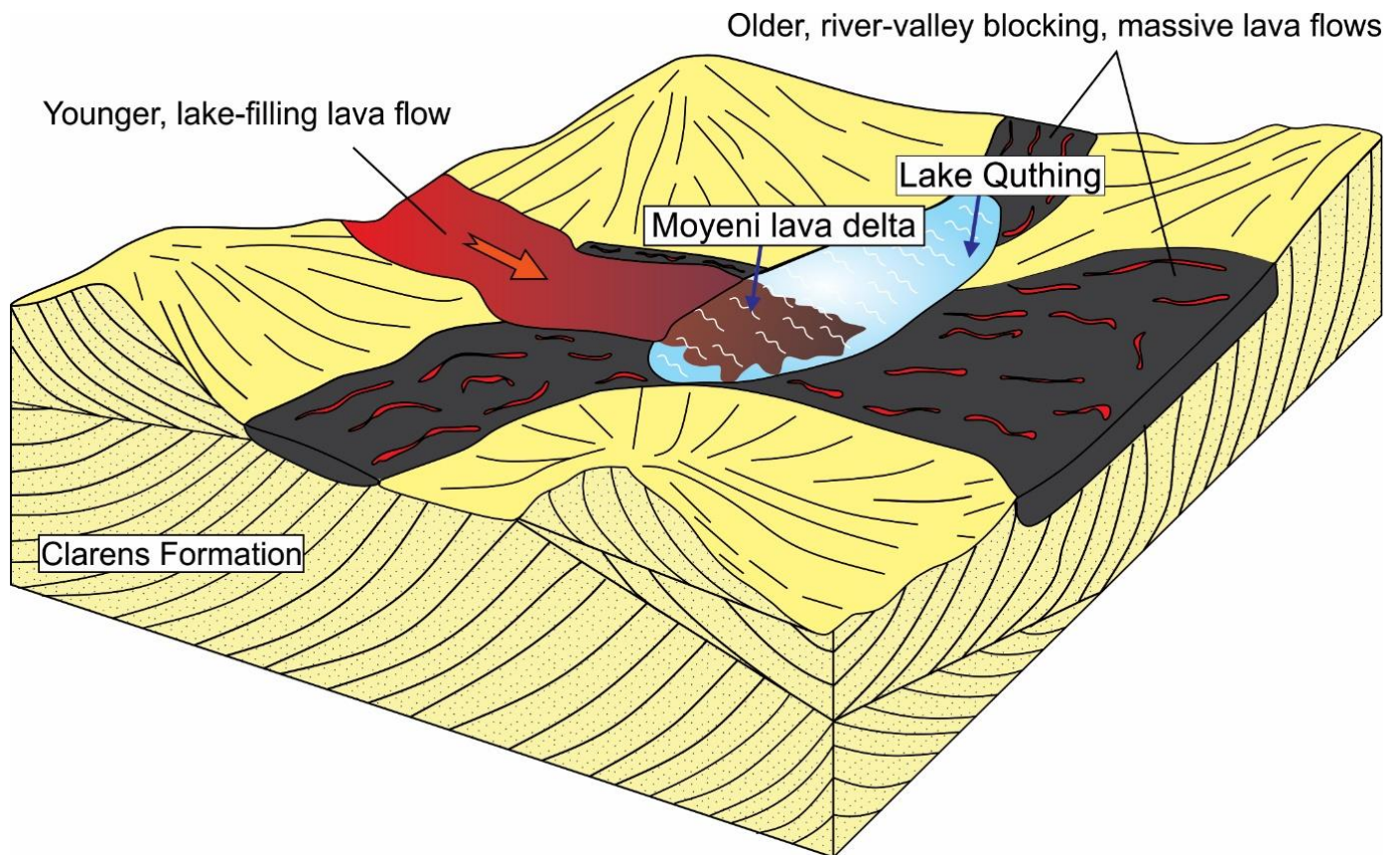


Figure 4.1: Schematic illustration of a lake environment within the lowermost Drakensberg Group. 'Lake Quthing' formed as a massive lava flow dammed the valley and gave rise to deeper temporary depression in the landscape in which surface water could pool. Younger subaerial lavas flowed into 'Lake Quthing' and formed the 'Moyeni lava delta' as well as the pillow lavas along the foreset beds of the subaqueous delta front (see Figure 4.2 as well). Not to scale.

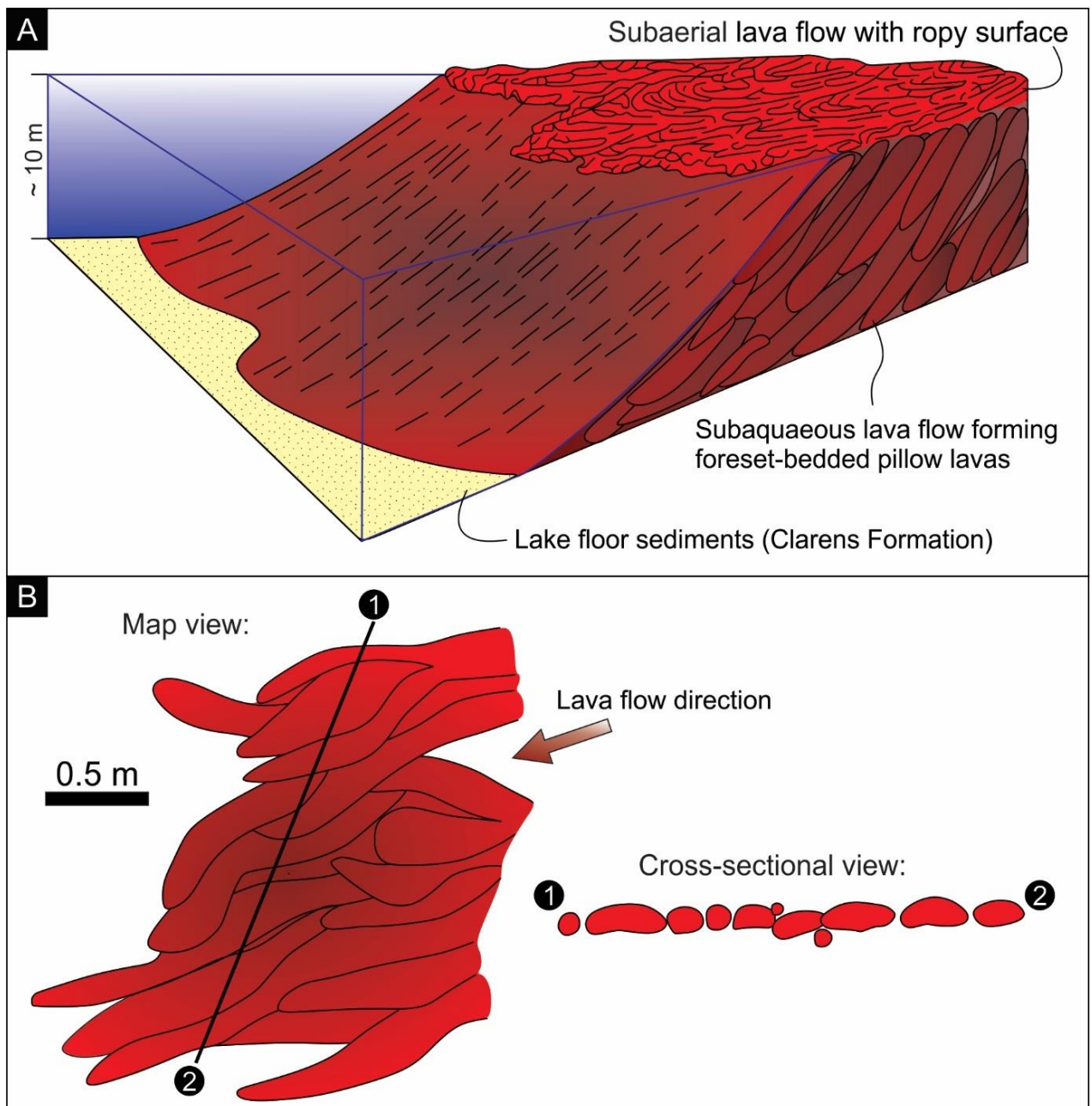


Figure 4.2: Formation of the prograding “Moyeni lava delta” in ‘Lake Qutuig’ as subaerial lava flows turned into subaqueous lava flows upon entering a standing body of water. Through time, this resulted in the lateral expansion of the delta along inclined foreset beds and filling of the lake basin by pillow lavas (modified after Cas and Wright, 1987). (B) Schematic illustration of foreset beds in map view (left) and cross-sectional view (right) to show the diameter variation of tube-like pillow lavas in 2D outcrops.

Over time, the front of the 'Moyeni lava delta' advanced from the lake shoreline into the deeper part of 'Lake Quthing', building a ~9.5-m-thick pile of pillow lavas (Figures 3.12 & 3.13). Using this pillow lava thickness as a proxy, 'Lake Quthing' could have been at least 10 m deep. The impounding of the lake water occurred in topographic low of the uneven land surface that was underlain by unconsolidated aeolian and alluvial sediments of Clarens Formation (Figure 3.13A). The formation of 'Lake Quthing' is linked here to an early subaerial lava flow that obstructed the valley of a local, semi-active river or larger stream (Figure 4.1). The obstruction may be linked to the blockage and inflation of the lava flow due to temporary reductions in lava supply (cf. Jay et al. 2018). When a younger lava flow, subsequent to the formation of Lake Quthing, flowed into the lake, the lava cooled rapidly and formed the foreset bedded pillow lavas along the inclined foreset of the 'Moyeni lava delta' (Figures 3.11B and 4.2). Some of the first pillows that landed on the lake floor, sank into soft lake floor sediment and deformed it further (Figure 3.14C) which also indicates that there was no geological time gap between the deposition of the lake sediments and the extrusion of the lavas. In addition to pillows, Lake Quthing, soon after its formation, also trapped wood-bearing debris flow sediments (Figures 3.13A and 3.14). However, field evidence indicates that except for this initial plant-fragments-bearing, debris flow, 'Lake Quthing' was exclusively filled by pillow lavas (and minor inter-pillow volcanoclastic sediments; Figure 3.11B-D) via the lateral accretion of the subaqueous deltaic foresets on the expanding lava delta. The pillows are capped by a massive, semi-horizontal lava sheet (Figure 3.12), and this can suggest that the lake dried up by the time the next lava flow reached the area. This may also imply that Lake Quthing was not only shallow, but geologically speaking, short-lived. Collectively these findings indicate that when the earliest Karoo lavas poured to the surface, water bodies and vegetation covered the area of Moyeni in Late Pliensbachian - Early Toarcian.

The sills (Figure 3.15), which are documented from the western part of Moyeni, indicate that in addition to the extrusive lavas, the region was prone to subvolcanic activities in form of dolerite intrusions. The impact of the sills is seen in the slight deformation of the uEF

sandstones into which the sills intruded. This occurs when the horizontally propagating magma, which mostly migrates laterally along the bedding planes, cuts across the horizontal strata exploiting a shallow-angle weakness zone (e.g., facies changes, older joints, faults). Because of the virtually identical geochemical composition and similar radiometric ages of the extrusive and intrusive Karoo igneous rocks, they are considered to have formed essentially simultaneously from a huge volume of magma reservoir beneath the surface of southern Africa in the late Early Jurassic (e.g., Marsh and Eales, 1984; Duncan et al., 1997; Moulin et al., 2017).

4.1.4 Breccia Facies

The polygomic breccia facies associated with the eastern fault (Figure 3.16) is interpreted as the product of a hydrovolcanic explosive activity (or phreatic volcanic event), which forms when magma comes into contact with groundwater and subsequently generates steam in the subsurface. The hot steam rises to the surface with explosive violence while penetrating and brecciating the horizontally stratified, older sedimentary rocks and excavating pipe- or funnel-shaped conduits (i.e., diatremes or explosion vents) with the shallow parts of the crust (Svenson et al., 2006). The hydrothermal events within the Karoo Basin have been linked to one or a couple of phreatic events during the Toarcian igneous events of the Karoo-Ferrar LIP (Svenson et al., 2006; Planke et al., 2005).

The clasts in the polymictic parabreccia comprise of green mudstone that are consistent with the uEF, sandstone that are consistent with the Clarens Formation, and amygdaloidal basalts that are consistent with the Drakensberg lavas (Figure 3.16D-G). Thus, the clast lithologies of this breccia facies demonstrate that the brecciation event cut across and fragmented all the geological formations of Moyeni, including the Pliensbachian–Toarcian basalts. The brecciated area also contains a large (tens of meters in diameter) block of basaltic lava that lies below the Clarens-Barkly East contact (Figure 3.24D & 3.16C). These observations

demonstrate that the brecciation (or diatreme event) postdates not only the deposition of the uEF and Clarens Formation but also the extrusion of the initial Drakensberg basalts. The diatreme also postdates the earliest faulting event in this area and its spatial proximity to the fault zone suggests that it may have exploited a weakened damage zone associated with faulting.

4.2 Petrographic analysis

The petrography of sedimentary rocks reflects the main source of the detritus. Although the original composition may be altered through physical and chemical processes, petrography allows for a better understanding of the depositional processes if considered together with other lines of geological evidence. However, it needs to be emphasized that given the few petrographic samples in this study, these petrographic interpretations are preliminary at best. The results of the thin section assessments are summarised in Appendix Table 1A and Figure 3.17. The comparison of the petrographic samples from the three formations exposed at Moyeni shows some similarities and differences, and these are discussed below.

4.2.1 Mineral composition and grain size

As mentioned in the results, based on the mineral composition, the uEF sandstone is classified as a sublitharenite whereas the sandstones from the Clarens Formation and the Barkly East Formation are subarkosic rocks (Figure 3.17A). The macroscopic grain-size evaluations of the five sandstone samples are corroborated by the microscopic observations. The absence of polycrystalline quartz within the uEF sandstone (sample A in Figure 3.17A) may be related to the relative textural maturity of this fine-grained sandstone sample (i.e., polycrystalline quartz fragments are usually larger and common in coarser grained, less mature sandstones in the

Elliot Formation – see Bordy et al., 2004c). The Clarens Formation sandstone samples (Figure 3.17B & C) are very similar compositionally and texturally, except for the slight grain size difference with sample B being relatively coarser grained than sample C (Appendix Table 1A). Microscopically, sample C which was taken directly at the Clarens-Barkly East contact contains no lithic fragment that could be positively identified as basalt. The sandstone interbeds from the Barkly East Formation (lower Drakensberg Group; Figure 3.17E & F) show similarities to the Clarens sandstones in terms of grain size (they are all medium grained sandstones) and mineral composition (Appendix Table 1A), which may be an indication of a similar sedimentary source and processes of deposition. For example, Eriksson (1981) suggested that parts of the Clarens Formation are loess deposits, and while direct evidence for this idea is not found in the petrographically studied samples (e.g., very angular silt size grains are uncommon), given the overall sedimentological properties of the Clarens Formation (e.g., very large- scale cross-beds), this proposition cannot be dismissed here.

The presence of the feldspars within the samples may be used to infer climatic conditions. For example, a high feldspar content may be indicative of a dry, arid depositional setting and may also suggest an increase in sediment supply (Visser and Botha, 1980; Visser, 1984; Eriksson et al., 1994; Bordy et al. 2004c). Although, it appears that the feldspar content in the studied sandstone samples increases with increasing stratigraphic age (from the uEF to the Barkly East Formation), this cannot be linked to a relative increase in aridity over time not only because the samples are not statistically robust in number, but also because other more reliable field evidence suggests that the depositional setting was wet in the lowermost Barkly East Formation (see section 4.1 in this chapter).

Due to the very fine grain sizes of the minerals in the mudstone (Figure 3.17D), it is difficult to identify their exact mineral composition with the sole use of optical petrography. However, the scope of sectioning of this mudstone sample was not for classification, but to identify the nature of lamination in the sample, which seems to be due to the alignment of the flat mineral particles. The angularity of the silt to very fine-grained sand particles are expected in this

sample, because this grain size population is usually transported in suspension where rounding is limited (Boggs, 2009).

4.2.2 Sorting

The moderate to well-sorted grains across the samples indicate that there were regular sedimentary processes occurring that increased the sorting of the samples (e.g., high intensity traction currents in stream flow, recycling, aeolian transport - Boggs, 2009). However, the poorly sorted sample C of the Clarens Formation (Figure 3.17C) may indicate that this sample that resulted from rigorous, but intermittent, short-lived sedimentary process typical in sediment transporting agents in semi-arid systems such as ephemeral streams, playa lakes and sheet flows or relatively weak aeolian processes (Eriksson, 1981; 1994).

4.2.3 Maturity

The abundance of the more resistant monocrystalline and lack of the less resistant polycrystalline quartz in all samples can suggest these rocks were deposited further away from the source or close to the source but via high intensity transporting agents. However, the low to moderate level of maturity across the sandstone samples suggest that the travel distance and rigour of transport were relatively moderate (Boggs, 2009). The sub-angular to sub-rounded of the grains in all medium-grained sandstone samples (Figure 3.17; Appendix, Table 1A) can also be attributed to the moderate to short travel distance, or many be an indication of deposition with in low-energy sub-aqueous environment (Eriksson, 1981).

4.2.4 Source rocks

The source rocks for the sandstone samples is interpreted by using the theoretical sandstone provenance fields determined by Dickinson (1985) in combination with the Qm-F-Lt ternary

diagram (Figure 4.3). The distribution of the five samples in the ternary diagrams (Figure 4.3) shows no distinct temporal changes in the composition, as the samples plot in the 'continental block provenance' field apart from the uEF sample which plots in the 'recycled orogen' field (Figure 3.17A). Continental block provenances are generally located within continental interiors (i.e., cratonic areas) and basement uplift provenances (Dickinson, 1985). The subarkose sandstones of the Clarens and Barkly East Formations reflect a continental source with exposed granitic-source rocks and recycled sedimentary rock types typical in continental rift settings (Boggs, 1995; Bordy et al., 2004c). The sublitharenite/litharenite of the uEF has composition indicative of a recycled orogen source, which means that sample was sourced from orogenic belts where the parent rocks are typically sedimentary (Ingersoll et al., 1984; Dickinson, 1985; Boggs, 1995). Consequently, a plausible sediment source for this sample is the Cape Fold Belt and the older Karoo rocks to the south, which themselves have a recycled sediment history (Catuneanu, 1998; Bordy et al., 2004c).

4.2.5 Sandstone classification

The mineral composition (normalised to 100 and free of accessory minerals; Appendix Table 1A) of all the samples with exception to the mudstone sample D, are plotted on the Quartz-Feldspar-Lithic fragment ternary diagram (Figure 4.3). The mudstone sample is not shown as the ternary diagram is exclusively for the classification of sandstone. The sandstone samples of this study are illustrated in the compositional context of Stormberg Group sandstones, which is a regional database compiled by Hanson et al. (2009) and is based on previous studies (Eriksson, 1984, Johnson, 1991; Hancox, 1998; Bordy et al., 2004c; Figure 4.3).

The ternary diagram indicates that the uEF sandstone is a sublitharenite/ litharenite as it plots on the boundary of these fields, whilst the rest of the sandstone samples from both the Clarens Formation and the sandstone interbeds within the Drakensberg Group are classified as subarkoses (Figure 4.3A). Using the classical sandstone provenance ternary diagram of

Dickinson (1985; Figure 4.3A), the samples plot in provenance fields that indicate that the source of the sediments is a recycled orogen during the uEF time, and a continental block later on during the deposition of the Clarens and Barkly East Formations (Figure 4.3B). The samples from the uEF and Clarens Formation plot outside their respective uEF and Clarens fields, which were established by Hanson et al. (2009; Figure 4.3B). This is due to the fact that visual estimates were used for this study, thus there may be slight discrepancies in the mineral compositions. Moreover, except for the Elliot Formation samples, the number of samples for the Clarens formation from the previous studied are low thus preliminary and the field itself may not be reliable.

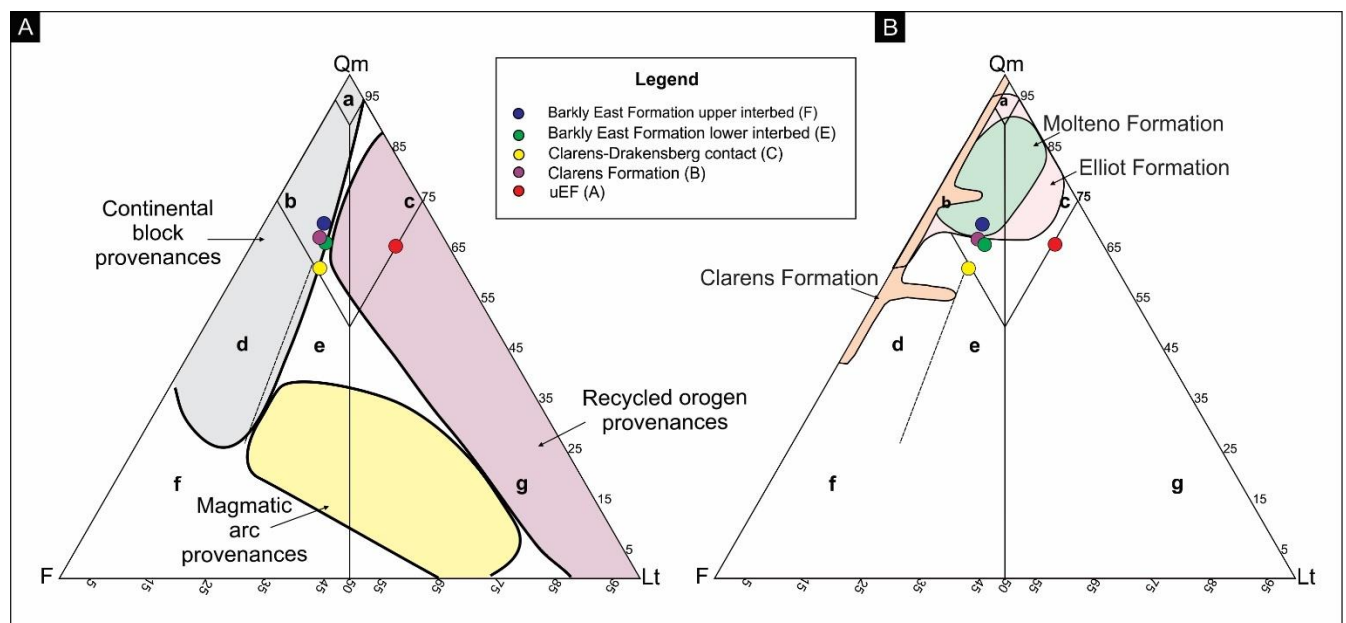


Figure 4.3: Sandstone classification ternary diagrams showing: (A) the Moyeni sandstones relative to classical sandstone provenance fields and (B) relative to the other regional upper Karoo samples. Classification fields a-g are after Pettijohn et al. (1987), provenance fields are after Dickinson (1985) and the Karoo sandstone fields are based on work by Hanson et al. (2009), who derived the Molteno field from Eriksson (1984), Johnson (1991) and Hancox (1998); the Elliot field from Eriksson (1984), Johnson (1991) and Bordy et al. (2004c); the Clarens field from Eriksson (1984) and Johnson (1991). Abbreviations: Qm = Monocrystalline quartz; F = Feldspar; Lt = Total lithic fragments; a = quartz arenite, b = subarkose, c = sublitharenite, d = arkose, e = lithic arkose, f = arkosic arenite, g = litharenite.

4.3 Ichnology

The results of the ichnological analysis in the uEF and Clarens Formation in Moyeni offers insight into the diverse life forms that existed in the Hettangian to the Pliensbachian palaeoenvironments. It appears that in spite of climatic changes suggested by the sedimentary facies of these rocks (see previous sections), these ecosystems were suitable for the survival and growth of both numerous vertebrates and invertebrates.

4.3.1 Lower Moyeni

The ripple marked sandstone palaeosurface with abundant and diverse vertebrate tracks and invertebrate traces (Figure 3.19A-B), as well as the massive mudstone below and above the palaeosurface, are interpreted to have deposited in a low energy fluvial depositional environment. Specifically, according to Smith et al. (2009) and Wilson et al. (2009), the palaeosurface was preserved on the inside of a meandering river loop, over a sandy point bar unit. The algal matted surface (Figure 3.19C) also demonstrates very gentle currents or no currents, a suitable environment for microbial activity (Smith et al., 2009), which together with the nutrient-rich sediments, sustained a diverse community of burrowing invertebrates.

The dominant tridactyl tracks with the robust and rounded digits (Figure 3.18B & C) can be classified into the ichnogenera *Anomoepus* (Wilson et al., 2009; Marsicano et al., 2014), which was originally termed as *Moyenisauropus* by Ellenberger (1974). Although, the tracks do show varying morphological detail (e.g. some tracks have more rounded digits than other tracks), which could be attributed to behavioural or preservation variation and the substrate and track interaction (Wilson et al., 2009), the main diagnostic features of *Anomoepus* tracks are the tridactyl pes with the splayed and broad digits, which are fairly blunt at their tips (Figure 3.18C; Ellenberger, 1974; Wilson et al., 2009). The tridactyl pes print indicates that the trackmaker

was functionally bipedal, however the preservation of the slightly impressed five-digit manus, in some cases, suggest that the trackmaker shifted between a quadrupedal and bipedal stance (Olsen and Rainforth, 2003; Wilson et al., 2009). Based on this evidence, these tracks can be attributed to herbivorous ornithischian dinosaurs, which are documented from the body fossil record of the Elliot Formation (e.g., Knoll, 2005; Butler et al., 2007). The specific ornithischian dinosaurs that could have been roaming in lower Moyeni are *Heterodontosaurus* and *Lesothosaurus* (Knoll, 2005).

The larger tracks with elongate pointy digits and preserved claw marks (Figure 3.18D) are interpreted as tracks of a bipedal dinosaur. The narrow digit morphology and the projection of digit III relative to the other digits allow for these tracks to be identified as the ichnogenera *Grallator* (Ellenberger, 1974; Wilson et al., 2009; Marsicano et al., 2014). *Grallator* tracks can be attributed to theropod dinosaur as the tracks have no metatarsal traces and the functionality of the elongate digit III of the pes allows for a bipedal posture (Olsen et al., 1998; Wilson et al., 2009). Depending on the size of the *Grallator* tracks, the specific track-maker dinosaur can be narrowed down to the common Early Jurassic theropods, which are either to the larger *Dracovenator regenti* and/or to the smaller *Coelophysis* (Yates, 2005; Wilson et al., 2009).

The 4-toed manus and 5-toed pes pairs with the associated drag marks (Figure 3.18E) has been suggested to be part of an *Episcopopus ventrosus* trackway (Ellenberger, 1974; Smith et al., 2009; Marsicano et al., 2014). It is evident that the track maker was quadrupedal due to the presence of the preserved manus and pes pairs. The initially interpreted trackmaker was that of a primitive crocodylian (Ellenberger 1974) that was described from uEF body fossil remains. However, Marsicano et al. (2014) attributed the tracks to a temnospondyl, a long amphibian tetrapod with a stout body and short-limbs. This animal dragged its body along the substrate, similar to that of a modern-day crocodylian, which is indicated by the persevered drag marks alongside the tracks. Finally, the much smaller ~2 - 3 cm manus and pes tracks (Figure 3.18F) can be tentatively assigned to *Batrachopodiscus* ichnotaxa and attributed to a small quadrupedal amphibian-like, crocodylomorph track maker.

4.3.2 Upper Moyeni

The morphological features (e.g., claw marks) and measurements of the large tridactyl tracks found on the palaeosurface at upper Moyeni (Figure 3.20B-3) are consistent with the diagnostic features of the ichnogenus *Eubrontes* (cf. Olsen et al., 1998). *Eubrontes* are generally characterised as tracks made by large bipedal and tridactyl theropods with average pes length of >25 cm, a L/W ratio of 1.4-1.5 and a heel area of the track accounting for 29% of the of the footprint length (e.g., Lockley and Mickelson, 1997; Olsen et al., 1998; Lucas et al., 2006). Based on this, the large upper Moyeni tracks are attributed to large theropod dinosaur trackmakers, specially *Dracovenator*, which is known from the body fossil record of the uEF. However, based on the morphological features and lengths up to ~ 48 cm, the largest upper Moyeni ichnites are broadly similar to the large Hettangian tracks (L = ~ 54 cm) from Poland as well as *Megalosauripus*, which is 10 cm larger than that of *Eubrontes*, has a L/W ratio ranging between 1.45-1.85 and heel area of the track accounts for 33% of the total foot length (Lockley et al., 1996; Gierlinski et al., 2001). Five of the upper Moyeni tracks that are smaller than 25 cm are classified as either smaller *Grallator* or larger *Anchisauripus* ichnotaxa, although the latter can be considered synonymous with *Eubrontes* (Milner et al., 2006). Similar to the track makers at lower Moyeni, the associated trackmaker of these smaller tracks are theropod dinosaurs that are either smaller individuals of *Dracovenator* and/or larger *Coelophysis* (Yates, 2005; Sciscio et al., 2016).

This ichnotaxonomic uncertainty of the upper Moyeni tridactyl tracks adds to the debate stemming around the *Grallator-Anchisauripus-Eubrontes* plexus and lack of reliable diagnostic features to distinguish these ichnogenera (Lucas et al., 2006; Lockley, 2010). Furthermore, the varying degrees of preservation and morphological features (Figure 3.20B), which possibly reflects changes in the rheology of the substrate from wetter, water-saturated to drier, more consolidated areas (Lockley, 1986; Buatois and Mangano, 2011; Sciscio et al., 2016), further complicates the ichnotaxonomic assessment of these tracks.

The upper Moyeni vertebrate burrow cast (Figure 3.21) in the uEF is interpreted to be a tetrapod burrow similar in size and morphology to the only other vertebrate burrow cast that was reported to-date from the uEF (Bordy et al., 2016). Because of its kidney-shaped cross-sectional outline, this upper Moyeni vertebrate burrow cast can be attributed to *Reniformichnus* ichnogenera (Krummeck and Bordy, 2017). The exact trace maker responsible for the construction of the burrow is not certain but based on the presence of the scratch marks on the side of the burrow cast (Figure 3.21C & D), the burrowing animal had claws and excavated sideways in a downward motion (Bordy et al., 2009). The burrow-hosting, pedogenically altered mudstone unit (Figure 3.21A) suggests that the animal burrowed into a soil ecosystem. The scratch marks also suggest that the sediment was competent enough, possibly due to some slight pedogeneis, to prevent caving in of the open burrow but was also moist enough to preserve the scratch marks (Bordy et al., 2009). The isolated, semi-horizontal burrow cast with its fairly uniform diameter could suggest that the burrow may have been a temporary hiding or resting place and not necessarily a permanent habitat (e.g., Hasiotis et al., 1999; Groenewald et al., 2001; Bordy et al., 2009). The bioturbation on the topside of the burrow cast indicates that the burrow-filling sediment was nutrient rich for other smaller, burrowing invertebrate organisms that were likely part of the soil biota.

4.3.2 Phahameng

The two-step trackway in the lowermost Clarens Formation at Phahameng (Figure 3.22) shows similarities to the tracks of upper Moyeni. Based on the measurements of the tracks (average L = ~ 34 cm), these represent *Eubrontes* tracks with the trackmaker being a larger theropod dinosaur, possibly *Dracovenator* (cf. Yates, 2005; Sciscio et al., 2016).

4.4 Structural geology of Moyeni

4.4.1 Normal Faulting

Normal faults, as seen in the study area (Figures 3.23-3.25), are non-vertical faults which downthrow the hanging wall from the underlying footwall. These faults displace rocks which have been deformed along a slip surface through intense shearing, which in turn deforms the surrounding rocks through more gentle and brittle deformation (Fossen, 2010). Due to the mostly horizontal attitude of the strata in the study area it is relatively easy to determine the displacement of the faults. The abrupt change in lithology indicates the stratigraphic separation which, combined with the dip of the fault, can be used to calculate the fault displacement. Faulting often occurs along pre-existing weaknesses in the rocks, which may be along the lithological interfaces or along dolerite dykes (Fossen, 2010). Once a fault occurs along a weak zone and a fault surface is established, it is highly likely that the build-up of renewed stress will cause failure. The deformation of a porous rock such as the sandstones in the Clarens Formation, allows for the faulting to occur along a slip surface. A slip surface is mechanically weak and therefore can accumulate meters of slip, which is what has been observed in the study area. The dipping of the small-scale faults towards the larger scale fault is a clear characteristic of antithetic faulting (Fossen, 2010; Figure 3.25). The antithetic faults that are associated with these normal faults can be interpreted as part of the damage zone that surrounds the main fault or fault core. The damage zone is characterised by the deformed wall rocks around the fault core, as a result of the initiation, propagation and build-up of the slip along the fault (Cowie and Scholz, 1992; Kim et al., 2004). The faults mapped generally trend in the ENE-WSW direction which is a similar trend to the dolerite dykes that dominate area around Moyeni. The general trends of the mean structural features observed during the geological mapping of Moyeni is corroborated by the 1: 100 000 scale geological map of the Quthing District (3027B; Lesotho Government, 1982).

4.4.2 Timing of the faulting

One of the main indicators of the timing of the faults is the variation in thickness within the Clarens Formation in the eastern region of the study area. Determining the exact time of commencement of the faulting is difficult. However, the fact that the relatively coarse-grained cliff forming sandstone within the lower units of the Clarens Formation does not increase in thickness across the fault, but the upper relatively finer-grained sandstone layer thickens towards the south (Figure 3.23B), suggests that the fault at least initiated sometime during the deposition of the Clarens Formation. Because the fault does not displace the Clarens-Barkly East contact in that locality (Figure 3.23B), the deformation on that fault strand ceased by the end of the deposition of the Clarens Formation. The fault-related variation in thickness of the Clarens Formation on both the eastern and western part of the area (most clearly seen in the east, Figure 3.23), is a key observation which serves as evidence for syn-sedimentary faulting (i.e. the normal faulting) that occurred during the deposition of the Clarens Formation (Childs et al., 2003; Bordy et al., 2004a). Syn-sedimentary faulting is synonymous with growth faulting (Childs et al., 2003). In general, growth faults develop due to contemporaneous faulting and sedimentation, and are characterized by the abrupt increase in thickness of the related strata across the fault (Edwards, 1976; Hardin and Hardin, 1961). Therefore, as the faulting occurs, and the hanging wall is displaced, the accommodation space increases, allowing for sediments to be deposited within the faulting zone. The other faults observed (Figure 3.24C & D) offset the Clarens-Barkly East contact, and therefore must have been active after the deposition of the Clarens Formation ended. However, it is not possible to determine if these fault strands collectively record a single period of deformation spanning the boundary between the deposition of the Clarens Formation and Barkly East Formation or if some of the faulting represents a much later reactivation of the fault zone.

These normal faults (Figures 3.23-3.25) could be interpreted as evidence for the changeover from a compressional to extensional tectonic regime in the basin during the Early Jurassic and could be linked to the first signs of Gondwana break-up (Bordy et al., 2004a). Prior to the deposition of the upper Stromberg Group deposits, the Karoo Basin was a compressive system, and the deformation in and near the Cape Fold Belt was predominantly represented as high angle thrust faults and associated gravity folds (Lock, 1974; Catuneanu et al., 1998). The thrust faulting may have had an influence on the sedimentary rocks of the basin up to the deposition of the lower Elliot Formation, however the thrusting completely diminished by the time the uEF deposited (Bordy et al., 2004a). Deformation within the Stromberg Group, specifically the Elliot and Clarens Formations is rare, however, these rocks especially the upper Elliot Formation represents an important time period tectonically for the timing of pre-break-up rifting (Bordy et al., 2004a). A previous study by Bordy et al. (2004a) has also reported pene-contemporaneous deformation features, which includes one large 'epi-depositional' normal fault and one large-scale convolute bedding structures, the latter tentatively linked to seismic activity. These deformation features were found in the upper Elliot Formation, ~ 80 km south-southwest from Moyeni in the Eastern Cape of South Africa. The normal fault mentioned by Bordy et al. (2004a) is also interpreted to have been a consequence of the change to in tectonic regime and as early heralds of Gondwana break-up during the early part of the Early Jurassic. Thus, the occurrence of the normal faults in Moyeni can be associated with the rifting phase within the Karoo Basin. The faults indicate that there was extensional tectonic movement during the deposition of the Clarens Formation and it is plausible that the normal faulting occurred along pre-existing structural weaknesses in the northern part of the Namaqua-Natal Mobile Belt, which is the basement below the main Karoo Basin in the Moyeni area (Bordy et al., 2004a; 2005). Further structural studies however, within the Karoo may aid in better understanding of the structural evolution of syn-sedimentary faulting and the impact on the rifting event of Gondwana.

Alternatively, this fault zone could be related to local stresses associated with the intrusion of dolerite sills. According to Dusat (1979), who observed the structures within the Stormberg-Drakensberg contact around Lesotho, large structural “highs” and “lows” can be recognised based on the changes in elevation of the Stormberg-Drakensberg contact. The highs were presumed to be caused by doming, as a result of dolerite intrusions, and the lows forming troughs. Quthing district in which Moyeni is located, is situated within a structural low. The boundaries between the structural highs and lows are either gradual transitional zones or marked by faults or monoclinical flexures. Dusat (1979) noted one significant fault which sharply defined the transition from the Thaba-Phechela-Mafeteng high (~ 80 km northwest from Moyeni) to the Quthing-Makhaleng low. The downthrow of the faults observed, are all towards the side of the structural lows (Schmitz and Rooyani, 1987). The faulting described in Moyeni is not necessarily similar to the faulting noted by Dusat (1979) in that the faulting occurred within the structural low rather than at the interface between the structural high and low. Furthermore, the changes in elevation of the Stormberg-Drakensberg contact may be also explained with palaeotopographic features, because the dune fields of the Clarens Formation could have had a significant relief of up to several tens of metres that was buried by the rapid outpouring of the continental flood basalts (e.g., Beukes, 1970).

The Moyeni dolerite sills form part of the subvolcanic plexus of dykes and sills which intruded, in enormous number, across southern Africa (Duncan et al, 1997). The regional commencement of the dolerite intrusions is considered coeval with the extrusion of the Karoo continental flood basalts, both of which are part of the Karoo-Ferrar Large Igneous Province (LIP; Duncan et al., 1997). The timing of the main basaltic magmatism in the Karoo-Ferrar LIP was repeatedly constrained to a Pliensbachian–Toarcian age (183 ± 1 Ma – see Duncan et al., 1997; Moulin et al., 2017). Thus, timing of the dolerite sills of Moyeni are synchronous with the emplacement intrusive and extrusive rocks of the Karoo-Ferrar LIP in the region. According to Encarnacion et al. (1996), however, the rifting event which triggered Gondwana break-up may have occurred >10 Ma after the main eruptive phase in Karoo-Ferrar LIP.

Therefore, the normal faults in Moyeni may range in age from 173 to 183 Ma (from late Pliensbachian to early Aalenian), however the syn-Clarens normal faulting at Moyeni, together with the syn-sedimentary normal fault in the Eastern Cape, pre-date the effusion of the Karoo lavas, and may be considered as either very early heralds of Gondwana break-up or a localized extensional event in the Pliensbachian that was unrelated to Gondwana break-up.

4.5 Palaeoenvironmental changes

4.5.1 Hettangian

The sedimentological evidence (i.e. facies analysis of the uEF mudstone, sandstone, gravel facies associations) suggests that during the deposition of the uEF, Moyeni was part of a low energy fluvial system, which was prone to episodes of flash flooding as well as desiccation. The presence of the mudstones indicates the lower energy floodplain environments with the overbanks dotted by shallow standing bodies of water i.e. lakes. The large-scale desiccation cracks that cut the mudstone beds are evidence for pervasive drying out of the initially moist muddy strata. In contrast, the fine- to medium-grained, massive to low-angle cross bedded sandstone beds indicate the periods of relatively higher energy currents and flash floods. These flooding events brought relatively coarser-grained sediments via wide yet shallow fluvial channels and/or crevasse splays (Bordy et al., 2004b). The occasional but very high energy events are also implied by the gravel facies deposits which were transported through vigorous yet rare debris flow events. The climatic conditions at this time was semi-arid, with seasonal, and likely high intensity rain. The palaeoenvironment and climate during the Hettangian was also able to support large vertebrates such as carnivorous theropods, herbivorous ornithischian dinosaurs, unknown burrowing vertebrates, various invertebrates as well as flora. Although a similar description and palaeoenvironmental reconstruction of the uEF has been proposed in previous studies undertaken in Lesotho as well South Africa specifically by Visser and Botha (1980), Eriksson (1984), Smith et al. (1993), Bordy et al. (2004a, b, c), the current study corroborates and reinforces these previous interpretations.

4.5.2 Sinemurian – Pliensbachian

The transition from the uEF to the deposition of the Clarens Formation clearly displays the gradual change in depositional environment and the change in climate. The shift from moderate to high energy fluvial deposits to mainly aeolian deposits indicates that the environment was initially seasonally wet with lakes and rare flash floods in the form of rivers, streams and debris flows, and thus, allowed for the preservation of fluvial-lacustrine sediments. Evidence is seen in the lower and upper parts of the Clarens Formation such as the mudstone deposits representing the low energy floodplain and/or lake deposits and the massive to cross-bedded sandstone representing the fluvial channels. However, overtime aridification gave rise to an aeolian system, which was dominated by eastward migrating, large sand dunes (Bordy and Head, 2018). The aridification is manifested by the thick prominent large-scale cross-bedded sandstone. The palaeoclimate thus, shifted from semi-arid with moderate to low rainfall, which provided water to rivers or streams along the desert margin, to an arid climate, dominated by aeolian processes with very little precipitation (Beukes, 1970). However, during the terminal Clarens times the environment in Moyeni comprised of temporary streams and lakes, attesting to a wet desert environment.

The presence of fossilised flora as well as the vertebrate tracks not only at the base but also towards the upper part of the Clarens Formation do, however, imply that the palaeoenvironmental conditions in Sinemurian-Pliensbachian were not too harsh and could, at least episodically, sustain a diverse biota (e.g., Haughton, 1924; Truter, 1945; Meijs, 1960; Ellenberger 1970; van Eeden and Keyser, 1971; Jubb, 1973; Forey and Gardiner, 1973; Van Dijk et al., 1978; Kitching and Raath 1984; Tasch 1984; Olsen and Galton 1984; Van Dijk 2001; Bordy and Catuneanu, 2002; Bamford, 2004; Knoll, 2005; Raath and Yates, 2005; Bordy, 2008; Bordy et al., 2009; Bordy and Head, 2018). These interpretations are substantially corroborated by studies conducted through sedimentary facies analysis by Beukes (1969; 1970), Eriksson (1979; 1981; 1986), Holzförster (2007) and summarized in Bordy and Head (2018). Beukes (1970) specifically attributed the sediments of the Clarens

Formation to both a wet and dry depositional environment. He also postulated that sedimentation occurred with the interior of a large desert basin near the centre of Gondwana during the Sinemurian-Pliensbachian.

4.5.3 Pliensbachian – Toarcian

Towards the end of the Pliensbachian and into the early Toarcian, the palaeoenvironment was dominated by the Karoo volcanic event, as seen by thick package of basaltic lavas (Drakensberg Group). However, the palaeoclimate reverted back from arid to semi-arid conditions, and seasonally wet periods allowed sedimentation in ephemeral rivers and lakes. The presence of the sandstone interbeds and their sedimentary structures indicate that sedimentation occurred within a fluvio-lacustrine environment, which in turn suggests that the volcanic activity was intermittent, and when it was brought to a halt, the accumulation of clastic sediments took place. The presence of the pillow lavas also serves as evidence that the land surface was again partially covered by temporary rivers and lakes. The pillow lavas found within southern Moyeni and elsewhere in the lower Drakensberg Group of South Africa (e.g., Lock et al. 1974), support the notion of Bond et al. (1970) and McCarthy (1970) who suggested that wet conditions persisted, during the Early Jurassic (Toarcian), periodically over large areas of southern Africa. Currently, the potential link between this wet period in the Toarcian and the atmospheric perturbations due to the gas emissions of the Karoo-Ferrar LIP (e.g., Moulin et al., 2017) remains unstudied in southern Africa (Bordy et al., 2018).

4.5.4 Early Jurassic Palaeogeography

The main factor that influenced the palaeoclimate and in turn the palaeoenvironment in the Early Jurassic of the study area was the position of the study area within southern Gondwana as well as the latitudinal position of the supercontinent during that time, or in short, the Early Jurassic palaeogeography of Gondwana. Because southern Gondwana moved out of its

position near the South Pole the since Latest Carboniferous by slowly drifting and rotating in a northward direction, the climate and in turn the depositional environments in the MKB shifted progressively from polar to semi-arid subtropical conditions (Anderson and Schwyzer, 1977; Smith et al., 1993). In this case, during the Early Jurassic, this region of Gondwana was situated within the subtropical belt (~45° latitude) where the southern subtropical high-pressure cell dominated the circulation pattern. The area was also dominated by a north-westerly wind system (Scotese et al., 1999; Bordy and Catuneanu, 2002; Veevers, 2004). Modern analogues of these type of environments, where the depositional environment is dominated by north-westerly winds are found in the present-day subtropical belts i.e. the Kalahari Desert of Namibia (southern Africa) and the northern part of the Sahara Desert (Scotese et al., 1999; Bordy and Catuneanu, 2002). While the deposition of the uppermost Karroo succession in a predominantly semi-arid and arid environment can be confidently linked to the subtropical position of Gondwana in the Early Jurassic, the position of the study area within Gondwana and the diminishing orographic effect of the Cape Fold Belt on the regional rainfall pattern during that time require further regional investigation.

5 Conclusion

The upper Karoo rocks at Moyeni present evidence for changes within the depositional environment, palaeoclimate and regional geodynamics. Describing the regional sedimentary lithofacies of the area has shown the following trends within the uEF, Clarens and Barkly East Formations:

The uEF was dominated by a fluvio-lacustrine setting with thick mudstone packages and channel sandstones. The very fine- to fine- grained channel complex sandstone deposits are characterised as massive, ripple cross-laminations (Sr) and/or low-angle cross-bedding (Sp) beige sandstones. The sandy siltstone and mudstone facies with *in-situ* carbonate nodules and desiccation cracks represent the flood plain deposits within a semi-arid climate. The gravel deposits are not as frequent but indicate events of the highest energy levels which occurred through fluvial processes and debris flows. Sedimentological evidence indicates that in the Hettangian the area was prone to flash floods and drying in a generally low-energy depositional system with small rivers and shallow lakes.

The uEF-Clarens contact occurs at irregular elevations throughout the study area, which can reflect the gradual transition from a fluvio-lacustrine to an aeolian depositional environment within a wet desert setting. On the other hand, the increasing abundance of water-laid deposits (channel sandstones and subordinate mudstones) and decreasing large-scale cross-bedded sandstone proportion towards the top of the Clarens Formation suggest that with time the aeolian depositional environment gradually diminished, and wetter conditions became more established. The ichnological diversity from both uEF and the Clarens Formation (Figure 3.14-3.18), indicate that during the Early Jurassic (Hettangian- Sinemurian) the environment could sustain a relatively varied and abundant biota.

The extrusion of the early Drakensberg lavas, specifically where the pillow lavas are present (Figure 3.10), occurred before the consolidation of the Clarens Formation could take place.

The evidence for this is seen in the localised soft-sediment structures in the uppermost Clarens beds into which pillow lavas are deeply embedded. On one hand, this indicates the rapid environmental transition between the Clarens and Barkly East Formations, and demonstrates that the contact between the two units is conformable (i.e., no stratigraphic gap between the Stormberg and Drakensberg Groups) at Moyeni. Furthermore, this also supports the idea that wetter conditions, that became more established in the late Clarens times, persisted and became even more dominant during the outpouring of the first Karoo lavas.

The geological mapping of the Moyeni area shows that the study area was structurally deformed by ~ESE-WNW trending normal faults, some of which appear to have been active during the deposition of the Clarens Formation. This syn-sedimentary normal faulting, even though localised, may be associated with incipient rifting and thus with the changeover from a compressional to extensional tectonic regime in the main Karoo Basin during the Early Jurassic. In this way, the Moyeni rock record contains one of the earliest signs of Gondwana break-up.

6 References

Abrahams, M., Bordy, E.M., Sciscio, L., Knoll, F. 2017. Scampering, trotting, walking tridactyl bipedal dinosaurs in southern Africa: ichnological account of a Lower Jurassic palaeosurface (upper Elliot Formation, Roma Valley) in Lesotho. *Historical Biology*, 29, 958–975.

Allen, J.R.L. 1984. *Sedimentary structures, their character and physical basis* (Developments in Sedimentology, 30). Elsevier, Amsterdam, 544-560.

Anderson, J. M. and Schwyzer, B. U. 1977. The biostratigraphy of the Permian and Triassic. Part 4. Palaeomagnetic evidence for largescale intra-Gondwana plate movements during the Carboniferous to Jurassic. *Transactions Geological Society of South Africa*, 80, 211-234.

Bamford, M.K. 2004. Diversity of the Woody Vegetation of Gondwanan Southern Africa. *Gondwana Research*, 7, 153-164.

Bangert, B., Stollhofen, H., Lorenz, V., Armstrong, R. 1999. The geochronology and significance of ash-fallout tuffs in the glaciogenic Carboniferous-Permian Dwyka Group of Namibia and South Africa. *Journal of African Earth Sciences*, 29(1), 33-49.

Beukes, N.J. 1970. Stratigraphy and sedimentology of the Cave Sandstone stage, Karoo System. In: *Proceedings 2nd IUGS Symposium on Gondwana Stratigraphy and Palaeontology*, Pretoria, CSIR, 321–341.

Blackburn, T.J., Olsen, P.E., Bowring, S.A., McLean, N.M., Kent, D.V., Puffer, J., McHone, G., Rasbury, E.T., Et-Touhami, M. 2013. Zircon U-Pb geochronology links the end-Triassic extinction with the Central Atlantic Magmatic Province. *Science*, 340(6135), 941-945.

Blodgett, R.H. 1988. Calcareous palaeosols in the Triassic Dolores Formation, southwestern Colorado. *Geological Society of America Special Paper*, 216, 103-121.

Boggs, S. Jr. 1995. *Principles of sedimentology and stratigraphy* 2nd edition. Englewood Cliffs, New Jersey, USA: Prentice-Hall Inc.

Boggs, S. Jr. 2009. *Petrology of sedimentary rocks*, 2nd edition. Cambridge, England: Cambridge University Press.

Bond, G., Wilson, J. F., and Raath, M. A. 1970. Upper Karoo pillow-lava and a new sauropod horizon in Rhodesia. *Nature*, 227, 1339.

Bordy, E.M. and Catuneanu, O. 2001. Sedimentology of the upper Karoo fluvial strata in the Tuli Basin, South Africa. *African Earth Sciences*, 33, 605-629.

Bordy, E.M. and Catuneanu, O. 2002. Sedimentology of the Beaufort-Molteno Karoo fluvial strata in the Tuli Basin, South Africa. *South African Journal of Geology*, 105, 51-66.

Bordy, E.M., Hancox, P.J. and Rubidge, B.S. 2004a. Basin development during the deposition of the Elliot Formation (Late Triassic - Early Jurassic), Karoo Supergroup, South Africa. *South African Journal of Geology*, 107, 397-412.

Bordy, E.M., Hancox, P.J. and Rubidge, B.S. 2004b. Fluvial style variations in the Late Triassic-Early Jurassic Elliot formation, main Karoo Basin, South Africa. *Journal of African Earth Sciences*, 38, 383–400.

Bordy, E.M., Hancox, P.J., Rubidge, B.S. 2004c. Provenance Study of the Late Triassic – Early Jurassic Elliot Formation, main Karoo Basin, South Africa. *South African Journal of Geology*, 107, 587-602.

Bordy, E.M., Hancox, P.J. and Rubidge, B.S. 2005. The contact of the Molteno and Elliot formations through the main Karoo Basin, South Africa: A second-order sequence boundary. *South African Journal of Geology*, 108, 351-364.

Bordy, E.M., Hancox, P.J. and Rubidge, B.S. 2005. Turner, B.R. and Thomson, K., Discussion on 'Basin development during deposition of the Elliot Formation (Late Triassic – Early Jurassic), Karoo Supergroup, South Africa'. *South African Journal of Geology*, 107, 397-412 – A Reply. *South African Journal of Geology*, 108, 454-461.

Bordy, E.M. 2008. Enigmatic trace fossils from the aeolian Lower Jurassic Clarens Formation, southern Africa. *Palaeontologia Electronica*, 11, 16A.

Bordy, E.M. and Prevec, R. 2008. Sedimentology, palaeontology and palaeo-environments of the Middle (?) to Upper Permian Emakwezini Formation (Lebombo Basin, South Africa). *South African Journal of Geology*, 111, 429-458.

Bordy, E.M., Brumby, A.J., Catuneanu, O. and Eriksson, P.G., 2009. Possible trace fossils of putative termite origin in the Lower Jurassic (Karoo Supergroup) of southern Africa. *South African Journal of Science*, 105, 356-362.

Bordy, E.M., Sztano, O., Rubidge, B.S., Bumby, A. 2009. Tetrapod burrows in southwestern main Karoo Basin (Lower Katberg Formation, Beaufort Group), South Africa. *Palaeontologica Africana*, 44, 95-99.

Bordy, E.M., Knoll, F. and Bumby, A. 2010. New data on the palaeontology and sedimentology of the Lower Jurassic Lisbon Formation (Karoo Supergroup), Ellisras Basin, South Africa. *Neues Jahrbuch für Geologie und Paläontologie - Abhandlungen*, 258, 145–155.

Bordy, E.M. and Eriksson, P. 2015. Lithostratigraphy of the Elliot Formation (Karoo Supergroup), South Africa. *Geological Society of South Africa*, 118, 311–316.

Bordy, E.M., Sciscio, L., Abdala, F., McPhee, B., Choniere, J. 2016. First Lower Jurassic vertebrate burrow from southern Africa (upper Elliot Formation, Karoo Basin, South Africa). *Palaeogeography, Palaeoclimatology, Palaeoecology*. 468, 362-372.

Bordy, E.M., Abrahams, M., Sciscio, L. 2017. The Subeng vertebrate tracks: stratigraphy, sedimentology and a digital archive of a historic Upper Triassic palaeosurface (lower Elliot Formation), Leribe, Lesotho (southern Africa). *Bollettino della Società Paleontologica Italiana*, 56(2), 181-198.

Bordy, E.M., Bowen, D.A., Moore, J., Garnett, M.H., Tsikos, H. 2018. A Holocene “Frozen Accident”: Sediments of extreme paleofloods and fires in the bedrock-confined upper Huis river, Western Cape, South Africa. *Journal of Sedimentary Research*, 88(8), 696-716.

Bordy, E.M and Head, H.V. 2018. Lithostratigraphy of the Clarens Formation (Stormberg Group, Karoo Supergroup), South Africa. *Geological Society of South Africa*, 121, 119-130.

Bordy, E.M., Abrahams, M., Rampersadh, A., Haupt, T., Head, H. 2018. The Fire Walkers: tracking the last Karoo dinosaurs. *Proceedings of the 20th Biennial Conference of the Palaeontological Society of Southern Africa*, Bloemfontein, 4-6 July, 9.

Bromley, R.G. and Asgaard, U. 1993. Endolithic community replacement on a Pliocene rocky coast. *Ichnos*, 2, 93–116.

Buatois, L.A., Mángano, M.G. and Aceñolaza, F.G. 2002. Trazas Fósiles: Señales de Comportamiento en el Registro estratigráfico. *Museo Paleontológico Egidio Feruglio, Trelew*, 382.

Buatois, L.A. and Mángano, M.G. 2007. Invertebrate ichnology of Continental Freshwater Environments. In: Miller, W. (ed), *Trace Fossils: Concepts, problems, prospects*. Amsterdam, Netherlands: Elsevier, 285-323.

Buatois, L.A. and M.G Mángano, 2011. *Ichnology: Organism-substrate interactions in space and time*. Cambridge, United Kingdom: Cambridge University Press.

Burgess, S.D., Bowring, S.A. 2015. High-precision geochronology confirms voluminous magmatism before, during, and after Earth's most severe extinction. *Science Advances*. 1, 1–14.

Butler, R.J., Smith, R.M.H. and Norman, D.B. 2007. A primitive ornithischian dinosaur from the Late Triassic of South Africa, and the early evolution and diversification Ornithischia. *Proc Biol Sci.*, 274(1621), 2041-2046.

Cas, R.A.F. and Wright, J.V. 1987. *Volcanic Successions, modern and ancient: A geological approach to processes, products and successions*. London, United Kingdom: Allen and Unwin.

Catuneanu, O., Hancox, P.J., and Rubidge, B.S. 1998. Reciprocal flexural behavior and contrasting stratigraphies: a new basin development model for the Karoo retroarc foreland system, South Africa. *Basin Research*, 10, 417-439.

Catuneanu, O., Wopfner, H., Eriksson, P.G., Cairncross, B., Rubidge, B.S., Smith, R.M.H. and Hancox, P.J. 2005. The Karoo basins of south-central Africa. *Journal of African Earth Sciences*, 43, 211-253.

Chakraborty, T. and Chaudhuri, A.K. 1993. Fluvial-aeolian interactions in a Proterozoic alluvial plain: example from the Mancherai Quartzite, Sullavai Group, Pranhita-Godavari Valley, India. Geological Society, London, Special Publications, 72, 127-141.

Childs, C., Nicol, A., Walsh, J.J., Watterson, J. 2003. The growth and propagation of syn-sedimentary faults. *Journal of Structural Geology*, 25(4), 633-648.

Cole, D.I. 1992. Evolution and development of the Karoo Basin. In: De Wit, M.J. and Ransome, I.G.D. (Eds.), *Inversion Tectonics of the Cape Fold Belt, Karoo and Cretaceous Basins of South Africa*, Rotterdam: Balkema, 87-99.

Cooke, R.U. and Warren, A. 1973. *Geomorphology in Deserts*, Berkeley, Los Angeles: University of California Press, 374.

Cowie, P.A. and Scholz, C. H. 1992. Growth of faults by accumulation of seismic slip. *Journal of Geophysical Research: Solid Earth*, 97(B7), 11085-11095.

De Gibert, J.M., Martinell, J. and Domenech, R. 1998. *Entobia ichnofossils in fossil rocky shores, lower Pliocene, northwestern Mediterranean*. *Palaios*, 13(5), 476-487.

de Wit, M.C.J. 2016. Early Permian diamond-bearing proximal eskers in the Lichtenburg/Ventersdorp area of the North West Province, South Africa. *South African Journal of Geology* 119, 585-606.

Dickinson, W.R. 1985. Interpreting provenance relations from detrital modes of sandstones. In: Zuffa, G.G (Eds.), *Provenance of arenites*. Dordrecht: D. Reidel, 333-361.

Directorate of overseas surveys, Lesotho Government, Department of Mines and Geology. 1982. *Quithing 3027B [Map]*. Edition 1. Scale 1:100 000. Maseru, Lesotho.

Duncan, R.A., Hooper, P.R., Rehacek, J., Marsh, J.S. and Duncan, A.R. 1997. The timing and duration of the Karoo igneous event, southern Gondwana. *Journal of Geophysical Research* 102(B8), 18127-18138.

Dusar, M. 1979. *Structural outline of Lesotho*. Department of Mines and Geology. United Nations development programme exploration for minerals project, special report, MD/8, Maseru.

Du Toit, A. 1954. *The Geology of South Africa*. London: Oliver and Boyd, 611.

Edwards, M.B. 1976. Growth Faults in Upper Triassic Deltaic Sediments, Svalbard. The American Association of Petroleum Geologists Bulletin, 60, 341-355.

Ellenberger, F., Ellenberger, P., Fabre, J., Mendrez, C. 1963. Deux nouvelles dalles à pistes de Vertébrés fossiles découvertes au Basutoland (Afrique du Sud) [Two new slabs of fossil vertebrate trackways discovered in Basutoland (southern Africa)]. *Compte Rendus de la Société Géologique de France*, 315-317.

Ellenberger, P. 1970. Les niveaux paléontologiques de première apparition des mammifères primordiaux en Afrique du Sud et leur ichnologie. Etablissement de zones stratigraphique détaillées dans le Stormberg du Lesotho (Afrique du Sud) (Trias superior a Jurassique). *Proceedings and Papers of the second Gondwana Symposium*, 343–370.

Ellenberger, P. 1972. Contribution à la classification des Pistes de Vértébrés du Trias: les Stormberg d'Afrique du Sud (I). In: *Paleovertebrata, Memoire Extraordinaire*. Montpellier: Laboratoire de paléontologie, 152.

Ellenberger, P. 1974. Contribution a la classification des pistes de Vértébrés du Trias; les types du Stormberg d'Afrique du Sud, (2). In: *Palaeovertebrata, Memoire Extraordinaire*. Montpellier: Laboratoire de paléontologie, 170.

Encarnación, J., Fleming, T.H., Elliot, D.H., Eales, H. V. 1996. Synchronous emplacement of Ferrar and Karoo dolerites and the early breakup of Gondwana. *Geology*, 24, 535-538.

Eriksson, P.G. 1981. A palaeoenvironmental analysis of the Clarens Formation in the Natal Drakensberg. *Transactions Geological Society of South Africa*, 84, 7-17.

Eriksson, P.G. 1984. A palaeoenvironmental analysis of the Molteno Formation in the Natal Drakensberg. *Transactions Geological Society of South Africa*, 87, 237-244.

Eriksson, P.G. 1985. The depositional environment of the Elliot Formation in the Natal Drakensberg and north-east Orange Free State. *Transactions Geological Society of South Africa* 88, 19-26.

Eriksson, P.G. 1986. Aeolian dune and alluvial fan deposits in the Clarens Formation of the Natal Drakensberg. *Transactions Geological Society of South Africa* 89, 389-393.

Eriksson, P.G. 1987. A note on the red colouration in sedimentary rocks of the Molteno, Elliot and Clarens formations. *Annals of the Geological Survey of South Africa* 21, 89-94.

Eriksson, P.G., McCourt, S. and Snyman, C.P., 1994. A note on the petrography of upper Karoo sandstones in the Natal Drakensberg: implications for the Clarens Formation palaeoenvironment. *Transactions of the Geological Society of South Africa*, 97, 101-103.

Forey, P. and Gardiner, B.G. 1973. A new dictyopygid from the Cave Sandstone of Lesotho, Southern Africa. *Palaeontologia Africana*, 15, 29-31.

Fossen, H. 2010. *Structural Geology*. New York, USA: Cambridge University Press.

Ghosh, P., Sarkar, S. and Maulik, P. 2006. Sedimentology of a muddy alluvial Deposit: Triassic Denwa Formation, India. *Sedimentary Geology*, 191, 3-36.

Gierlinski, G., Niedzwiedzki, G. and Pienkowski, G. 2001. Gigantic footprint of a theropod dinosaur in Early Jurassic of Poland. *Acta Palaeontologica Polonica*, 46(3), 441-446.

Gondwana context of the southeastern Cape – Karoo Basin. *South African Journal of Geology*, 94, 137-145.

Goudie, A.S. 1996. Organic agency in calcrete development. *Journal of Arid Environments*, 32, 103-110.

Groenewald, G.H., Welman, J. and Maceachern, J.A. 2001. Vertebrate burrow complexes from the Early Triassic Cynognathus Zone (Driekoppen Formation, Beaufort Group) of the Karoo Basin, South Africa. *Palaios* 16, 148-160.

Gustavson, T.C. 1991. Buried vertisols in lacustrine facies of the Pliocene Fort Hancock Formation, Hueco Bolson, West Texas and Chihuahua, Mexico. *Geological Society of America*, 103(4), 448-460.

Halbich, I.W. 1978. Fold profiles and tectonic shortening in the Cape Fold Belt. 81, 403–408.

Hancox, P.J. 1998. The Beaufort-Molteno contact revised: ramifications for the development of the Karoo retro-foreland basin during the Triassic. *Journal of African Earth Sciences*, 27, 103-104.

Hancox, P.J. and Rubidge, B.S. 2001. Breakthroughs in biodiversity, biogeography, biostratigraphy, and basin analysis in of the Beaufort Group. *Journal of African Earth Sciences* 33, 563-577.

Hancox, P.J. and Rubidge, B.S. 2018. Mid-Late Triassic Beaufort-Stormberg contact – Implications for Triassic Karoo Basin development. *Geocongress 2018*, University of Johannesburg, 18-20 July, 91.

Hansma, J., Tohver, E., Schrank, C., Jourdan, F. and Adams, D. 2016. The timing of the Cape Orogeny: New $^{40}\text{Ar}/^{39}\text{Ar}$ age constraints on deformation and cooling of the Cape Fold Belt, South Africa. *Gondwana Research*, 32, 122–137.

Hanson, E.K., Moore, J.M., Bordy, E.M., Marsh, J.S., Howarth, G., Robey, J.V.A. 2009. Cretaceous erosion in central South Africa: Evidence from upper-crustal xenoliths in kimberlite diatremes. *South African Journal of Geology*, 112, 125–140.

Hardin, F.R. and Hardin, G.C. 1961. Contemporaneous normal faults of Gulf Coast and their relation to flexures. *The American Association of Petroleum Geologists Bulletin*, 45, 238-248.

Hasiotis, S.T., Miller, M.F., Isbell, J., Babcock, L.E., Collinson, J.W. 1999. Triassic trace fossils from Antarctica: burrow evidence of crayfish or mammal-like reptiles? Resolving crayfish from tetrapod burrows. *Freshwater Crayfish*, 12, 71-81.

Haughton, S.H. 1924. The Fauna and stratigraphy of the Stormberg Series Annals of the South African Museum, 8, 1-517.

Haughton, S.H. 1969. Geological history of Southern Africa. The Geological Society of South Africa, Cape Town: Cape and Transvaal printers Ltd, 536.

Heinz, J. and Aigner, T. 2003. Hierarchical dynamic stratigraphy in various Quaternary gravel deposits, Rhine glacier area (SW Germany): implications for hydrostratigraphy. International Journal of Earth Sciences, Geologische Rundschau, 92, 923-938.

Hogg, S.E., 1982. Sheetfloods, sheetwash, sheetflow or. . .? Earth-Science Reviews 18, 59-76.

Holzförster, F. 2007. Lithology and depositional environments of the Lower Jurassic Clarens Formation in the Eastern Cape, South Africa. South African Journal of Geology, 110, 543-560.

Hunter, R.E. 1977. Basic types of stratification in small eolian dunes. Journal of the International Association of Sedimentologists, 24(3), 361-387.

Ingersoll, R. V., Bullard, T.F., Ford, R.L., Grimm, J.P., Pickle, J.D., Sares, S.W. 1984. The Effect of Grain Size on Detrital Modes: A Test of the Gazzi-Dickinson Point-Counting Method. SEPM J. Sediment. Res., 54, 103-116.

Isbell, J.L., Cole, D.I. and Catuneanu, O., 2008. Carboniferous-Permian glaciation in the main Karoo Basin, South Africa: Stratigraphy, depositional controls, and glacial dynamics. Geological Society of America Special Papers, 441, 71-82.

Jay, A.E., Marsh, J.S., Fluteau, F. and Courtillot, V. 2018. Emplacement of inflated Pāhoehoe flows in the Naude's Nek Pass, Lesotho remnant, Karoo continental flood basalt province: use of flow-lobe tumuli in understanding flood basalt emplacement. Bulletin of Volcanology, 80.

Johnson, M.R. 1991. Sandstone petrography, provenance and plate tectonic setting in Gondwana context of the southeastern Cape-Karoo basin. South African Journal of Geology, 94, 137-154.

Johnson, M.R., Van Vuuren, C.J., Hegenberger, W.F., Key, R., Shoko, U. 1996. Stratigraphy of the Karoo Supergroup in southern Africa: An overview. Journal of African Earth Sciences, 23, 3–15.

Johnson, M.R., Van Vuuren, C.J., Visser, J.N.J., Cole, D.I., de Wickens, H.V., Christie, A.D.M. Roberts, D.L. 1997. The Foreland Karoo Basin, South Africa. In: R.C. Selly (ed.): African Basins. Sedimentary Basins of the World, 3. Amsterdam: Elsevier Science B.V, 269-317.

Johnson, M.R., Van Vuuren, C.J., Visser, J.N.J., Cole, D.I., de Wickens, H., Christie, A.D.M., Roberts, D.L., Brandl. G. 2006. Sedimentary Rocks of the Karoo Supergroup. In: Johnson, M.

R., Anhaeusser, C.R. and Thomas R J. (Eds.), The Geology of South Africa. Geological Society of South Africa, Johannesburg/Council for Geoscience, Pretoria, 461-501.

Jones, M.T., Jerram, D.A., Svensen, H.H. and Grove, C. 2016. The effects of large igneous provinces on the global carbon and sulphur cycles. *Palaeogeography, Palaeoclimatology, Palaeoecology*, 441, 4–21.

Jones, J.G. and Nelson, P.H.H. 1970. The flow of basalt lava from air into water- its structural expression and stratigraphic. *Geological magazine*, 107(1), 13-21.

Jubb, R.A. 1973. Brief synthesis of present information on the geographical and stratigraphical distribution of fossil fish within the Stormberg Series, South Africa. *Palaeontologia Africana*, 16, 17-23.

Kim, Y., Peacock, D.C.P. and Sanderson, D.J. 2002. Fault damage zones. *Journal of Structural Geology*, 26, 503-517.

Kitching, J.W. 1977. The distribution of the Karoo vertebrate fauna. Bernard Price Institute for Palaeontological Research Memoir, 1, 1-131.

Kitching, J.W. and Raath, M.A. 1984. Fossils from the Elliot and Clarens formations (Karoo Sequence) of the northeastern Cape, Orange Free State and Lesotho, and a suggested biozonation based on tetrapods. *Palaeontologia Africana*, 25, 111-125.

Knoll, F. 2004. Review of the tetrapod fauna of the 'Lower Stormberg Group' of the main Karoo Basin (southern Africa): implication for the age of the Lower Elliot Formation. *Bulletin de la Société géologique de France*, 175, 73-83.

Knoll, F. 2005. The tetrapod fauna of the Upper Elliot and Clarens formations in the main Karoo Basin (South Africa and Lesotho). *Bulletin de la Société Géologique de France*, 176, 81-91.

Krummeck, D.W. and Bordy, E.M. 2017. *Reniformichnus katikatii* (new ichnogenus and ichnospecies): continental vertebrate burrows from the Lower Triassic, main Karoo Basin, South Africa. *Ichnos*, 25, 138-149.

Lindeque, A.S., de Wit, M.J., Ryberg, T., Weber, M. and Chevallier, L. 2011. Deep crustal profile across the Southern Karoo basin and Beattie magnetic anomaly, South Africa: An integrated interpretation with tectonic implications. *South African Journal of Geology*, 114, 265-292.

Lock, B.E., Paverd, A.L. and Broderick, T.J. 1974. Stratigraphy of the Karoo volcanic rocks of the Barkly East district. *Transactions of the Geological Society of South. Africa*, 77, 177-129.

Lock, B.E. 1980. Flat-plate subduction and the Cape Fold Belt of South Africa. *Geology*, 8, 35–39.

Lockley, M.G. 1986. The paleobiological and paleoenvironmental importance of dinosaur footprints. *Palaios*, 1, 37-47.

Lockley, M.G., Meyer, C.A. and dos Santos, V.F. 1996. *Megalosauripus*, *Megalosauropus* and the concept of megalosaur footprints. In: M. Morales (Ed.), *The Continental Jurassic*. Museum of Northern Arizona Bulletin, 60, 113-118.

Lockley, M.G. and Mickelson, D.L. 1997. Dinosaur and pterosaur tracks in the Summerville and Bluff (Jurassic) beds of eastern Utah and northeastern Arizona. *New Mexico Geological Society Guidebook, 48th Field Conference. Mesozoic Geology and Paleontology of the Four Corners Region*, 133-138.

Lockley, M.G., Meyer, C.A. and dos Santos, V.F. 1998. *Megalosauripus* and the problematic concept of megalosaur footprints. *Gaia*, 15, 313–337.

Lockley, M.G., 2010. New perspectives on morphological variation in tridactyl footprints: clues to widespread convergence in developmental dynamics. *Geological Quarterly*, 53(4), 415-432.

Lucas, S.G., Klein, H., Lockley, M.G., Spielmann, J.A., Gierlinski, G.D., Hunt, A.P., Tanner, L.H., 2006. Triassic-Jurassic stratigraphic distribution of the theropod footprint ichnogenus *Eubrontes*. *New Mexico Museum of Natural History and Science Bulletin*, 37, 86-93.

MacEachern, J.A., Bann, K.L., Gingras, M.K., Zonneveld, J., Dashtgard, S.E., Pemberton, S.G. 2012. The Ichnofacies Paradigm. In: Knaust, D. and Bromley, R.G. (Eds.), *Developments in sedimentology: Trace Fossils as indicators of sedimentary environments*. Amsterdam, Netherlands: Elsevier, 64, 103-138.

Marsh, J.S. and Eales, H.V. 1984. The chemistry and petrogenesis of igneous rocks of the Karoo central area, Southern Africa. In: Erlank, A.J. (Eds.), *Petrogenesis of the Volcanic Rocks of the Karoo Province*. Special Publication Geological Society of South Africa, 27-67.

Marsh, J.S., Hooper, P.R., Rehacek, J.J., Duncan, R.A. Duncan, A.R. 1997. Stratigraphy and age of Karoo basalts of Lesotho and implications for correlations within the Karoo igneous province. *Large Igneous Provinces: Continental, Oceanic, and Planetary Flood Volcanism*, 247-272.

Marsicano, C.A., Wilson, J.A. and Smith, R.M., 2014. A temnospondyl trackway from the early Mesozoic of western Gondwana and its implications for basal tetrapod locomotion. *PLoS one*, 9(8), 103255.2.

Martins, U.P. and Pfefferkorn, H.W. 1988. Genetic interpretation of a Lower Triassic Paleosol complex based on soil micromorphology. *Palaeogeography, Palaeoclimatology, Palaeoecology*, 64, 1-14.

McCarthy, M. J. 1970. An occurrence of pillow-lava in a basal flow of the Drakensberg Volcanic Stage, Ndedema Valley, Natal. *Proceedings, 2nd Gondwana Symposium, South Africa*, 433-440.

McIlroy, D. 2008. Ichnological analysis: The common ground between ichnofacies workers and ichnofabric analysts. *Palaeogeography, Palaeoclimatology, Palaeoecology*, 270, 332–338.

McPhee, B.W., Bordy, E.M., Sciscio, L. and Choiniere, J.N., 2017. The sauropodomorph (Dinosauria) biostratigraphy of the Elliot Formation of southern Africa: tracking the evolution of Sauropodomorpha across the Triassic–Jurassic boundary. *Acta Palaeontologica Polonica*, 62(3), 441-465.

Meijs, L. 1960. Notes on the occurrence of petrified wood in Basutoland. Roma, Basutoland: Pius XII University Collage, 2, 8.

Melchor, R.N., Bedatou, E., Valais, S. De and Genise, J.F. 2006. Lithofacies distribution of invertebrate and vertebrate trace-fossil assemblages in an Early Mesozoic ephemeral fluvio-lacustrine system from Argentina: Implications for the Scoyenia ichnofacies. 239, 253–285.

Miall, A.D. 1978. Lithofacies types and vertical profile models in braided river deposits: a summary. *Fluvial Sedimentology*, 5, 597–600.

Miall, A.D., 1985. Architectural-element analysis: a new method of facies analysis applied to fluvial deposits. *Earth-Science Reviews*, 22, 261-308.

Miall, A.D. 1996. *The geology of fluvial deposits*. Berlin Heidelberg, Germany: Springer.

Miall, A.D. 2006. How do we identify big rivers? And how big is big? *Sedimentary Geology*, 186, 39-50.

Milner, A.R., Lockley, M.G. and Johnson SB. 2006. The story of the St. George Dinosaur Discovery Site at Johnson Farm: an important new lower Jurassic dinosaur tracksite from the Moenave Formation of Southwestern Utah. *The Triassic-Jurassic Terrestrial Transition*. New Mexico Museum of Natural History and Science Bulletin, 37, 315-328.

Moore, J.G. 1975. Mechanism of Formation of Pillow Lava: Pillow lava, produced as fluid lava cools underwater, is the most abundant volcanic rock on earth, but only recently have divers observed it forming. *American Scientist*, 63(3), 269–277.

Moulin, M., Fluteau, F., Courtillot, V., Marsh, J., Delpech, G., Quidelleur, X. and Gérard, M. 2017. Eruptive history of the Karoo lava flows and their impact on early Jurassic environmental change. *Journal of Geophysical Research: Solid Earth*, 122(2), 738-772.

Nemec, W and Steel, R.J. 1984. Alluvial and Coastal Conglomerates: Their significant features and some comments on gravelly mass-flow deposits. *Sedimentology of Gravels and Conglomerates*, 10, 1-31.

Olsen, P.E., and Galton, P.M. 1984. A review of the reptile and amphibian assemblages from the Stormberg Group of southern Africa with special emphasis on the footprints and the age of the Stormberg. *Palaeontologia Africana*, 25, 87-110.

Olsen, P.E., Smith, J.B. and McDonald, N.G. 1998. Type material of the type species of the classic theropod footprint genera Eubrontes, Anchisauripus, and Grallator (Early Jurassic, Hartford and Deerfield basins, Connecticut and Massachusetts, USA). *Journal of Vertebrate Paleontology*, 18(3), 586-601.

Olsen, P.E. and Rainforth, E.C. 2003. The Early Jurassic Ornithischian Dinosaurian Ichnogenus. 2, 314-367.

Parizot, M., Eriksson, P.G., Aifa, T., Sarkar, S., Banerjee, S., Catuneanu, O., Altermann, W., Bumby, A.J., Bordy, E.M., Rooy, J.L. Van and Boshoff, A.J. 2005. Suspected microbial mat-related crack-like sedimentary structures in the Palaeoproterozoic Magaliesberg Formation sandstones, South Africa. *Precambrian Research*, 138, 274–296.

Percival, L.M.E., Witt, M.L.I., Mather, T.A., Hermoso, M., Jenkyns, H.C., Hesselbo, S.P., Ruhl, M. 2015. Globally enhanced mercury deposition during the end-Pliensbachian extinction and Toarcian OAE: A link to the Karoo–Ferrar Large Igneous Province. *Earth and Planetary Science Letters*, 428, 267-280.

Pettijohn, F.J., Potter, P.E. and Siever, R. 1987. *Sand and Sandstone*. 2nd Edition. New York, USA: SpringerVerlag.

Planke, S., Rassmussen, T., Rey, S.S., Myklebust, R. 2005. Seismic characteristics and distribution of volcanic intrusions and hydrothermal vent complexes in the Vøring and Møre basins. In: Dore, A. and Vining, B. (Eds.), *Petroleum Geology: North-West Europe and Global Perspectives*. Proceedings of the 6th Geology Conference. Geological Society, London, 833-844.

Prevec, R., Gastaldo, R.A., Neveling, J., Reid, S.B. and Looy, C. V. 2010. An autochthonous glossopterid flora with latest Permian palynomorphs and its depositional setting in the Dicynodon assemblage zone of the southern Karoo Basin, South Africa. *Palaeogeography, Palaeoclimatology, Palaeoecology*, 292, 391-408.

Prevec, R. 2011. A structural re-interpretation and revision of the type material of the glossopterid ovuliferous fructification *Scutum* for South Africa. *Palaeontologia Africana*, 46, 1-19.

Pye, K. and Tsoar, H. 1990. *Aeolian Sand and Sand Dunes*. London, United Kingdom: Unwin Hyman.

Pysklywec, R.N. and Mitrovica, J.X. 1999. The role of subduction-induced subsidence in the evolution of the Karoo basin. *Journal of Geology*, 107, 155–164.

Rayhani, M.H.T., Yanful, E.K. and Fakher, A. 2008. Physical modeling of desiccation cracking in plastic soils. *Engineering Geology* 97, 25-31.

Retallack, G.J. 2005. Pedogenic carbonate proxies for amount and seasonality of precipitation in palaeosols. *Geological Society of America*, 33(4), 333-336.

- Rubidge, B.S. 2005. Re-uniting lost continents—Fossil reptiles from the ancient Karoo and their wanderlust. *South African Journal of Geology* 108,135-172.
- Rubidge B.S., Erwin D.H., Ramezani J, Bowring S.A., de Klerk W.J. 2013. High-precision temporal calibration of Late Permian vertebrate biostratigraphy: U-Pb zircon constraints from the Karoo Supergroup, South Africa. *Geology*, 10,1-4.
- Scheiber-Enslin, S.E., Ebbing, J. and Webb, S.J. 2015. New depth maps of the main Karoo Basin, used to explore the Cape Isostatic Anomaly, South Africa. *South African Journal of Geology*, 118.3, 225-248.
- Schmitz, G. and Rooyani., F. 1987. Lesotho, Geology, Geomorphology, Soils. National University of Lesotho,12–42.
- Sciscio, L. and Bordy, E.M., 2016. Palaeoclimatic conditions in the Late Triassic-Early Jurassic of southern Africa: a geochemical assessment of the Elliot Formation. *Journal of African Earth Sciences*, 119, 102-119.
- Sciscio, L., Bordy, E.M., Reid, M. and Abrahams, M. 2016. Sedimentology and ichnology of the Mafube dinosaur track site (Lower Jurassic, eastern Free State, South Africa): a report on footprint preservation and palaeoenvironment. *PeerJ*, 4, e2285.
- Sciscio, L., Bordy, E.M., Abrahams, M., Knoll, F., McPhee, B.W. 2017a. The first megatheropod tracks from the Lower Jurassic upper Elliot Formation, Karoo Basin, Lesotho. *PLoS ONE*, 12(10), e0185941.
- Sciscio, L., de Kock, M., Bordy, E.M., Knoll, F. 2017b. Magnetostratigraphy across the Triassic-Jurassic boundary in the main Karoo Basin. *Gondwana Research* 51, 177-192.
- Sciscio, L., Knoll, F., Bordy, E.M., de Kock, M., Redelstorff, R. 2017c. Digital reconstruction of the mandible of an adult *Lesothosaurus diagnosticus* with insight into the tooth replacement process and diet. *PeerJ*, 5, e3054.
- Scotese, C.R., Boucot, A.J. and Mckerrow, W.S. 1999. Gondwanan palaeogeography and palaeoclimatology. *Journal of African Earth Sciences*, 28(1), 99-114.
- Seilacher, A. 1964. Biogenic sedimentary structures. In: Imbrie, J. and Newell, N. (Eds.), *Approaches to Paleoecology*. New York, USA: Wiley, 296-316.
- Seilacher, A.1967. Bathymetry of trace fossils. *Marine Geology* 5, 413-428.
- Sell, B., Ovtcharova, M., Guex, J., Bartolini, A., Jourdan, F., Spangenberg, J.E., Vicente, J.-C., Schaltegger, U. 2014. Evaluating the temporal link between the Karoo LIP and climatic-biologic events of the Toarcian stage with high-precision U–Pb geochronology. *Earth Planetary Science Letters*, 408, 48–56.
- Selley, R.C., 1970. Studies of sequences in sediments using a simple mathematical device. *Geological Society of London Quarterly Journal*, 125, 557-581.

- Shi, B., Tang, C.S., Liu, C., Zhao, L., Wang, B.J. 2008. Influencing factors of geometrical structure of surface shrinkage cracks in clayey soils. *Engineering Geology*, 101, 204-217.
- Smith, R.M.H. 1990. A review of stratigraphy and sedimentary environments in the Karoo Basin of South Africa. *Journal of African Earth Sciences*, 10(1), 117-137.
- Smith, R.M.H., Eriksson, P.G. and Botha, W.J. 1993. A review of the stratigraphy and sedimentary environments of the Karoo-aged basins of Southern Africa. *Journal of African Earth Sciences*, 16, 143-169.
- Smith, R.M., Marsicano, C.A. and Wilson, J.A., 2009. Sedimentology and paleoecology of a diverse Early Jurassic tetrapod tracksite in Lesotho, southern Africa. *Palaios*, 24(10), 672-684.
- Snyder, G. and Fraser, G. 1963. Pillowed lavas, I: Intrusive layered lava pods and pillowed lavas Unalaska Island, Alaska. *Geological Survey professional paper*, 454, 11-22.
- Svensen, H., Jamtveit, B., Planke, S., Chevallier, L. 2006. Structure and evolution of hydrothermal vent complexes in the Karoo Basin, South Africa. *Journal of the Geological Society*, 163, 671-682.
- Tasch, P. 1984. Biostratigraphy and palaeontology of some conchostracan-bearing beds in southern Africa. *Palaeontologia Africana*, 25, 61-85.
- Tankard, A.J., Welsink, H., Aukes, P., Newton, R., Stettler, E. 2009. Tectonic evolution of the Cape and Karoo basins of South Africa. *Marine and Petroleum Geology*, 26, 1379-1412.
- Tankard A, Welsink H, Aukes P, Newton R, Stattker E. 2012. Geodynamic interpretation of the Cape and the Karoo basins, South Africa. *Phanerozoic Passive Margins, Cratonic Basins and Global Tectonics Maps*. USA and UK: Elsevier, 869.
- Terry, R.D. and Chilingar, C.V. 1955. Summary of "Concerning some additional aids in studying sedimentary formations" by M.S. Shvetsov. *Journal of Sedimentary Petrology*, 25 (3), 229-234.
- Turner, B.R. 1983. Braidplain deposition of the Upper Triassic Molteno Formation in the main Karoo (Gondwana) Basin, South Africa. *Sedimentology*, 30, 77-89.
- Turner, B.R. 1999. Tectonostratigraphical development of the Upper Karoo foreland basin: orogenic unloading versus thermally-induced Gondwana rifting. *Journal of African Earth Sciences* 28, 215-238.
- van Dijk, E.D., Hobday, D.K. and Tankard, A.J. 1978. Permo-Triassic lacustrine deposits in the Eastern Karoo Basin, Natal, South Africa. *Special Publications of the International Association of Sedimentology*, 2, 225-239.
- van Dijk, E.D. 2001. Jurassic bipeds that could hop? perch? pounce? fly? *South African Journal of Science* 97: 373-374.

- van Eeden, O.R. and Keyser, A.W. 1971. Fossielspore in die Holkrans-sandsteen op Pont Drift, Distrik Soutpansberg, Transvaal. *Annals of the Geological Survey of South Africa*, 9, 135-137.
- Veevers, J.J., Cole, D.I. and Cowan, E.J. 1994. Southern Africa: Karoo Basin and Cape Fold Belt. In: J.J. Veevers and McA. Powell: Permian-Triassic Pangean Basins and Foldbelts along the Panthalassan Margin of Gondwanaland. *Geological Society of America Memoir*, 184, 223-280.
- Veevers, J.J. 2004. Gondwanaland from 650-500 Ma assembly through 320 Ma merger in Pangea to 185-100 Ma breakup: supercontinental tectonics via stratigraphy and radiometric dating. *Earth-Science Reviews*, 68, 1-132.
- Visser, J.N.J. and Botha, B.J.V. 1980. Meander belt, point bar, crevasse splay and aeolian deposits from the Elliot Formation in Barkly Pass, northeastern Cape. *Transactions of the Geological Society of South Africa*, 83, 55-62.
- Visser, J.N.J. 1984. A review of the Stormberg Group and Drakensberg volcanics in southern Africa. *Palaeontologia Africana*, 25, 5-27.
- Visser, J.N.J. 1990. The age of the late Palaeozoic glaciogene deposits in southern Africa. *South African Journal of Geology* 93, 366-375.
- Walker, R.G. 1984. General introduction: facies, facies sequences and facies models. In: Walker, R.G. and James, N.P. (Eds.), *Facies Models Response to Sea Level Change*. Geological Association of Canada.
- Walker, R.G. 1992. Facies, facies models and modern stratigraphic concepts. In: Walker, R.G. and James, N.P. (Eds.), *Facies Models: Response to Sea-level Change*. Geological Association of Canada, 1-14.
- Waters, A.C. 1960. Determining Directions of Flow in Basalts. *American Journal of Science*, 258-A, 350-366.
- Wilson, J.A., Marsicano, C.A. and Smith, R.M.H. 2009. Dynamic locomotor capabilities revealed by early dinosaur trackmakers from Southern Africa. *PLoS ONE*, 4, 1-8.
- Wright, V.P. and Tucker, M.E. 1991. Calcretes: An introduction. In Wright V.P., Tucker M.E. (Eds.), *Calcretes*. International Association of Sedimentologists. Reprint Series Vol. 2. Oxford: Blackwell Scientific Publications, 1-22.
- Xiuman, H., Chengshan., W., Xianghui, L., Luba., Jansa. 2006. Upper Cretaceous oceanic red beds in southern Tibet: Lithofacies, environments and colour origin. *Science in China Series D: Earth Sciences*, 49(8), 785-795.
- Yates, A. 2005. A new theropod dinosaur from the Early Jurassic of South Africa and its implications for the early evolution of theropods. *Palaeontologica Africana*, 41, 105-122.

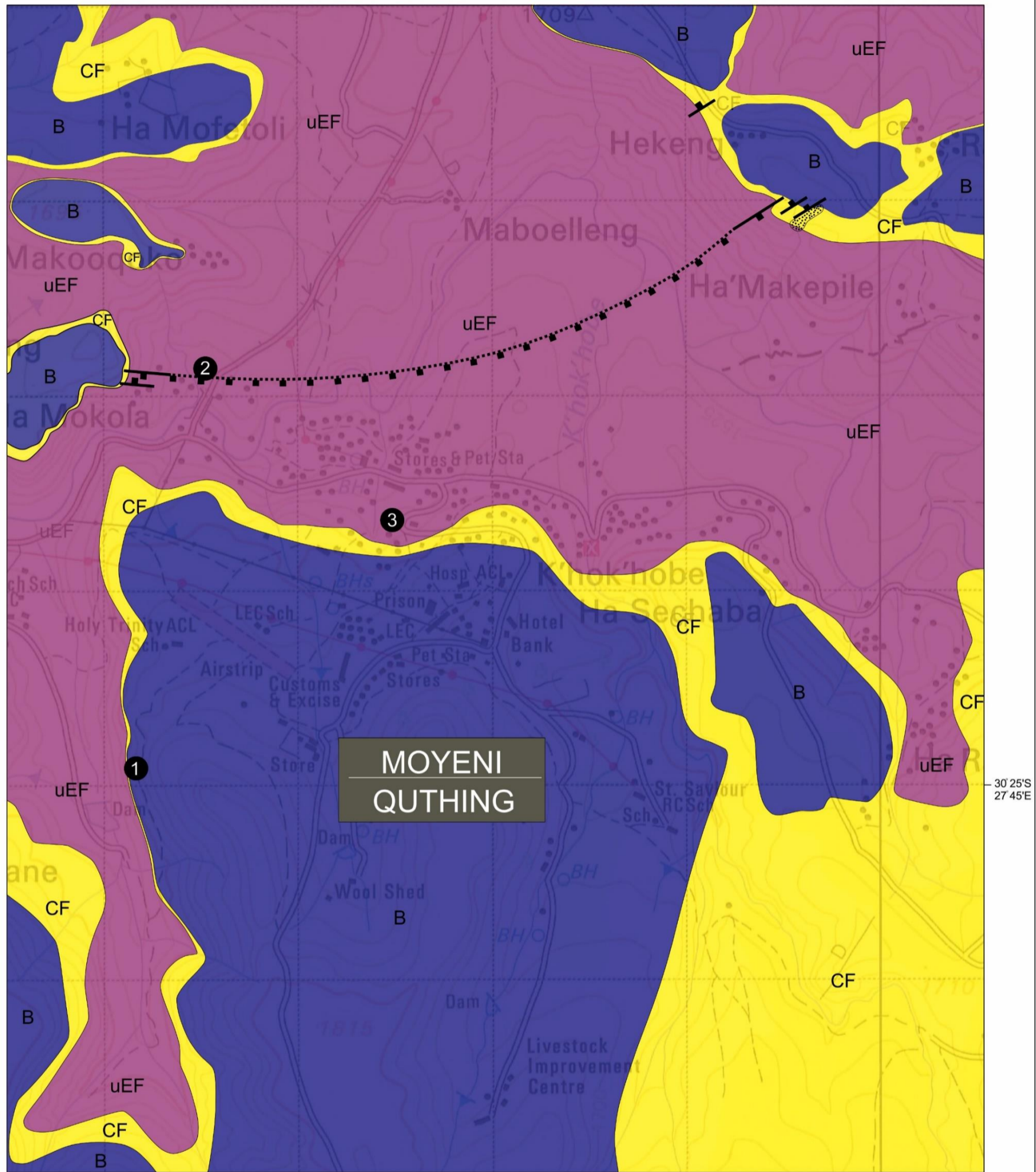
7 Appendix

Table 1A: Petrographic descriptions for sandstones and mudstone sample.

SAMPLE	A	B	C	D	E	F
FORMATION	uEF	Clarens	Clarens	Clarens (mudstone facies)	Barkly East (lower interbed)	Barkly East (upper interbed)
TEXTURE						
Grain size	medium	medium	medium	fine (clay-sized)	medium	fine-medium
Sorting	poor/moderate	moderate/well	poor	moderate	moderate	well
Sphericity	low	low	high		moderate	moderate
Roundness	angular/ sub- rounded	angular/sub- rounded	subangular- subrounded	very angular-angular quartz	sub-rounded- angular	sub-angular/sub- rounded
Fabric	homogenous	homogenous	homogenous	laminated	homogenous	homogenous
Grain packing	closely packed	closely packed	closely packed	closley packed	closely packed	closely packed
Grain contacts	concavo-convex	point/concavo- convex	concavo-convex		point/concavo- convex	point/concavo- convex
Matrix %	<12%	<10%	~10%		<15%	<10%
Maturity	submature	immature	immature		sub-mature-mature	mature
MINERAL COMPOSITION %						
Quartz	65	65	55	~70 % clay minerals	60	70
Feldspar	10	20	25		20	20
Lithic	25	10	15		15	10
Accessory minerals	trace	5	5		5	trace
Normalised %						
Quartz	65	68	58		63	70
Feldspar	10	21	26		21	20
Lithic fragments	25	11	16		16	10
Total	100	100	100		100	100
Classification	Sublitharenite	Subarkose	Subarkose		Subarkose	Subarkose
Provenance	Recycled Orogen	Continental Block	Continental Block		Continental Block	Continental Block

MOYENI (QUTHING DISTRICT) LESOTHO

Geological Map



- B Barkly East Formation
- CF Clarens Formation
- uEF upper Elliot Formation
- normal fault zone
- smaller antithetic faults
- breccia facies
- ⊗ study localities

Drakensberg Group
Stormberg Group
Karoo Supergroup

contour vertical interval 25 metres

1 km



Figure 1A: Geological map of Moyeni (Quthing District), southwestern Lesotho. Note the main study localities are also labelled; (1) pillow lava succession, (2) lower Moyeni ichnosite and (3) upper Moyeni ichnosite.